Universita' degli Studi di Milano-Bicocca
Dipartimento di Biotecnologie e Bioscienze
Dottorato di ricerca in Biotecnologie Industriali
XXVIII Ciclo

New nanostructured biomaterials for regenerative medicine

Antonella Sgambato
Matr. 077393

Relatore: Prof. Laura Cipolla
Coordinatore: Prof. Marco Vanoni

Anno accademico 2014-2015

“May the wind always be at your back and the sun upon your face. And may the wings of destiny carry you aloft to dance with the stars.”

Table of Contents

Abstract

Innovative approaches in tissue engineering and regenerative medicine based on decellularized extracellular matrix (ECM) scaffolds and tissues are quickly growing. ECM proteins are particularly adequate toward tissue regeneration applications, since they are natural biomaterials that can be bio-activated with signalling molecules able to influence cell fate, driving cell responses and tissue regeneration. Indeed, it is well recognized that cells perceive and respond to their microenvironment; the underlying mechanisms are generally complex and sometimes still poorly understood. Carbohydrates, found as complex polysaccharides or conjugated to other structural and functional proteins, are relevant components of the cell environment and cell membrane, contributing to cell interactions at several levels: for example, proteoglycans are a major constituent of the extracellular matrix (ECM) surrounding a cell, and glycosoaminoglycans (GAGs) participate in cell-ECM interactions and mediate cell-cell communications. It is now well recognized that glycans play an essential role in a plethora of biological processes, including cellular adhesion, migration, and differentiation, disease progression, and modulation of immunological responses. Although this relevant role, carbohydrates have been rarely considered as signalling cues for ECM derived scaffold functionalization and activation, due to their complexity in synthetic manipulations.

Nevertheless, recent data highlight that they can be promising tools for tissue engineering and regenerative medicine applications. Collagen and elastin, in form of 2D matrices or in their hydrolyzed forms have been bioactivated with different glycidic epitopes; characterizations and biological evaluations have been made. In particular this neo-glycosylated biomaterials have been tested for their ability to influence cell fate; we found that glucose-functionalized biomaterials are able to drive neuronal differentiation, and sialic acid, depending on the regiochemistry of its glycosidic bond, drives mesenchymal stem cells to differentiate in osteogenic or chondrogenic direction.

Inspired by the aggrecan, a natural proteoglycans found in cartilaginous tissues, with a bottlebrush structure, another work has been based on the design and production of a synthetic macromolecule, composed of collagen, as core protein, modified with the natural glycosaminoglycan chondroitin sulfate. Due to the high morbidity of some cartilage and bone diseases, and the difficulty, or impossibility, to restore ailing joints, the synthesis of these macromolecules is interesting and could be useful in cartilage tissue regeneration.

The area of hydrogels as biomaterials has also been taken into account. Hydrogels are three-dimensional hydrophilic polymer networks obtained from synthetic and/or natural polymers. They are able to swell and retain a large portion of water when placed in an

aqueous solution. We synthesized hydrogels, by using modified gelatin with different functional groups, or gelatin in combination with cross-linking agents. Hydrogels have become increasingly studied as matrices for tissue engineering. This kind of material are able to guarantee a 3D environment for cell culture.

Chapter 1

Introduction

Tissue engineering is an interdisciplinary field dedicated to the regeneration of functional human tissues. Despite the body having intrinsic self-healing properties, the extent of repair varies amongst different tissues, and may also be undermined by the severity of injury or disease. The combination of biomaterial scaffolds, cells, and bioactive molecules to orchestrate tissue formation and integration within the host environment are the basis of tissue engineering. In 1986, the Consensus Conference of the European Society for Biomaterials defined a biomaterial as “a nonviable material used in a medical device, intended to interact with biological systems”. The general approach in tissue engineering is based on the design and generation of biomaterials that can contribute to regenerative processes by efficiently transporting cells and therapeutic drugs and providing structural scaffolding that confer sufficient mechanical properties to a tissue. Additionally, the biomaterial degradation at the site of implantation should be obtained.[1]

Throughout history, biomaterials have occupied an important role in the improvement of health care and in the treatment of disease. Ancient biomaterials encompass metals such as gold, used in dentistry over 2,000 years ago, wooden teeth and glass eyes.[2] With the advent of synthetic polymers at the end of the nineteenth century, these materials became increasingly used in health care. For example, polymethylmethacrylate, PMMA, was used in dentistry in the 1930s[3] and cellulose acetate was used in dialysis tubing in the 1940s. Dacron was used to make vascular grafts; polyetherurethanes were used in artificial hearts; and PMMA and stainless steel were used in total hip replacements. Naturally available materials such as collagen,[4] elastin, hyaluronic acid, and chitosan have also been used as biomaterials in regenerative medicine. Scientists are creating new materials including those with improved biocompatibility, stealth properties, responsiveness (smart materials), specificity and other critical properties. Currently, biomaterials science is focused on a growing attention on identification of specific design parameters that are critical to achieve, and the requirement to combine biomaterials design with the basis of interactions of cells with the extracellular matrix, cellular signalling pathways, and systems biology. Nowadays, biomaterials have an extensive effect on medicine. Controlled drug delivery systems that largely involve polymers[5] are used by tens of millions of people annually. Recent examples are polymer-coated stents, which have recently been approved both in Europe and the

United States. Hundreds of thousands of lives are expected to be saved each year. In addition, various controlled release systems for proteins, such as human growth hormone, as well as molecules decorated with polyethylene glycol (PEG), such as pegylated interferon,[6] have recently been approved by regulatory authorities, and are showing how biomaterials can be used to positively affect the safety, pharmacokinetics and duration of release of important new drugs. By combining biomaterials with mammalian cells, patients with burns or skin ulcers can have new skin for the replacement, and many other polymer/cell combinations are in clinical trials, such as cartilage, bone, liver, and corneas.[7] The field of biomaterials is also having a great impact in dentistry, with dental implants, sutures, and numerous medical devices.[8]

Naturally derived biomaterials, including extracellular matrix (ECM) components, such as glycoproteins and proteoglycans, are being studied for many applications such as direct tissue replacement; the ECM complex, in fact, provides a good model for biomaterials design for tissue engineering.[9] Collagen, and other ECM-macromolecules, have been used in the last years as biomaterials for tissue regeneration applications; nowadays, it is possible to design and produce artificial/synthetic analogues of the extracellular matrix proteins using recombinant DNA technology.[10]

Polysaccharides have been used for biomaterials production in order to evaluate their *in vivo* performance; alginate-based hydrogels have

been used for cell encapsulation and transplantation, giving promising results in the field of bone tissue engineering.[11] The perspective of growing tissues from small numbers of precursor cells is an interesting alternative to harvesting and encapsulating large cell masses before transplantation.

Initially, scientists have designed materials with specific mechanical properties, being preferably "inert" without interaction with the host organism to prevent rejection.[12,13] Early research studies and unplanned accidents linking materials chemistry to biological responses provided a rational basis for developing new biomaterials. The molecular biology revolution of the seventies, and advances in genomics, proteomics, and more recently in glycomics, significantly influenced the ways in which biomaterials are designed, produced and used nowadays. The biomaterials implantation into the human body involves a series of interactions between the surface of biomaterials and the biological environment. Therefore, the biomaterials surface plays an extremely important role in the response of artificial medical devices to the surrounding biological environment. The functionalization of biomaterials with biomolecules to promote a specific biological response is a smart strategy to increase the chances of local regeneration.[14] Different classes of biomolecules have been used to produce cell-responsive biomaterials, including: peptides, like the adhesive cue arginine (Arg) – glycine (Gly) – asparagine (Asp), targeting cell adhesion receptors

(such as integrin or syndecan);[15] other regulatory molecules (i.e. cytokines, growth factors) and small molecules, such as kartogenin (KGN) promoting chondrocytes differentiation for cartilage repair[16] or acetylcholine targeting guanine nucleotide-binding protein (G protein)–coupled receptor used for neural repair.[17] In this field, an important class of biomolecules, the glycans,[18] has been neglected; their use for biomaterials functionalization should be take into account, since they are involved in a plethora of molecular recognition bioprocesses.[19] It is now well established that glycan interactions with their receptors play a fundamental role in various critical intra- and intercellular events.[20,21,22] Moreover, glycan structures encode information that regulates interactions between cells and the extracellular matrix (ECM).[23,24] On the basis of these premises, the use of saccharidic motifs has undoubted attractiveness for the functionalization of synthetic or natural materials to generate innovative and smart scaffolds with the capability to interact with the biological environment. Unlike most man-made materials, materials used in living systems are frequently multifunctional and dynamic.[25] The use of natural macromolecules, such as proteins, could be an advantage due to their related properties with the natural biological environment, and their natural predisposition to proteolytic degradation and remodeling. In contrast, disadvantages of using naturally-derived materials are the difficulty and costs to manufacture and lack of biostability. For these reasons, in some cases

researchers prefer to design and develop synthetic materials for tissue engineering applications, potentially suitable for many medical, but also non-medical applications.[26] The system simplification achieved with the use of synthetic biomaterials is one of the driving forces behind their use. The use of artificial components, such as polymers, provides a good alternative as they are often easy to manufacture, require low costs, and exhibit high stability over different conditions. Independently from the nature and mechanical properties, these materials can be decorated with biologically active biomolecules (i.e. peptides, growth factors, and glycans) that are able to mimic the natural biochemical and structural properties of the ECM, interacting and stimulating cells and directing their fate.

1.1 Biomaterials encountered in the clinics

In the following section there is a description of traditional biomaterials currently used in clinical procedure and tissue engineering and how their limitations have led to advanced technological developments in order to improve their *in vivo* performance.[27]

1.1.1 Metals and metal alloys

Stainless steel-based implants, cobalt-chromium, titanium and its alloys have been used for decades in classical biomaterials research.

Until today, knee, hip, spinal and dental metal implants are abundantly used worldwide.[28] Limitations of these metal implants are due to corrosion in the body environment; nickel, chromium and cobalt can be release by causing toxicity or hypersensitivity reactions, and, at worst, inducing carcinogenesis.[29,30] Titanium and its alloys-based materials are able to reduce the extent of stress-shielding by impeding bone resorption and improving bone remodeling. Titanium forms an extremely stable passive layer of TiO_2 on its surface and so providing ideal corrosion resistance and higher biocompatibility. Moreover, titanium is an interesting material due to its high specific strength. On the other hands, it shows some disadvantages, such as low shear strength, so its application as plates or screws is limited.[31] Metal is classified as a bioinert material. The activation of metal implants surface, *via* physical and chemical approaches, has been made. New advancements in the field of magnesium-based metal implants may break the paradigm of the insolubility of metallic materials in the future.[32]

1.1.2 Ceramics and glasses

The majority of ceramics are naturally hard and brittle materials with higher elastic moduli if compared to bone. Classical ceramics are characterized of high compressive but low tensile strength. However, mechanical and biological properties are extremely dependent on the applied manufacturing process. Alumina (Al_2O_3) and zirconia (ZrO_2)

are non-bioactive ceramics coated with a non-adherent fibrous layer at the interface after implantation. Their use in orthopedics as artificial femoral heads or acetabular liners is due to their great mechanical strength and resistance in conjunction with low friction and wear coefficients.[33] For these properties, they are also largely used in dentistry, for crown and bridge. In the clinic, bioactive calcium phosphate ceramics, such as hydroxyapatite (HA) and tricalcium phosphate (TCP, $Ca_3(PO_4)_2$), are largely used in bone substitutions. Currently, they are subject of many studies to design and produce materials for tissue engineering applications. The calcium-to-phosphate ratio of these ceramics closely resembles the mineral phase of bone, important for their osteoconductive features. Their surface chemistry is favourable to protein adsorption; moreover, these ceramics exhibit osteoinductive potentials.[34] Other examples are calcium phosphate cements (CPC) for vertebral augmentation of vertebral fractures in children, [35] and octacalcium phosphate (OCP) as good alternative for bone regeneration, in fact OCP is a biological precursor of bone apatite crystals and it is able to enhance bone formation if compared to HA or TCP, driving osteogenic differentiation of mesenchymal stem cells (MSCs).[36] The introduction of bioactive glasses (Bioglasses) was made by Hench in the 1970s.[37] They can be produced either by melt or sol–gel processing. They have been widely used as bone void fillers in clinical settings. Bioactive glasses are mainly composed of sodium, calcium,

silicon and phosphorous oxides in different proportions; their bioactivity is due to the presence of a hydrated silicate-rich layer, which forms when is in contact with human fluids. This layer has catalytic effects on the deposition of HA, which subsequently leads to a stable bond between glass and bone. These bioglasses show a higher osteogenic potential when compared to HA alone. Different studies could show that bioactive glass scaffolds completely dissolve within 6 months.[38] However, the brittleness and low fracture toughness of bioglasses impede their application for load-bearing applications.

1.1.3 Polymers

- Synthetic polymers: polymethylmetacrylate (PMMA), silicone rubber, polyethylene (PE), acrylic resins, polyurethanes or polypropylene are examples of biostable synthetic polymers. Acrylic bone cements have been used in orthopedic and dental surgery for many decades to attach metal or plastic components, but their use does not allow any biological fixation. Disadvantages are the considerable exothermic reaction and the toxicity of residual monomers. Polyethylene, and recently introduced highly cross-linked polyethylene (HXLPE) are available materials for acetabular liners or knee implants having a low friction rate and high impact strength.[39] Polyglycolic acid (PGA), polylactide (PLA) and polydioxanone

(PDS) have been used as resorbable bone fixation devices or suture materials. The mechanical properties of these materials can be increased by self-reinforcing processes; the polymer matrix is strengthened by oriented fibers of the same material. New scaffolds composed of bioactive polymers aim to mimic some aspects of the native ECM while displaying suitable degradability. Synthetic polymers, such as poly(α-hydroxyesters), PGA, and their copolymers poly(lactic-co-glycolic acid) (PLGA) and poly-ε-caprolactone (PCL) are widely used; they were granted FDA approval for different applications in humans.[40]

- Natural polymers: alternatively to synthetic polymers, polymers isolated from ECMs of natural materials with or without additional modifications have been used. To reduced potential pathogen contamination and, by this, disease transmission, detailed purification protocols need to be followed. Collagen is one of the mainly used natural polymers in different clinical applications; it is found in connective tissues such as ligaments, tendons, cartilage, bone, and skin.[41] Collagen can be obtained in form of sponges, 2D-films, nanofibrous non-woven meshes, fleeces or hydrogels. By cross-linking collagen with chemical agents (for examples, glutharaldheyde or EDC) or physical stimuli, the mechanical properties and stability of these scaffolds can be enhanced.[42]

Collagen-based biomaterials are naturally degraded by matrix metalloproteinases (MMPs) and serine proteases, which allow cell-mediated degradation. Gelatin is derived from denaturation of collagen in either acid or alkaline conditions giving charged polyelectrolytes, in particular types A and B gelatin. This denaturation step leads to gelatin characterized by lower antigenicity when compared to collagen. One of the major problems of gelatin is that at physiological temperature (37°C) it dissolves, so it needs to be cross-linked.[43] Fibrin is a protein matrix, which is produced by polymerization of fibrinogen under the enzymatic action of thrombin. It forms a gel like nano-/micro-fibrillar network, to mediate the blood coagulation process. Fibrin glue (composed of fibrinogen plus thrombin) has been largely used as a tissue adhesive for surgical wound repair.[44] Due to its biomimetic features, fibrin is for instance used as a scaffold material for muscle and cartilage engineering. Glycosaminoglycans (GAGs), found in many connective tissues, are constituents of the native ECM; they regulate the function of various proteins, thus modulating cell adhesion, migration, proliferation and differentiation.[45] GAGs account for tissue hydrodynamics and regulate the viscoelastic properties of cartilage. Their incorporation into collagen scaffolds extensively influences collagen matrix structure.[46] Hyaluronic acid, a non-sulphated

glycosaminoglycan, can be applied as a hydrogel cell carrier by covalent cross-linking with hydrazide derivatives, and, to obtain a more stable design, it can also be associated with other materials. Hyaluronic acid has the property to degrade within a few months with the enzymatic activity of hyaluronidase, which exists ubiquitously in serum and cells.[47] Nowadays, hyaluronan is used into clinical applications as a scaffold material for cartilage, skin, bone and soft tissue substitutes.[48] Chondroitin sulfate (CS) is a sulphated glycosaminoglycan that is found covalently linked to a core protein forming proteoglycans. As hyaluronan, CS is water soluble; cross-linking procedures or the development of hybrid constructs are needed to produce stable scaffolds.[49] Chitosan reveals structural similarity to natural glycosaminoglycans. Due to its biocompatibility, low-toxic and non-antigenic properties, it is another attractive material for tissue engineering applications.[50] Chitosan is produced with N-deacetylation of chitin, the natural polysaccharide that is found in exoskeletons of crustaceans and cell walls of fungi. Chitosan is degraded by *in vivo* action of lysozyme, which is produced by macrophages. Nevertheless, it is generally insoluble in neutral organic solvents, so many derivatives have been developed to increase its *in vivo* solubility and processability.[51] The cationic nature of chitosan leads to an

interaction with anionic molecules such as glycosaminoglycans and proteoglycans, which again can make this polymer an effective carrier for growth factors or cytokines. Chitosan can be used alone or in combination with other materials to form hydrogels, fibers, granules or sponges. Alginate is a polysaccharide polymer obtained from marine brown algae. In aqueous solution, alginates reversibly undergo gelation with divalent cations forming hydrogels.[52] Thus, alginate was applied as a cell or growth factor delivery system,[53] wound dressing or immobilization matrix.[54]

1.2 The "biomimetic" approach in tissue engineering

Tissue development and remodeling *in vivo* is coordinated by a plethora of regulatory factors interacting at multiple levels, in time and space. The use of whole animal models surely provides precise biological properties (at least within given species), but doesn't offer a complete control over the local environment, and limited real-time insight. On the other hand, traditional cell culture allows a good control over the cellular environment and processes, but in this case there is an oversimplified experimental context. In the field of tissue engineering, driving the cells to differentiate in the right manner, at the right time, in the right place, and into the right phenotype, also necessitates an environment that gives the same factors that rule cellular processes *in vivo*.[55]

Biomaterials composed of biologically derived building blocks, such as extracellular matrix (ECM) components (for example collagen and fibronectin), are being studied for a lot of applications in the field of regenerative medicine. In fact, proteins, glycoproteins and proteoglycans, are important models for biomaterials design, providing chemical and physical structures and biochemical properties able to mimic cellular microenvironment (**Figure 1.1**).[56] Like a scaffold that provides the framework for a high-rise building, the extracellular matrix, mechanically supports interactions between cells for healthy tissue generation and preservation. ECM is a dynamic mixture, produced and degraded by cells, in healthy and damaged/diseased tissues. Cell-ECM interactions drive a series of cellular effects, among which there are cell adhesion, migration, proliferation, and differentiation, thus directing cell fate. This dynamic interplay between cells and the ECM has significant effects on cell adhesion, migration, proliferation, and differentiation.[57]

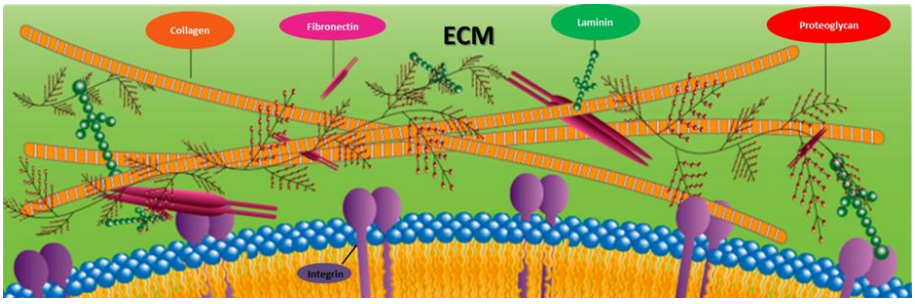

Figure 1.1. An overview of the extracellular matrix (ECM) molecular organization.

Moreover, it is well established that ECM has significant biochemical roles in biological processes such as angiogenesis, wound healing,

and immune cell migration. ECM components, such as glycosaminoglycans and proteoglycans are able to entrap and activate growth factors and other biomolecules in order to induce specific cell response. The well-known RGD (Arginine-Glycine-Aspartic acid) and IKVAV (Isoleucine-Lysine-Valine-Alanine-Valine) sequences, found in fibronectin and laminin respectively, are able to promote cell adhesion. Mimicking the natural ECM network is not an easy task, but with the increase in the knowledge about physicochemical and biochemical cell signaling processes, this approach is now feasible for the design and production of tissue engineering scaffolds. One of the most common properties of biomaterials should satisfy is cell adhesion. Initially, the strategy adopted was coating scaffolds with proteins, such as laminin or fibronectin, that are able to induce cell adhesion and spreading. Subsequently, cell-binding-domains (e. g., RGD, IKVAV) were used to covalently functionalized surface biomaterials, and by modulating their concentration and spacing, scientists were able to direct cell spreading in both 2D and 3D culture systems. Moreover, natural anionic proteoglycans and GAGs are able to interact with growth factors and cytokines, which are positively charged, inducing oligomerization and increased local concentrations. To alter growth factor release, one strategy is to combine heparan sulfate, a proteoglycan, with materials.[58]

Carbohydrates and receptors decorate, among others, the outer membrane of a cell; receptor activation is promoted by interactions with adjacent cells, ligand in the extracellular matrix, and secreted biomolecules. The high abundance in cells of proteins, playing different roles in the cell receptor stimulation, causes a plethora of responses (cell migration, organogenesis, wound repair). Putting together all these factors, a widely defined and specialized cell microenvironment, fundamental for correct tissue development and maintenance, is created.

Different tissues and different stages of development show diversity in ECM composition due to different isoforms, ratios and geometrical disposition of proteins like collagen, proteoglycans, elastin, fibronectins, and laminins.[59] This creates an environment that is replete with informational cues. Moreover, a wealth of molecular mechanisms modulates the dissemination of this information.[60]

1.3 Biomaterial functionalization strategies

Adaptation (or integration) of materials into biomedical devices and biological systems has been of great interest in recent years. Through the modification of existing materials one can control and tailor their properties, and confer them biological properties and functionalities to better allow their integration with biological systems. These modified materials can lead new and unique abilities to a variety of

biomedical applications ranging from implant engineering and regulated drug delivery, to clinical biosensors and diagnostics.[61]

The different applications in tissue regeneration require variable materials properties and functions; biomaterials modification can be lead with different methods, they can be modified and functionalized with different reagents in various ways including physical, chemical and biological techniques. Two things are often achieved by modifying the surface of nanostructured materials: 1) enhanced solubility and stability of nanostructured materials in aqueous media and 2) new material functions and properties.

The surface modification of materials with bioactive molecules is an easy way to fabricate smart materials. Different strategies can be used for the functionalization of materials with biomimetic molecules:

a) physical adsorption (van der Waals, electrostatic, affinity, adsorbed and cross linked);

b) physical entrapment attachment (barrier system, hydrogel, dispersed matrix system);

c) covalent surface immobilization, taking advantage of different natural or unnatural functional groups present both on the biomolecules and on the material surfaces (chemoselective ligation, *via* amino functionalities, heterobifunctional linkers, etc.).

The major methods of immobilizing a bioactive compound to a material surface are: adsorption *via* electrostatic interactions, ligand–

receptor pairing (e.g., biotin–avidin), and covalent attachment (**Figure 1.2**).[30]

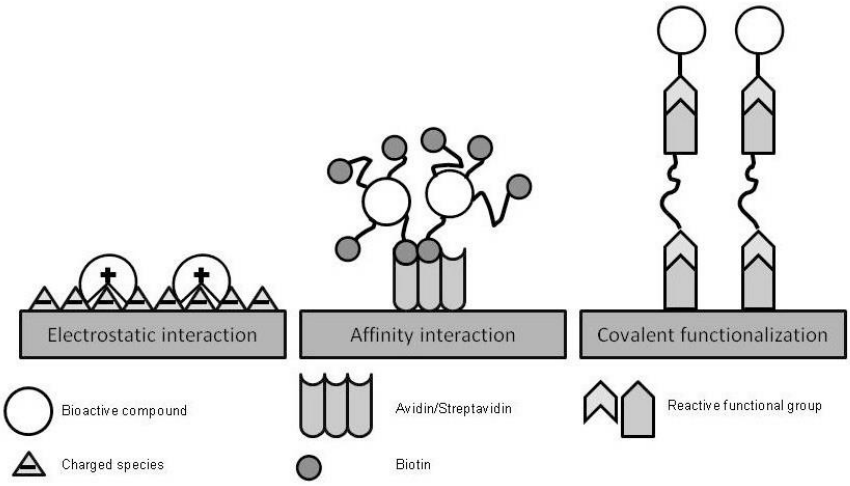

Figure 1.2. Different strategies for the introduction of biomimetic elements into synthetic materials.

Physical methods, such as molecular coating (or adsorption), surface entrapment, and physical treating with plasma, ozone, or UV have emerged as leading strategies for surface modifications of nanostructured materials. Through physical modifications, functional molecules, varying charges, or active chemical groups can be introduced on the surfaces of materials, leading to the functionalization and activation. The evident advantages of physical modifications are the simplicity in handling and mild interactions with biomolecules through little or null damage to their bioactivities. These methods, however, also show certain limitations, among which there are physical linkages, often formed between the substrates and coatings. These physical linkages and interactions are considered to

be weak if compared to chemical bonds. Moreover, functional molecules and entities may detach from the surfaces of modified materials, particularly when certain serum components compete for active binding sites in physiological conditions. Non-covalent adsorption is sometimes desirable, as in some drug delivery applications.[62] Covalent immobilizations offer several advantages by producing the most stable bond between the compound and the functionalized surface. A covalent immobilization can be used to extend the half-life of a biomolecule, prevent its metabolism, or allow continued bioactivity of indwelling devices.[63] Bioactive molecules (growth factors, ECM proteins, etc.) that are free in solution, may influence significantly different biological responses. Growth factors are regularly added to cultures *in vitro*, and have been incorporated and released from polymeric systems with retention of bioactivity, as shown for neurotrophins, BMPs, and VEGF.[64] *In vivo*, these soluble factors can be released from the delivery site, and one of the most important parameters is the duration over which therapeutic concentrations can be maintained. Otherwise, bioactive molecules can be covalently linked to the biomaterial, eventually in a reversible way or exploiting a degradable linking tether. For growth factor immobilization to fibrin, cell migration results in cell-activated plasmin degradation that can catalyze release of the factor. These scaffolds have been termed ‘‘cell-responsive’’[65] being characterized to release of the factor upon

cellular demand. These soluble factors can be released and then can bind their receptors and initiate a signaling cascade. Differently, immobilized biomolecules can interact with their receptors directly from the material surface; however, this type of interaction may not correctly replicate the signaling of soluble factors, as growth factor internalization can stimulate signaling pathways that are different from those activated at the surface. For example, neuronal growth factor NGF induces neurite outgrowth by signaling at the plasma membrane, yet promotes neuron survival when internalized.[66] Surface immobilization has been successfully used to attach several factors such as EGF,[67] BMP-7,[68] BMP-2,[69] VEGF,[70] NGF,[71] and NT-3[72] to a variety of natural and synthetic biomaterials. Signaling by these immobilized or locally released bioactive ligands may be more potent than signaling by soluble versions that are free added directly to culture media.[73] These studies also show that the immobilization strategy has to consider protein structure and active region topology, when designing adequate delivery systems in order to optimize and maximize bioactivity. Finally, some factors may be better delivered in a continuous manner, while others take advantage from direct attachment to the biomaterial surface.[74] Different methods have been developed for covalent functionalization of biomolecules to diverse biomaterials. For covalent functionalization to an inert solid polymer, the surface firstly has to be chemically modified to provide reactive groups (-OH, -NH_2, COOH, -SH) for a second functionalization

step. When the material does not contain reactive groups, they can be introduced by chemical and physical modification, on the polymer surfaces in order to allow covalent attachment of biomolecules. With this ambition, a wide number of surface modification techniques have been developed, including plasma, ionic radiation graft polymerization, photochemical grafting, chemical modification and chemical derivatization. For example peptides can react *via* the N-terminus with different functional groups on polymers (**Figure 1.3**). This is usually done with reactions that bring to the activation of carboxylic acid group with the nucleophilic N-terminus of peptides. Carboxylic groups can be activated with different coupling reagent, e.g. 1-ethyl-3-(3-dimethylaminopropyl)-carbodiimide (EDC, also referred to as water soluble carbodiimide, WSC), dicyclohexyl-carbodiimide (DCC) or carbonyl diimidazole (CDI).

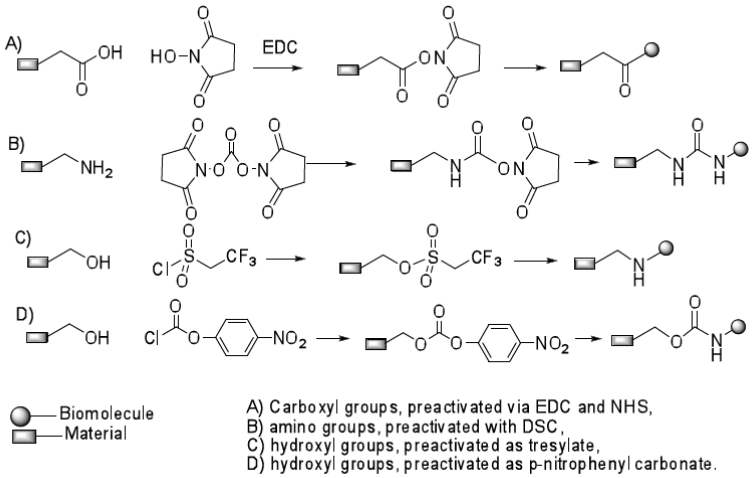

Figure 1.3. Coupling methods to different groups on materials.

Chemoselective ligation is a relatively new approach (**Figure 1.4**), where selected pairs of functional groups are used to form stable bonds without the need of an activating agent and without interfering with other functional groups that are usually encountered in biomolecules. Chemoselective reactions proceed usually under mild conditions and result in good yields.[75]

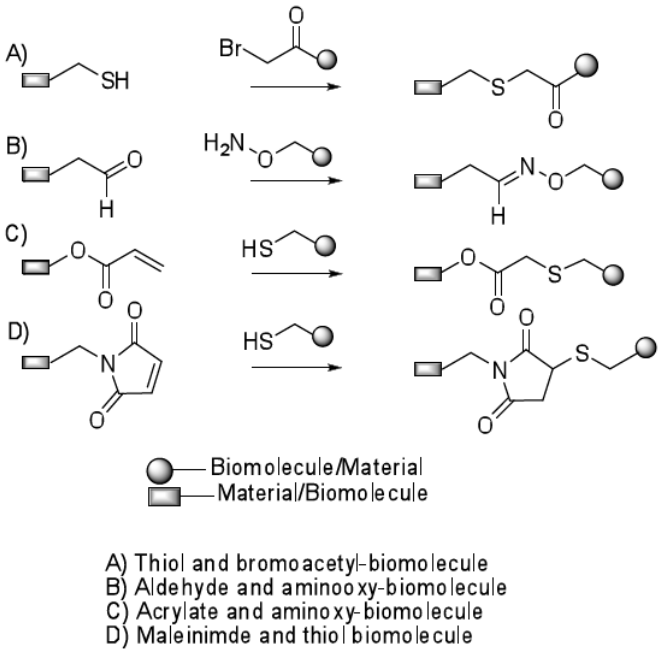

Figure 1.4. Examples of chemoselective strategies.

A biomolecule can also be linked, with these coupling methods, by using a spacer arm, in order to give better access to the specific target receptor. One useful and biocompatible spacer is polyethylene glycol (PEG) that can be differently functionalized at the two

extremities.[76] Metal or ceramic surfaces may also be silanised, exploiting functionalized triethoxysilanes.[77]

1.4 The importance of carbohydrates: a novel strategy to develop smart biomaterials

Carbohydrates are one of four major groups of biologically important macromolecules that can be found in nature in all forms of life. They have a lot of biochemical, structural, and functional features that could provide a series of evolutionary benefits or even stimulate or enhance evolutionary events. During evolution, carbohydrates served as a source of food and energy, provided protection against UV radiation and oxygen free radicals and participated in molecular structure of complex organisms. During time, simple carbohydrates became more complex through the process of polymerization and developed new functions. According to the one origin of life theory, called glycoworld, carbohydrates are thought to be the original molecules of life, which provided molecular basis for the evolution of all living things.[78] Ribose and deoxyribose are integral parts of RNA and DNA molecules and cellulose (glucose polymer) is the most abundant molecule on the planet. There is also evidence for catalytic properties of some carbohydrates[79] that further support theory about the capacity of glycans to enable evolution of life.

Carbohydrates are essential for all forms of life, but the largest diversification of their functions is found in higher eukaryotes. The

majority of eukaryotic proteins are modified by co-translational and post-translational attachment of complex oligosaccharides to produce the most complex epiproteomic modification–protein glycosylation. A lot of different glycans can be made by varying number, order and type of monosaccharide units. The most abundant monosaccharides found in animal glycan are fucose (Fuc), galactose (Gal), glucose (Glu), mannose (Man), *N*-acetylgalactosamine (GalNAc), *N*-acetylglucosamine (GlcNAc), sialic acid (Sia) and xylose (Xyl) (**Figure 1.5**). There are two main ways for protein modification with glycans: *O*-glycosylation and *N*-glycosylation. In *O*-glycosylation, the glycan is bound to the oxygen (O) atom of serine or threonine amino acid in the protein (less frequently hydroxylysine and tyrosine);[80] on the other hand, there is *N*-glycosylation where glycan is bound to the nitrogen atom of asparagine residues.

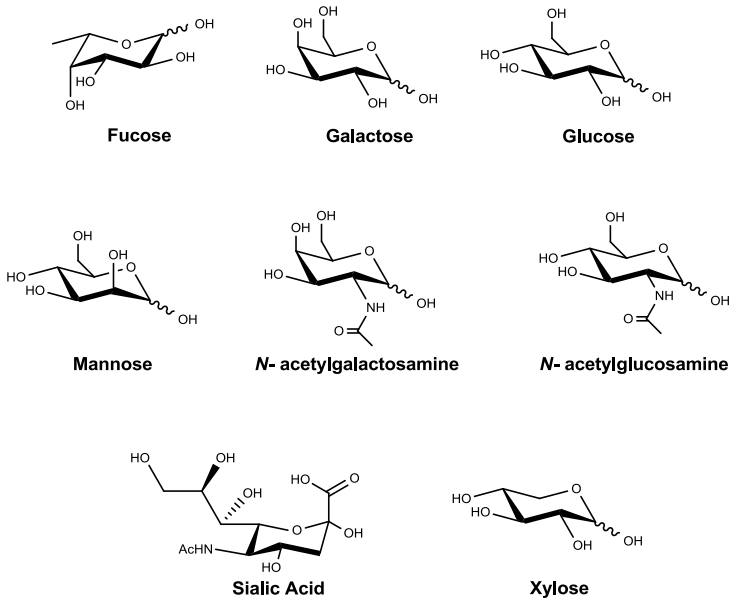

Figure 1.5. Structures of the most abundant monosaccharides found in animal glycan.

Surfaces of all eukaryotic cells are covered with a thick layer of complex glycans attached to proteins or lipids. Many cells in our organism can function without the nuclei, but there is no known living cell that can function without glycans on their surface. Anything approaching the cell, being it a protein, another cell, or a microorganism, has to interact with the cellular glycan coat.[81] One of the critical steps in the evolution of multicellular organisms was formation of extracellular matrix (ECM).[82] Extracellular matrix has huge importance for multicellular organisms. It has role in cell signaling, communication between cells, cell adhesion and in transmitting signal from the environment, and also provides structural support for cells, tissues and organs. Extracellular matrix

plays essential role in numerous fundamental processes such as differentiation, proliferation, survival, and migration of cells. The main components of ECM are glycoproteins and proteoglycans and the same molecules are responsible for functional properties of ECM. Extracellular matrix evolved in parallel with first multicellular organisms; therefore, glycans of the early ECM probably participated in evolution of multicellular organisms by enabling communication between cells and thus provided signals for cooperation and differentiation.[83]

Despite their importance, glycans have not been given as much attention as signaling molecules in biomaterial design for tissue engineering and regenerative medicine applications.

Chapter 2

Aim of the work

The general aim of my PhD project has been focused on the development of innovative biomaterials for regenerative medicine, and in particular on the design of smart biomaterials decorated with specific signalling molecules able to direct and regulate cell proliferation and differentiation. Biomaterials decorated with biomolecules, in particular carbohydrates, are not only able to give a good mechanical support for cell proliferation, but, especially, they are able to influence cell fate. Biomaterials functionalized with different carbohydrate epitopes should be capable of eliciting specific cellular responses and directing cell differentiation, which can be manipulated by altering design parameters. Biomaterials should be non-toxic, non-attractive and nonstimulatory of inflammatory cells, and also non-immunogenic, which would be detrimental. Finally, the scaffolds should provide easy handling under clinical conditions, enabling fixation of the materials into the implant site. New smart biomaterials were designed and synthesized to obtain innovative

scaffolds useful in directing neuronal differentiation, osteogenic and chondrogenic differentiation. Moreover, new biocompatible gelatin-based hydrogels have been produced.

Hence the following proteins have been taken into consideration for the design of smart biomaterials for regenerative medicine:

a) Collagen: the most studied protein of the extracellular matrix (ECM), the major component of skin and bone; it represents approximately 25% of the total dry weight of mammals. Moreover, the use of collagen-based biomaterials, from either acellular matrix or extracted collagen, has a wide range of applications, both *in vivo* and *in vitro*.

b) Elastin: an extracellular matrix protein with the ability to provide elasticity to tissues and organs, already used as biomaterials in different fields of tissue engineering.

c) Gelatin: a protein derived from collagen hydrolysis, good candidate for the production of new hydrogels, useful to give a 3D environment to support cell growth.

Chapter 3

Collagen-based biomaterials

3.1 Introduction

Collagen has been found in all connective tissues, making it one the most studied biomolecules of the extracellular matrix (ECM). This fibrous protein species is the major component of skin and bone and represents approximately 25% of the total dry weight of mammals. To this day, 29 distinct collagen types have been characterized and all exhibit a typical triple helix structure. Collagen types I, II, III, V and XI are known to form collagen fibers. Collagen molecules are composed of three α chains that assemble together due to their molecular structure; every α chain is composed of more than a thousand amino acids based on the sequence -Gly-X-Y-. The presence of glycine is essential at every third amino acid position in order to allow for a tight packaging of the three α chains in the tropocollagen molecule; the X and Y positions are mostly occupied by proline and 4-hydroxyproline. There are more or less twenty-five different α chain conformations, each produced by their unique gene, and their

combination, in sets of three, assembles to form the twenty-nine different types of collagen currently known. The most common are briefly described in **Table 2.1**.

Table 2.1. Collagen types, forms and distribution.

	Type	Molecular formula	Polymerized form	Tissue distribution
Fibril-Forming (fibrillar)	I	$[\alpha1(I)]_2\alpha2(I)$	Fibril	Bone, skin, tendons, ligaments, cornea (represents 90% of total collagen of the human body)
	II	$[\alpha1(II)]_3$	Fibril	Cartilage, invertebrate disc, notochord, vitreous humor in the eye
	III	$[\alpha1(III)]_3$	Fibril	Skin, blood vessels
	V	$[\alpha1(V)]_2\alpha2(V)$ and $[\alpha1(V)]\alpha2(V)\alpha3(V)$	Fibril (assemble with type I)	*Idem* as type I
	XI	$[\alpha1(XI)]\alpha2(XI)\alpha3(XI)$	Fibril (assemble with type II)	*Idem* as type II
Fibril-associated	IX	$[\alpha1(IX)]\alpha2(IX)\ \alpha3(IX)$	Lateral association with type II fibril	Cartilage
	XII	$[\alpha1(XII)]_3$	Lateral association with type I fibril	Tendons, ligaments
Network-forming	IV	$[\alpha1(IV)]_2\ \alpha2(IV)$	Sheet-like network	Basal lamina
	VII	$[\alpha1(VII)]_3$	Anchoring fibrils	Beneath stratified squamous epithelia

Even if many types of collagen have been characterized, only a few types are used to produce collagen-based biomaterials. The most used collagen in the field of tissue-engineering is collagen type I. Fibroblasts are cells that produce the majority of the collagen in

connective tissue. Collagen pro-α chain is synthesized from a unique mRNA within the rough endoplasmic reticulum and is then transferred to the Golgi apparatus of the cell. During this transfer, some prolines and lysines residues are hydroxylated by the lysyl oxydase enzyme. Specific lysines are glycosylated and then pro-α chains self-assemble into procollagen before their encapsulation in excretory vesicles. Following their passage through the plasma membrane, the propeptides are cleaved outside the cell to allow the auto-polymerisation by telopeptides. This step marks the initiation of tropocollagen self-assembly into 10 to 300 nm sized fibril and the agglomeration of fibril into 0.5 to 3 µm collagen fibers (**Figure 3.1**).

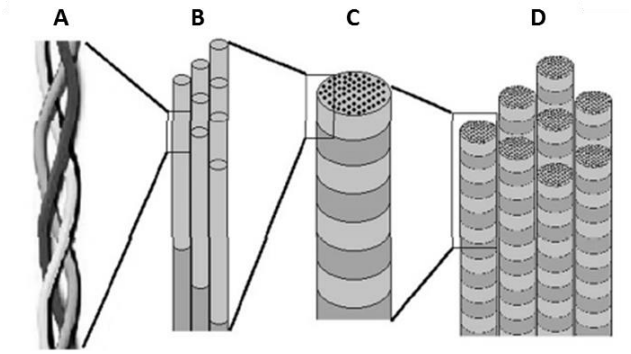

Figure 3.1. (A) Schematization of a collagen α chain triple helix segment. (B) Assembled tropocollagen molecules. (C) Collagen fibril ranging from 10 to 300 nm in diameter. (D) Aggregated collagen fibrils forming a collagen fiber with a diameter ranging from 0.5 to 3 µm.

Collagen is a key structural element in vertebrates. The way that led to complex life form, like human being, counts on three types of interactions. In 1985, Ruoslahti *et al.*[84] affirmed that cells and ECM relate each other by self-aggregation of matrix molecules, interaction

of these aggregated molecules with one another and eventually by their affinity for cell surface to allow cells binding to the ECM as well as proliferation. Cell-matrix interactions consist mainly in the interaction of cells with collagen, directly or indirectly. Direct cell-collagen interactions consist of cell receptors recognition of specific peptide sequence within collagen molecules, and these receptors are divided into four groups: the first group, like glycoprotein VI, is involved in the recognition of peptide sequence containing GPO motif (Gly-Pro-Hyp),[85] the second group concerns of collagen binding receptor members of integrin family and discoidin domain receptor 1 and 2 (DDR1 and DDR2). All these receptors bind to different specific motifs often including the GFO (Gly-Phe-Hyp) sequence.[86] The third group is composed of integrin-types that have the ability to recognize cryptic motifs, within the collagen molecule.[87] Finally, the fourth group consists of cell receptors that directly bind collagen having affinity for the non-collagenous domain of the molecule. The third and fourth groups of collagen binding receptors generally involve other cell-matrix interactions *via* indirect cell-collagen interactions in order to achieve stable adhesion of cell to the extracellular matrix. Fibronectin is one of the most important proteins involved in indirect-collagen interactions; on fibronectin the integrin recognized sequence RGD (Arg-Gly-Asp) was first identified,[88] moreover, other proteins show this RGD or other motifs, binding to collagen, thus allowing indirect cell-collagen interactions. Proteins like decorin and

laminin can bind either collagen or integrin promoting cell adhesion and proliferation.[89] This knowledge about collagen receptors and collagen binding molecules are important in order to do the correct choice of collagen or ECM source to produce collagen-based biomaterials. This is why the treatments used to extract collagen, to decellularized ECM or to sterilized biomaterials are very important. In addition, the molecular architecture of collagen and other correlated proteins in biomaterials are crucial for cell adhesion, migration and, finally, differentiation.

The use of collagen-based biomaterials, from either acellular matrix or extracted collagen, has a wide range of applications, both *in vivo* and *in vitro*. Collagen scaffolds are widely used to study cell behavior such as migration and proliferation, differentiation and phenotype expression. Furthermore, crucial findings about cells behavior in complex environments consider the ability of cells to grow *in vitro* in a 3D tissue-like scaffold.[90] Collagen hydrogels are also appropriate scaffolds when the access to cell membrane is needed, for example in electrophysiological protocols.[91] Collagen-based scaffolds were also used to visualize motor neuron myelinisation by Schwann cells.[92] 3D collagen scaffolds are also useful for cancer research; the invasive feature of cancer cells[93,94] and interaction between cancer cells and other cell types in a 3D environment can be analysed.[95] Moreover, 3D collagen-based biomaterials can be used as a 3D environment to test anticancer drugs.[96] Finally, collagen scaffolds could serve as

anchorage material to cultivate organs *ex vivo*[97] or as 3D models for bone and cartilage diseases like osteoarthritis.[98]

In light of the relevance of collagen, a significant part of my PhD project has been focused on the design, production and functionalization of collagen-based biomaterials in form of 2D films, by using insoluble collagen, and soluble collagen.

The functionalization has been performed with carbohydrates. Glycans are involved in many biological processes: they are used as source of energy or for their purely structural role, they are crucial for the development, growth, function, or survival of an organism. This variety and complexity is not unexpected if we keep in mind their structural diversity. Furthermore, glycans have very strategic locations on the cell surface. The functionalization with carbohydrates has been resulted in a novel approach towards the stimulation of selected cells.

3.2 Collagen films functionalization, characterization and biological evaluation

To study and design collagen based smart materials, we produced collagen films. Collagen Type I from bovine Achilles tendon was used for the preparation of two-dimensional (2D) scaffolds by a solvent casting method. The collagen matrices were produced as thin transparent films (1 mg cm^{-2}, **Figure 3.2**).

Figure 3.2. Photograph acquired by a standard camera of a collagen matrix.

Subsequently, we covalently modified collagen films with saccharidic structures and characterized them for their physico-chemical properties. In particular, we adopted three different strategies for the functionalization step: the first one has been the reductive amination that was achieved by reacting free lysine side-chain amino groups of the collagen with sugars in the presence of a reducing agent; the second one has involved a reaction with thiolated sugars and opportunely modified collagens. Finally, thiol groups were introduced on collagen matrices to allow a thiol–ene reaction between thiolated collagen with allyl α-glucopyranoside and allyl β-galactopyranoside. In particular, we have selected the following sugars for collagen functionalization: glucose, galactose, fucose, sialic acid and chondroitin sulfate.

3.2.1 Collagen functionalization *via* reductive amination

Collagen functionalization and characterization

The strategy of reductive amination on lysine residues was applied for collagen functionalization with different sugars; in fact, lysines

bear a primary amine moiety and, although their side chains are protonated under physiological pH, they can react as nucleophiles. Disaccharides maltose, lactose and cellobiose (in order to expose α-glucose, β-glucose, and galactose), trisaccharides 3'-sialyllactose and 6'-sialyllactose (in order to expose sialic acid) and the sulfated glycosaminoglycan chondroitin sulfate have been chosen. The choise of galactose is due to its presence in the monosaccharide motifs found in collagen glycosylation patterns, being it one of the most commonly found saccharidic residues. Collagen hydroxylysines can be further modified by the addition of the disaccharide Glc(α1-2)Gal(β1-*O*). The choice of sialic acid has been inspired by the bone sialoprotein (BSP); it is a component of mineralized tissues such as bone, dentin, cementum and calcified cartilage. BSP is a significant component of the bone extracellular matrix and has been suggested to constitute approximately 8% of all non-collagenous proteins found in bone and cementum. BSP, originally isolated from bovine cortical bone as a 23-kDa glycopeptide, is a protein with high sialic acid content.[99]

About chondroitin sulfate, the synthesis of a mechano responsive molecule, named collaggrecan, with molecular features borrowed from the natural aggrecan molecule has been achieved. The molecule has tuned molecular features to mimic the original brush-like molecular structure of the native aggrecan, the predominant proteoglycan found in cartilage extracellular matrix, difficult to

replicate synthetically due to its complex architecture. The lack of efficient treatment strategies for cartilage defects has motivated attempts to engineer cartilage constructs *in vitro*. However, none of the current strategies has generated long lasting hyaline cartilage replacement tissue that meets the functional demands placed upon this tissue *in vivo*.[100] The result is typically a suboptimal repair: the biochemical and mechanical properties of the regenerated cartilage do not match those of the native cartilage. The reason is that the astonishing behaviour of this tissue resides in the molecular features of the cartilage ECM. A possible solution to increase both the biochemical and the mechanical properties of new generation constructs would be the use of aggrecan itself or, and this has been our strategy, the synthesis of new biomimetic substituents of the aggrecan with simplified but effective and optimized molecular features. For collagen functionalization, we have used high molecular weight chondroitin sulfate, but also chodroitin sulfate with lower molecular weight (with 4, 8, and 16 saccharide units). Data showed later, concern collagen functionalized with high molecular weight chondroitin sulfate.

The reductive amination, in all cases, has been performed in aqueous solution (citrate buffer pH 6.00) in the presence of the reducing agent $NaCNBH_3$, producing a covalent stable neoglycosylation; collagen exposing α-glucose (**3.1**), β-glucose (**3.2**), galactose (**3.3**), sialic acid (**3.4** linked at position 3 and **3.5** linked at position 6 of the galactose

unit), and chondroitin sulfate (collaggrecan, **3.6**) have been obtained (**Figure 3.3**).

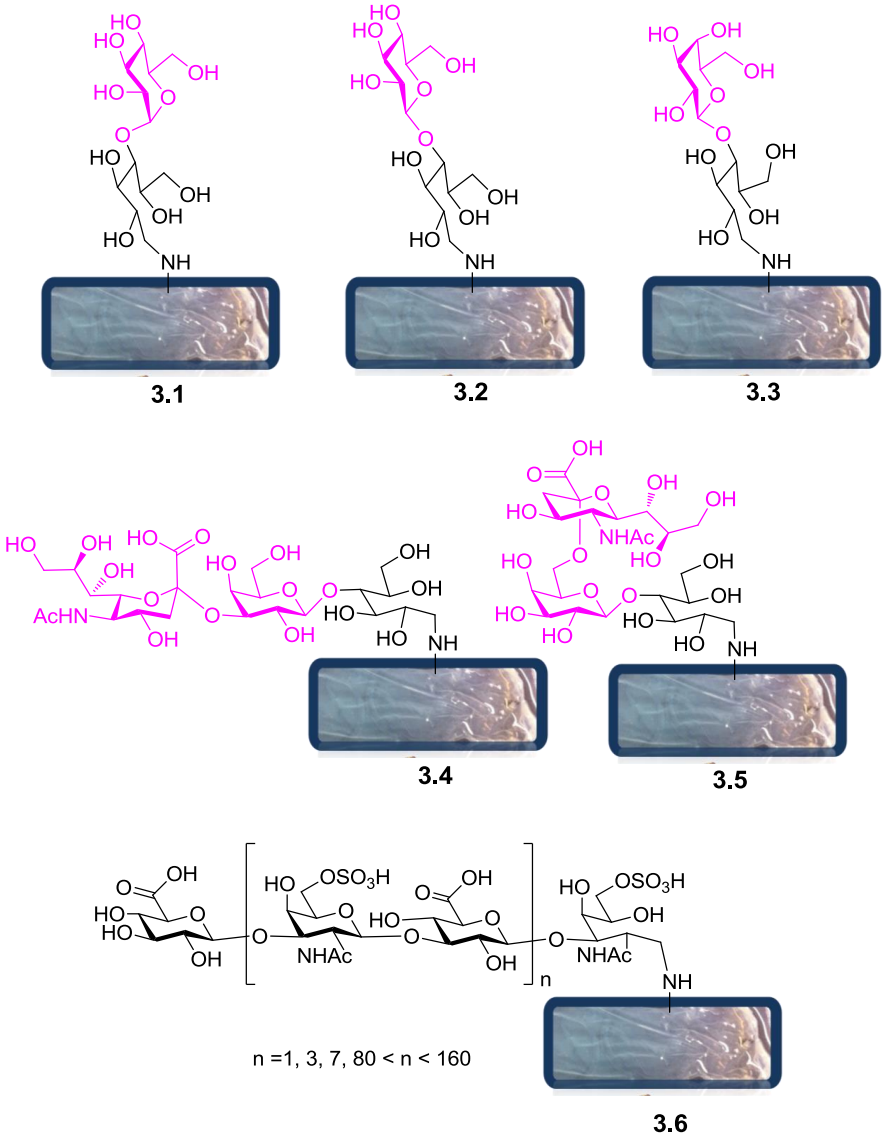

Figure 3.3. Schematic representation of functionalized collagen films.

To evaluate if the chemical process had any damaging effect on supramolecular structure of neoglycosylated collagens, we have characterized pristine and functionalized collagen matrices by Fourier transform infrared (FTIR) spectroscopy in attenuated total reflection (ATR) mode. In **figure 3.4** FTIR absorption spectra of pristine and neoglucosylated collagen **3.1** are shown. Intact collagen matrices displayed almost superimposable IR spectra also in the amide I band, which is due to the C=O stretching vibrations of the peptide bond, so the maintenance of the overall protein secondary structures is not altered after sample treatments. The analyses of the external layers of the collagen matrix proved the success of the neoglycosylation reaction as showed by the raising of the carbohydrate marker bands,[101,102] in the 1200-900 cm^{-1} region, only in the case of the functionalized sample. The spectrum of collagen functionalized with galactose moieties (collagen **3.3**) resulted almost superimposable to that of collagen functionalized with glucose (data not shown).

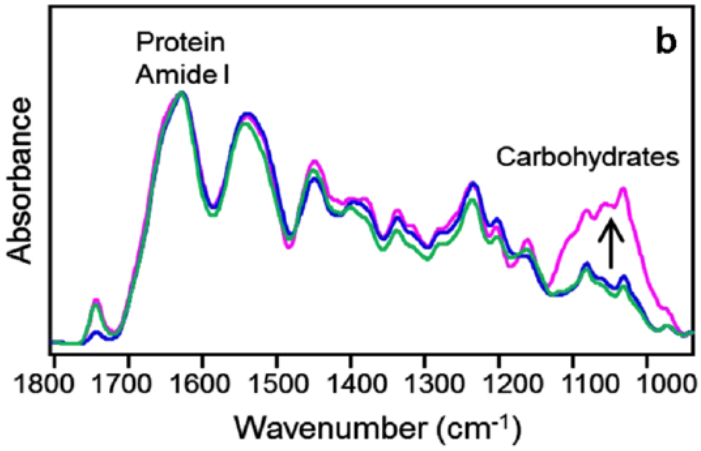

Figure 3.4. FTIR absorption spectra of intact pristine (green line) and neoglycosylated (blue line) collagen and external layers (pink line) of the neoglycosylated collagen sample.

The FTIR spectrum of collaggrecan **3.6**, is characterized by the absorption contributions of collagen and of chondroitin sulfate. In particular, the ~1225 cm^{-1} and the 1100-950 cm^{-1} bands, respectively assigned mainly to the S=O and the C-O vibrations of chondroitin sulfate, are present with a very high intensity. This result clearly demonstrated the success of the functionalization. The absorption spectra of the pristine collagen and of collaggrecan films are reported in **Figure 3.5**. The amide I band of collaggrecan is very similar to that of pristine collagen, indicating that the neoglycosylation does not induce major changes on the overall protein secondary structures. Indeed this band, mainly due to the CO stretching vibrations of the peptide bonds, is particularly sensitive to the protein backbone conformation. In comparison with the pristine collagen, the

collaggrecan spectrum is characterized by a higher absorption around 1225 cm^{-1} and in the 1100-950 cm^{-1} region, where the main absorption components of chondroitin sulfate occur (inset of **Figure 3.5**). These bands are more evident after subtraction of the collagen spectrum to that of collaggrecan, confirming the successful linkage of chondroitin sulfate to the collagen backbone.

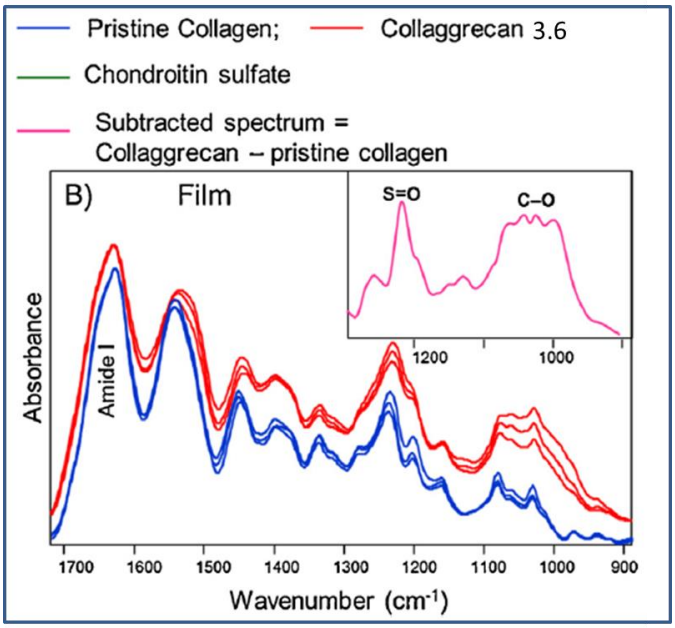

Figure 3.5. FTIR absorption spectra of pristine collagen and collaggrecan 3.6. For each sample three FTIR spectra were reported. The result of the subtraction of the control collagen spectrum to that of the collaggrecan is given in the inset.

FTIR absorption spectra of collagen functionalized with 3'-sialyllactose and 6'-sialyllactose, resulted almost superimposable to the spectrum of pristine collagen; this result indicates that the functionalization with these sugars is too low to be detectable with

this kind of analysis; to quantify collagen **3.4** and **3.5** functionalization we used ^{1}H NMR, reacting free amino groups of collagen with maleic anhydride, and resulted 6 nmol/cm^2. In the same way, we quantified collagen **3.1** and **3.2**; in this case NMR results have shown that roughly 20 nmol of saccharide/cm^2 have been added by reductive amination.

Moreover, we have done a morphological evaluation of collagen matrices structure by AFM analysis. Small fragments of collagen scaffolds were mounted on appropriate stubs and observed with a Digital Instruments MultiMode Scanning Probe Microscope with a Nanoscope IIIa controller and a phase Extender, fitted with Nanosensors TESP silicon probes (k ≈ 42 N m−1 and f ≈ 300 kHz). All images were taken in Tapping- Mode AFM at 512 × 512 pixel with a fast axis scan speed of 1.5 − 2 Hz. Pristine collagen scaffold (**Figure 3.6A**) exhibited a mottled, finely granular surface interspersed with occasional fibrous structures. Collagen matrices functionalized with glucose and galactose moieities (**3.1** and **3.3**) show a greater tendency to form ordered structures, more evident in the case of collagen **3.3**, and their patch shows short cross-banded segments randomly oriented, which are similar to short stretches of natural fibrils. We have also seen a longitudinal striation, corresponding to the layout of the molecules, within the banded segments (**Figure 3.6B-C**). This is a precise indication that the neoglycosylation process

does not modify the size and the shape of the collagen molecules, steel having the ability to create ordered banded structures.

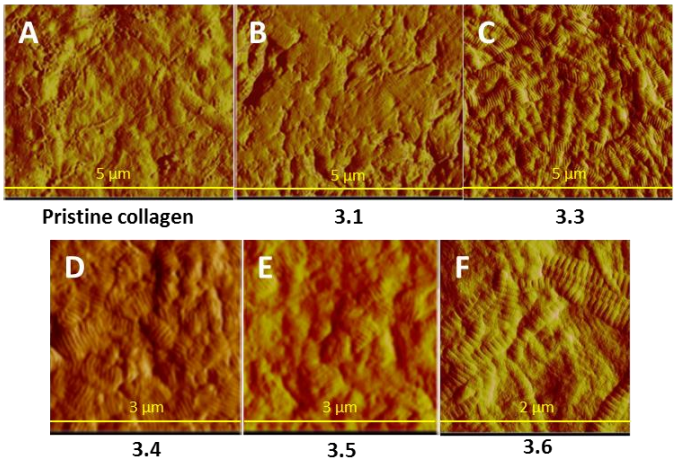

Figure 3.6. Atomic force micrographs of pristine and neoglycosylated collagen films.

In the case of collagen **3.4** and **3.5**, we observed that the surface of both specimens was mostly represented by numerous, randomly oriented tactoids, a few micron long and up to 500 nm wide, with the distinctive 67 nm cross-banding of collagen (**Figure 3.6D-E**). The space among the tactoids was occupied by a finely grainy, featureless surface. No significant differences were found between the 3'-sialyllactose (**3.4**) or the 6'-sialyllactose collagen (**3.5**). Finally, the collaggrecan (**3.6**) appeared composed of sparse, regularly banded collagen fibrils having heterogeneous diameter and random orientation dispersed into a finely textured, unstructured filamentous matrix (**Figure 3.6F**).

In order to assess if the exposed glucose moieties in collagen **3.1** could also exploit their biological signaling functions upon recognition

of its complementary receptor, we executed enzyme linked lectin assays (ELLAs)[103] on the neoglucosylated collagen matrices (**Figure 3.7**). We have used commercially available peroxidase-conjugated lectins for the recognition of the surface-bound carbohydrate; concanavalin-A (ConA) has been chosen having the ability to recognize α-glucosides, while peanut agglutinin (PNA) recognizing β-galactosides has been selected as negative control. In **figure 3.7** data show the effective recognition of exposed α-glucoside by its complementary lectin. The observed absorbance values clearly indicate the presence, but also the correct exposition, of the glucose residues on protein surfaces.

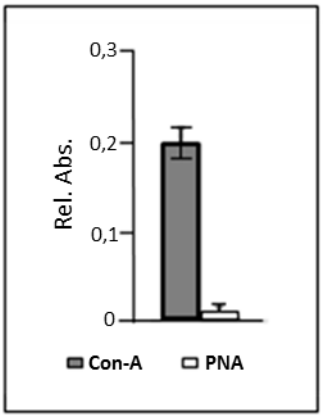

Figure 3.7. ELLA assays on collagen 3.1 from three independent experiments.

Moreover, the copper phthalocyanin Cupromeronic Blue has been used to characterize collagen **3.6**. Cupromeronic Blue is an intense blue cationic dye developed specifically for electron microscopic localization and characterization of proteoglycans and sulfated

glucosaminoglycans (dermatan, keratan and chrondroitin sulfates) and hyaluronan (hyaluronic acid). It acts like intercalating dyes but its unique steric hindrance, due to methyl group placement, prevents the dye from intercalating into the stacked base pairs. This dye precipitates onto collagen filaments turning them into thick cylinders (**Figure 3.8A**), confirming their glycosaminoglycan nature. Even at the unaided eye the reaction to Cupromeronic Blue is unequivocal, and clearly differentiates the collaggrecan-covered films from the pure collagen controls (**Figure 3.8B**).

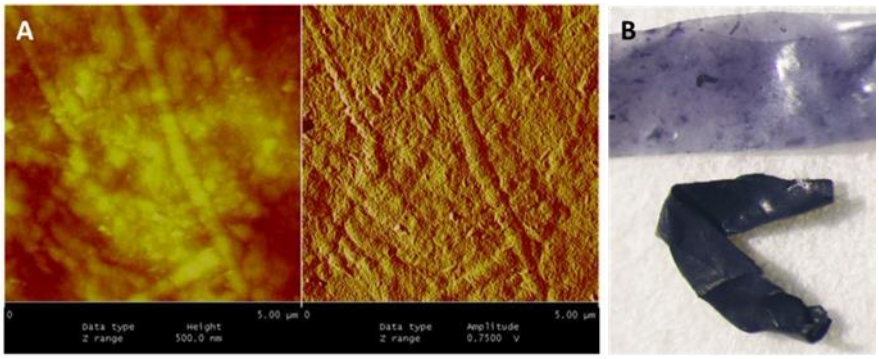

Figure 3.8. (A) Treatment with 0.05% Cupromeronic Blue leaves the surface covered with thick precipitates, betraying the presence of surface-bound glycosaminoglycans. (B) A fragment of collagen film 3.6 functionalized with chondroitin sulfate (below) reacts strongly with Cupromeronic Blue, while a control film exposed to the same reaction just shows occasional specks corresponding to local impurities.

The decoration with sugars has been conducted not only on collagen films, but also on hydrolyzed collagen, therefore soluble. Unlike collagen films that are insoluble and can be used as 2D-supports for cell growth or could be implanted in a body, soluble collagen could

be an efficient candidate as injectable biomaterial to repair, for example, damaged tissues.

As in the case of insoluble collagen, we functionalized soluble collagen *via* reductive amination; the purification step has considered the use of dialysis tubing (MWCO 14000 Da) to eliminate all unreacted reagents (sugar excess and $NaBH_3CN$). Selected carbohydrates are maltose, 3'-sialyllactose, 6'-sialyllactose, and chondroitin sulfate. In order to evaluate if all unreacted sugars were eliminated during the purification step, the reaction has been conducted also in absence of the reducing agent, and then purified as just described. This new biomaterials have been characterized by Fourier transform infrared (FTIR) spectroscopy. In **figure 3.9** the spectra of soluble collagen neoglycosylated with maltose (collagen **3.7**), 3'-sialyllactose (collagen **3.8**), and 6'-sialyllactose (**3.9**) are shown. The raising of the carbohydrate marker bands, in the 1200-900 cm^{-1} region, is visible only in the case of the functionalized samples (in presence of $NaBH_3CN$). In the case of collagen reacted in absence of the reducing agent the resulting spectrum is superimposed on the spectrum of pristine collagen.

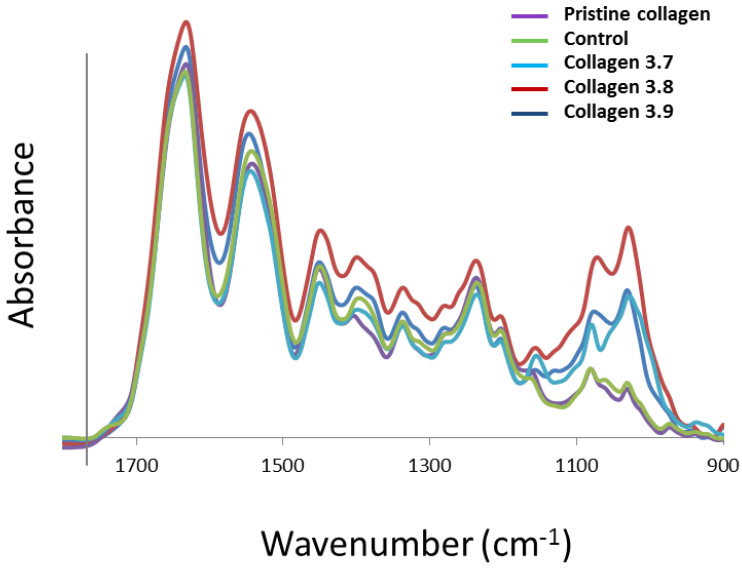

Figure 3.9. FTIR absorption spectra of pristine collagen (violet line), neoglycosylated collagens (light blue line - collagen 3.7 functionalized with maltose; red line - collagen 3.8 functionalized with 3'-sialyllactose; blue line- collagen 3.9 functionalized with 6'-sialyllactose) and collagen reacted with sugar in absence of $NaBH_3CN$ (green line).

The FTIR spectrum of soluble collaggrecan **3.10** is characterized by the absorption contributions of collagen and of chondroitin sulfate, as in the case of collagen film **3.6**. The FTIR results indicate that the extent of functionalization is higher for the collagen in soluble form (**3.10**) compared to the film **3.6**, as expected (**Figure 3.10**).

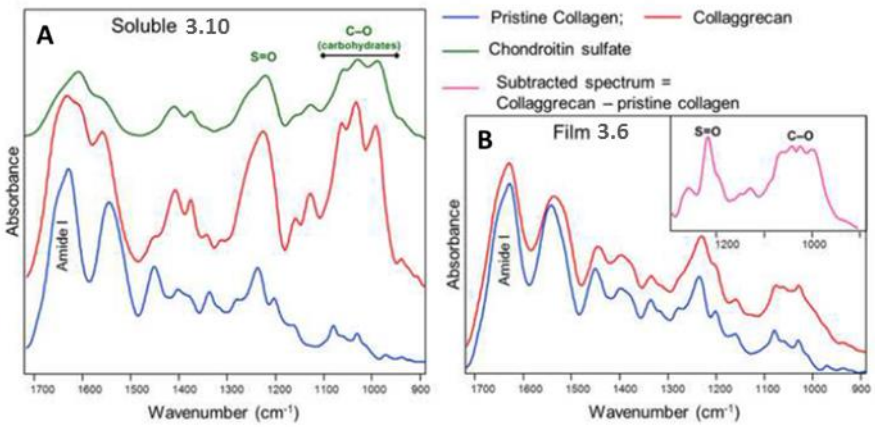

Figure 3.10. FTIR absorption spectra of pristine collagen and of collaggrecan. (A) The spectra of the soluble samples (3.10) are given after normalization at the Amide I band intensity. The spectrum of chondroitin sulfate is also reported. (B) Spectra of pristine collagen and of collaggrecan in form of film (3.6) presented as in A. The result of the subtraction of the control collagen spectrum to that of the collaggrecan is given in the inset.

Morphological analysis of soluble collaggrecan **3.10** has been performed. During AFM analysis, the collaggrecan suspension adheres to mica forming a dense, regular monolayer of molecules (**Figure 3.11A**). At higher magnification (**Figure 3.11B**) we can see that each collagen molecule shows a few ill-defined, slender side chains: these are more clearly detectable at their insertion on the collagen molecule, where they produce a sort of caterpillar figure.

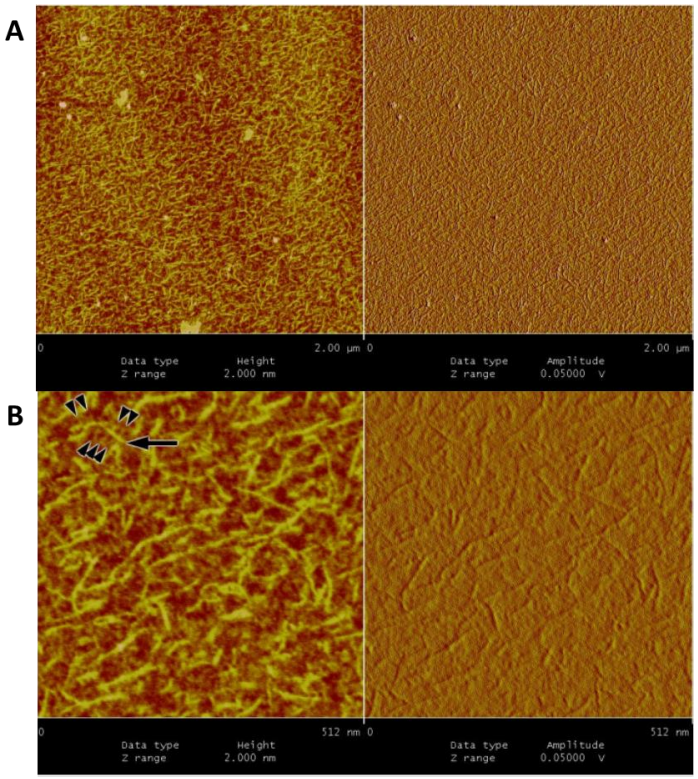

Figure 3.11. (A) Atomic force micrograph of collaggrecan molecules 3.10 adsorbed to mica. The molecules form an uniform monolayer on the substrate. (B) A higher magnification of the same specimen reveals the single molecules. A collagen molecule (indicated by the arrow) is covalently bound to several, barely visible chondroitin sulfate side chains (arrowheads) approximately orthogonal to the collagen axis.

3.2.2 Biological assays

3.2.2.1 Response of osteoblast-like MG63 on neogalactosylated collagen matrices

Given the relevance of collagen glycosylation and the predominant role of collagens in skeletal tissues, it seemed worthwhile to evaluate the interaction of chemically modified collagen matrices with galactose moieties with MG63 cells, an osteosarcoma-derived line that partially mimics the characteristics of human osteoblasts. For

these cells collagen-soaked surfaces relevantly implemented cell adhesion.[104] Moreover MG63 cells were shown to modify their metabolism and gene expression pattern according to the topography of their substrates,[105,106] ultimately affecting attachment and proliferation.

A rapid and extended colonization of all available surfaces and volumes of a suitable substrate by progenitor cells should be a prerequisite to maximize the regenerative effects of a cell loaded scaffold within a lesion site. In this respect, matrices able to drive and sustain a large proliferative burst may be beneficial, provided that they do not negatively influence the differentiation potential of the cells. For bone tissue engineering it is also relevant to note that proper glycosylation of collagen I is a prerequisite for the development of a suitable vessel network: angiogenesis does not occur if endothelial cells are grown on substrates derived from de-glycosylated collagen matrices or derived from normal fibroblasts. In contrast it becomes markedly sustained in over-glycosylated collagen I matrices derived from Osteogenesis imperfecta mutated fibroblasts.[107] Thus, a substrate providing such a pro-angiogenic signal may indeed be advantageous. Given these premises, the biological assays with the human osteosarcoma MG63 cell line were performed to determine if glycosylated matrices exerted any direct effect on the attachment and proliferation of this osteoblast-like cell line. Indeed, on over 20 independent experiments on native and

neoglycosylated collagen as cell culture platforms (for a total of 40), we did not notice any statistical variation in the number of adhered cells after seeding. However, the proliferation rates of the attached cells were quite different on the two collagen matrices. As shown in **figure 3.12A**, cells grown on plastic or on glycosylated collagen performed 3.8–4.0 doublings within the experimental timing (cell duplication time: 42 h), while cells grown on native collagen performed less than 3.0 doublings (cell duplication time: 58 h). These results are in agreement with the images of the cell-seeded matrices acquired at the end of the experimental timings (**Figure 3.12B**).

As a whole, the presented results evidenced that the neoglycosylated collagen can be recognized as a preferential substrate for the growth of cells of the skeletal system. Prospectively, this chemical modification could be used to implement cell colonization of collagen-based scaffolds for tissue engineering approaches.

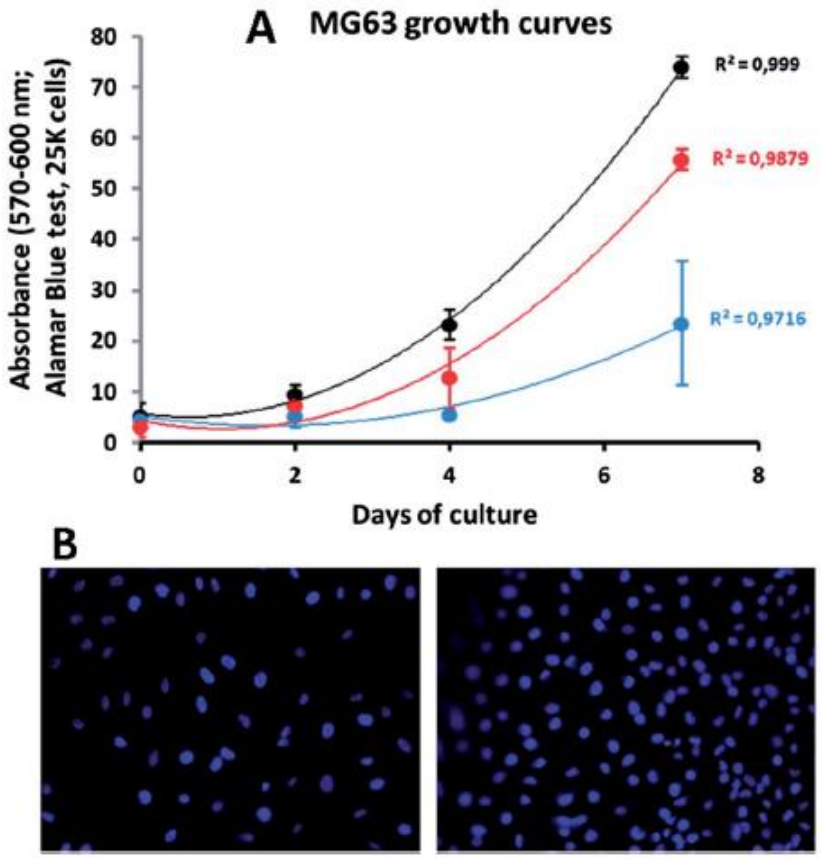

Figure 3.12. (A) MG63 growth rate on native and neoglycosylated collagen: (●) standard plastic; (●) control collagen; (●) glycosylated collagen 3.3; (—) best-fit standard plastic; (—) best-fit control collagen; (—) best-fit glycosylated collagen. Data points depict mean values ± SD of 6 independent determinations. (B) Fluorescence images of DAPI-stained MG63 nuclei after cells were grown for 7 days onto native or neoglycosylated collagen matrices 3.3, the left and right panel, respectively (images are representative of five different visual fields acquired for each substratum; 20x enlargements).

3.2.2.2 Effects of neoglycosylated collagen matrices on neuroblastoma F11 cell line

In the nervous system, post-translational glycosylation has important roles in neurite outgrowth and in fasciculation, in synapse formation

and modulation[108,109,110,111] in the developing and mature nervous system.[112,113,8] Additionally, the research of nature-mimicking cues with the ability to enhance the efficiency of synaptic connections is very significative in biomaterial design for nervous system regeneration.[114] Collagen is usually glycosylated with α-(1→2)-D-glucosyl-β-D-galactosides linked to hydroxylysine residues; glucose is added as the last residue and most propably has specific biological responses. In the light of this, we decided to examine the possible role of collagen neoglucosylation on neuronal differentiation.

We prepared collagen matrices decorated with different sugars at their surface in order to investigate neuroblastoma F11 cell line behavior on grafted sugars. In particular, collagen matrices **3.1**, **3.2**, **3.3**, **3.4**, and **3.5** were used as 2D supports for F11 cells growth. Most promising results were obtained with collagen **3.1**, functionalized with glucose moieties. These data will be discussed in detail in this paragraph. At the end of the paragraph, data obtained with all other collagen matrices, will be briefly discussed.

Effects of collagen functionalized with glucose moieties (**3.1**) on F11 cells

We compare the behavior of neuroblastoma F11 cells[115] plated on pristine and neoglucosylated collagen **3.1** with cells seeded on common Petri dishes. We first noticed that both native and neoglucosylated collagen did not have any negative effect on cell

viability. In this way we demonstrated that the neoglycosylation did not alter the biocompatibility of the matrices.

After 7 days, we performed morphological and functional analysis of cells seeded in the three conditions. Images at the confocal microscope have shown a significantly higher frequency of cells with neuritic-like processes when plated on neoglucosylated collagen **3.1** if compared to pristine collagen and Petri dishes (**Figure 3.13A-B**). Immunofluorescent staining with antibodies to the late neuronal marker β-tubulin confirmed that cells seeded for 7 days on neoglucosylated collagen were mature neurons (**Figure 3.13C**).

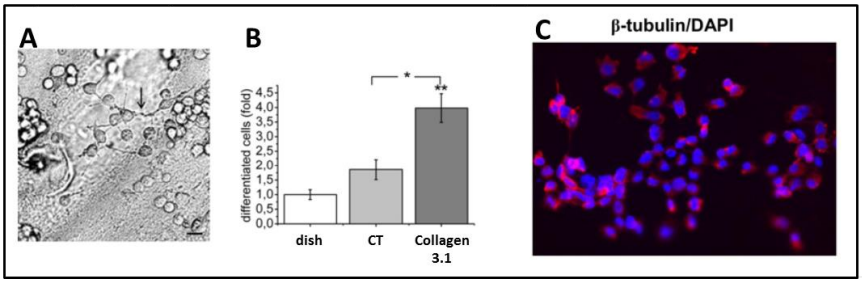

Figure 3.13. Morphological and electrophysiological properties of F11 cells maintained for 7 days on Petri dishes (dish), on pristine collagen (CT), and on neoglycosylated collagen 3.1. (A) Transmission image of F11 cells grown on neoglycosylated collagen: neuritic-like processes are indicated with an arrow; scale bar 30 µm. (B) Differentiated cell numbers, expressed in fold, relative to cells on Petri dishes. A significant difference was observed in cells plated on collagen 3.1 versus cells plated on Petri dishes (p < 0.01) and versus cells plated on pristine collagen (*p < 0.05). (C) Immunofluorescence of F11 grown on neoglucosylated collagen: β tubulin III antibody indentified neurons (red) and DAPI evidenced nuclei (blue).**

Neurite outgrowth could be a morphologic exhibition of differentiation.[116,117] For that reason, we decided to verify the acquisition of specialized neuronal properties by functional analysis investigating the electrophysiological properties of cells by the patch-

clamp technique in the whole-cell configuration. Voltage protocols were applied to measure sodium (I_{Na}) and potassium (I_K) current amplitudes and to compare current densities (**Figure 3.14A**). Na^+ current densities exhibited the tendency to increase from Petri dishes (47.3 ± 18.8 pA/pF, *n* = 15), to collagen (81.4 ± 21.8 pA/pF, *n* = 12) and to neoglucosylated collagen (91.5 ± 13.9 pA/pF, *n* = 17); additionally, a substantial higher mean I_K density was calculated for cells plated on neoglycosylated collagen (74.6 ± 7.4 pA/pF) if compared to both Petri dishes (41.1 ± 6.3 pA/pF) and untreated collagen (47.7 ± 7.3 pA/pF). Current recordings in voltage-clamp mode indicated that collagen matrices promoted the expression of sodium and/or potassium channels in cell membranes and this was clearer for the neoglucosylated matrices.

Switching the system to the current-clamp mode, we measured the resting membrane potential (V_{rest}) and we followed the electrical activity. Mean V_{rest} showed very depolarized values in cells from the Petri dish (−15.9 ± 4.6 mV, *n* = 15) but manifested a trend to hyperpolarize in cells plated on pristine collagen (−27.5 ± 4.9 mV, *n* = 11) and was significantly more negative in glycosylated collagen-plated cells (−34.8 ± 3.3 mV, *n* = 18, $p < 0.01$) (**Figure 3.14B**). The electrical activity was analyzed by applying depolarizing current pulses by the patch-electrode (**Figure 3.14C**). In Petri dishes, the majority of the cells showed slow depolarizations which were not able to reach 0 mV, whereas mature action potentials (APs) were

registered in 40% of cells. On the contrary, percentage of cells able to generate APs was higher on collagen (82%) and reached almost the totality (94%) on neoglycosylated collagen (**Figure 3.14D**).

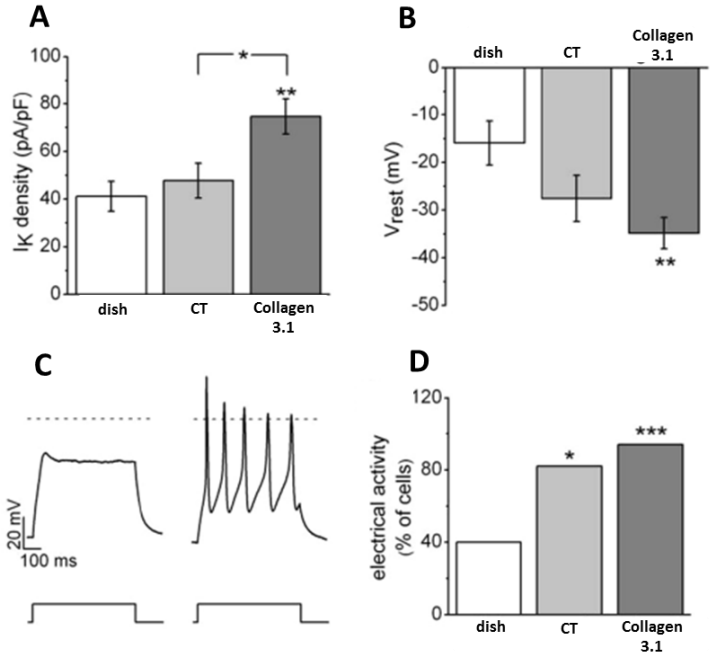

Figure 3.14. (A) Mean current density through potassium channels. A significant increase in the mean values was observed in cells plated on neoglucosylated collagen versus cells plated both on Petri dishes (p < 0.01) and on pristine collagen (*p < 0.05). (B) Mean resting membrane potential for cells in the three conditions. Compared to cells plated on Petri dishes, a hyperpolarizing trend was evident for cells plated on pristine collagen and a significant difference was even obtained for cells plated on neoglucosylated collagen 3.1 (**p < 0.01). (C) Representative response induced by a step current of 50 pA from a cell on the dish (left) and a cell on glc-collagen 3.1 (right). The depolarizing current elicited a passive response in the cell on the dish, but triggered action potentials in the cell on collagen 3.1. The action potential amplitude and duration is characteristic of differentiated F11 cells. The dot line in the traces represents the level of 0 mV. The current protocol is represented below the trace; holding potential, −75/−77 mV. (D) Percentage of cells endowed with electrical activity. Significantly higher values observed for both collagen (*p < 0.05) and functionalized collagen 3.1 (***p < 0.001).**

These differences were significant for collagen ($p < 0.05$, χ^2 test) and highly significant for the neoglycosylated collagen **3.1** ($p < 0.001$, χ^2 test). Overall, we noticed that cells maintained on collagen matrices showed a more differentiated phenotype compared to cells plated on Petri dishes, and this was sustained by morphological and physiological results: increasing frequency of cells with neuritic-like processes, we observed higher sodium and potassium current densities, more hyperpolarized mean V_{rest}, and major probability to generate mature overshooting action potentials. Moreover, we observed that differentiating pressure supplied by the neoglucosylated collagen matrix was the most evident. So we showed for the first time that F11 cells can be driven from proliferation to differentiation without the use of chemical differentiating agents in the culture medium.[118,119]

Generally, glycosylated proteins of the extracellular matrix are specifically recognized by cell surface proteins which are lectins or which contain characteristic lectin-domains.[120] Lectin-like proteins have been found on the surface of a neuroblastoma cell line, in association with many proteins in high molecular weight complexes, and in particular, calreticulin, was found to be essential for adhesion and neurite formation.[121] Other cellular receptors for extracellular matrix components have been shown to trigger signalling pathways for migration, proliferation, survival, and differentiation by regulating ion channel properties. Some types of integrins have been shown to

specifically activate a member of a potassium channel family, resulting in the control of neurite extension in neuroblastoma cells.[122,123] These observations suggest that glycosylated collagen might activate a signal pathway in which the activation of ion channels seems to represent a key step toward differentiation.

Effects of collagen matrices **3.2**, **3.3**, **3.4**, and **3.5** on F11 cells

As mentioned above, morphological and functional analysis with F11 cells have been performed also on collagen films functionalized with other different saccharidic structures, in particular galactose (collagen **3.3**), β-glucose (collagen **3.2**), and sialic acid residues (collagen **3.4** and **3.5**) have been exposed on collagen matrices surfaces. These neoglycosylated collagen films didn't drive F11 to differentiate into functional neurons. The only difference was observed with proliferation assays that have shown that collagen films functionalized with sialoside epitopes enhance cell proliferation rate, if compared with cells seeded on Petri dishes and on native collagen (data not shown).

3.2.2.3 Effects of collagen matrices functionalized with two different sialoside epitopes on mesenchymal stem cells

We performed a preliminary study with functionalized collagen containing sialoside epitopes by using mouse mesenchymal stem cells (mMSCs), considered the most valid candidates for

osteochondral tissue engineering.[124] In particular, we wanted to study whether these saccharidic structures might influence mMSCs behavior and the early stage of osteogenesis and chondrogenesis processes, in order to search new strategies for osteochondral tissue regeneration. These saccharidic structures differ by the linkage between the sialic acid and the galactose unit, being α-2→3 in 3'-sialyllactose and α-2→6 in 6'-sialyllactose. Sialic acids[125] are found in human as the outermost residues on glycoproteins of the cell surface and have carboxylate groups able to coordinate cations. Many studies have shown the function of α-2→6 and α-2→3 sialosides found on glycoproteins exposed on cell surfaces, as for examples in osteogenesis,[126] and in angiogenesis.[127,128]

We did biological evaluation of mMSCs morphology, viability, proliferation and we studied the expression of osteogenic and chondrogenic related genes. The morphological analysis showed that mMSCs well adhered to the collagen matrices after 1 day with their typical spindle/fibroblast-like morphology without any difference among the groups (**Figure 3.15A**). Additionally we evaluated the number of metabolically active cells by MTT assay. We observed an overall increase in cell proliferation from day 1 to day 14 for all groups, demonstrating that neoglycosylation process did not affect cell viability (**Figure 3.15B**). CT group (cells seeded on pristine collagen film) showed the higher cell number after the first 3 days ($p \leq 0.05$ at day 2 and $p \leq 0.001$ at day 3), if compared to the other

groups. However, we did not observe differences after 7 and 14 days of culture, when films **3.4** and **3.5** showed comparable cell number to CT group. Results indicate that the collagen films positively influence the mMSCs behavior in terms of viability and proliferation, and that, in the long-term culture (d7 and d14), the surface functionalization does not have negative effect on cell proliferation.

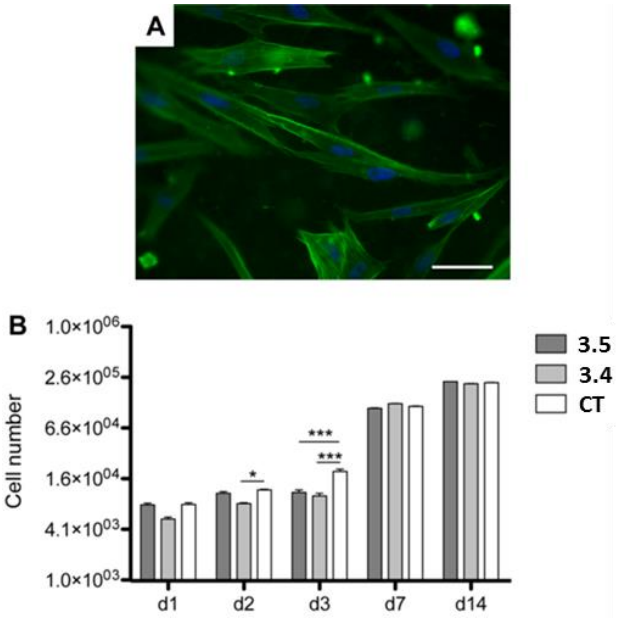

Figure 3.15. (A) Analysis of cell morphology by immunofluorescence image. Cells were spread with good morphology and firmly attached to the surface (day 1, CT group). Phalloidin in green stains for actin filaments and DAPI in blue stains for cell nuclei. Scale bars 50 µm. (B) Analysis of cell proliferation by the MTT assay, after 1, 2, 3, 7 and 14 days of MSCs culture on collagen films (control, 3.4 and 3.5). *p≤ 0.05, *** p≤ 0.001; n = 5.

In order to investigate the role of sialo-functionalized collagen matrices in osteogenic and chondrogenic stimulation, we evaluated the principal markers of these cell differentiative pathways. The progression of osteogenic differentiation was evaluated quantifying

RUNX2 and ALP gene expression, which are considered the main markers of osteoblast commitment.[129] In fact, during early osteogenic process, RUNX2 acts as a transcriptional downstream activator of bone morphogenetic protein signaling, essential for osteoblast differentiation.[130,131] In that phase, cells start with the synthesis of extracellular matrix (ECM), which consists primarily of collagen type I. Subsequently, cells produce ALP and a variety of non-collagenous proteins, followed by the induction of ECM calcification.[132] The quantification of mRNA demonstrated that film **3.4** significantly up-regulate the expression of RUNX2 and ALP after 14 days of culture: ~3.29 and ~2.88 fold change relative to CT, respectively (p=0.0042 and p=0.024). Additionally, a significant increase of both the osteogenic genes was observed (**Figure 3.16**) compared to film **3.5** (RUNX2 p=0.035 and ALP p=0.023).

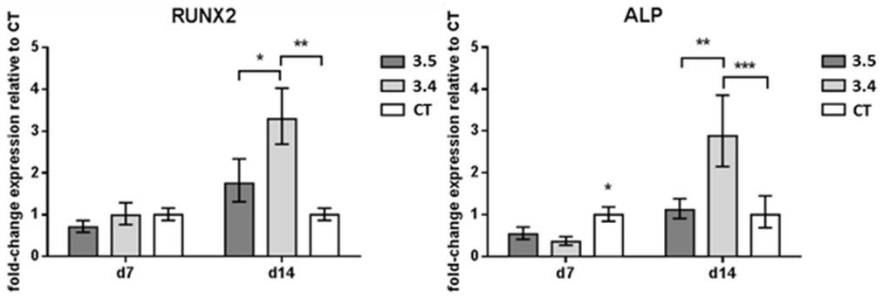

Figure 3.16. Relative quantification ($2^{-\Delta\Delta Ct}$) of osteogenic related gene expression after 7 and 14 days of MSCs cultured in direct contact with all the films. Mean, upper and lower value of the technical triplicate of RUNX2 and ALP respect to the expression of the CT, were indicated. Statistical significant differences among the samples are indicated in the graph. RUNX2: *p=0.035, **p= 0.0042. ALP: *p= 0.025, **p= 0.023, ***p=0.024.

The potential effect of sialylated collagen films in the chondrogenic inductions of MSCs was evaluated by the relative quantification of both early and late chondrocyte markers, SOX9 and ACAN. SOX9 is a transcription factor that plays a key role in chondrogenesis and skeletogenesis and it has been shown to directly regulate the expression of ACAN, that codify for the predominant proteoglycan of cartilage extracellular matrix.[133,134]

The results showed that, although no differences were found in the expression level of SOX9, film **3.5** significant up-regulated the expression of ACAN (**Figure 3.17**), compared to CT, after 7 and 14 days of culture (p=0.0015 and p=0.0003, respectively).

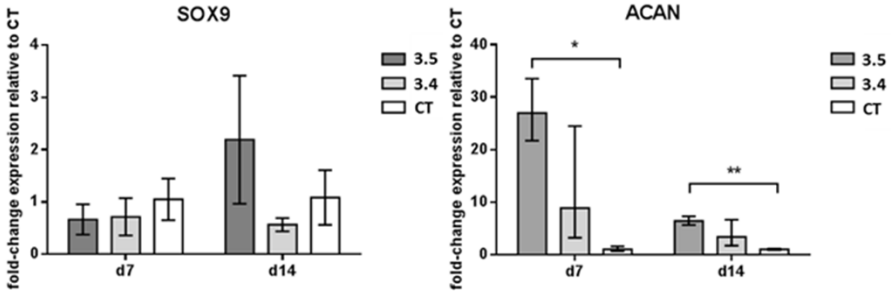

Figure 3.17. Relative quantification ($2^{-\Delta\Delta Ct}$) of chondrogenic related gene expression after 7 and 14 days of MSCs cultured on the films. Mean, upper and lower value of the technical triplicate of SOX9 and ACAN in respect to CT, were indicated. Statistical significant differences among the samples are indicated in the graph: * p= 0.0015 and ** p=0.0003.

We have to underline that cells were grown without any osteogenic or chondrogenic supplements in the culture medium, so the inductive effects highlighted by increased gene expression are uniquely a consequence of the sialoside moieties presented on collagen surface.

On the whole, with these data we have clearly shown that mMSCs are able to perceive the two different surface functionalizations of collagen films **3.4** and **3.5**, although they differ only by a glycosidic linkage. In conclusion, the two sialosides are able to convey different molecular signals.

We demonstrated that in general collagen-based films represent a suitable support for rapid cell adhesion and proliferation. In fact, we observed a great increase of cell number since day 1 after seeding (**Figure 3.15B**). Moreover, the chemical functionalization with sialoside epitopes gives the impression to provide mMSCs with different and specific *stimuli*, which are saccharide-dependent, in term of osteogenic and chondrogenic related gene expression.

These preliminary results show that sialylated collagen films supply a "functional network" for suitable mMSCs/material interactions and cell stimulations for osteochondral tissue engineering. Deeper biological studies are needed in order to clarify the critical role of different carbohydrates in the commitment process of precursors stem cells.

3.2.3 Collagen modification with thiolated sugars

Collagen functionalization and characterization

Differently from collagen functionalization already discussed, matrices functionalization with fucose has not been achieved *via* reductive amination. The chemical strategy exploited has considered

the modification of collagen lysine side-chains amino groups with maleic anhydride in order to make available, on collagen surfaces, functional groups able to specifically react with thiol-modified fucose. L-fucose (6-deoxy-L-galactose) is a monosaccharide that is a common component of many N- and O-linked glycans and glycolipids produced by mammalian cells. Two structural features distinguish fucose from other six-carbon sugars present in mammals. These include the lack of a hydroxyl group on the carbon at the 6-position (C-6) and the L-configuration. Fucose frequently exists as a terminal modification of glycan structures; however, recently glycosyltransferase activities capable of adding sugars directly to fucose have been identified. Specific terminal glycan modifications, including fucosylation, can confer unique functional properties to oligosaccharides and are often regulated during ontogeny and cellular differentiation. Important roles for fucosylated glycans have been demonstrated in a variety of biological settings. However, because of the diversity of fucose-containing glycoconjugates and the difficulties inherent in studying the biological function of carbohydrates, it is likely that many additional functions for fucosylated glycans remain to be uncovered.[135]

The reaction of collagen with maleic anhydride has been performed in tetrahydrofuran (THF) for 24 hours; in this way we have obtained a "maleimide-collagen" (**3.11)** suitable for the reaction with the sugar. On the other hand, starting from fucose, in a four-step synthesis, we

have synthesized the desired thiolated sugar (**3.15**); in more details, the starting fucose was reacted with allylic alcohol, in order to add an allylic functionality. In this way, we obtained a mixture of α and β anomers. To obtain the desired α anomer, we decided to do an acetylation reaction to facilitate the anomers separation by column flash chromatography. The following reaction with thioacetic acid, in the presence of azobisisobutyronitrile (AIBN) as initiator, and the final deacetylation have allowed the production of the final thiolated sugar **3.15** (**Scheme 3.1**).

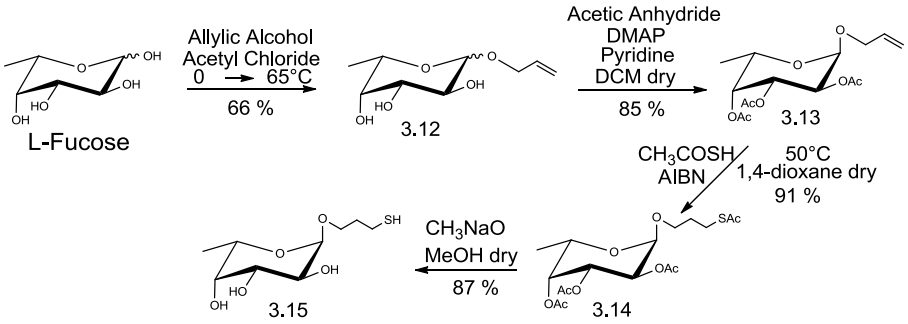

Scheme 3.1. Synthesis of thiolated fucose 3.15.

Then, the reaction with maleimide-collagen (**3.11**) and the thiolated fucose (**3.15**) has been conducted in PBS for 24 hours, obtaining the neofucosylated collagen **3.16** (**Scheme 3.2**)**.**

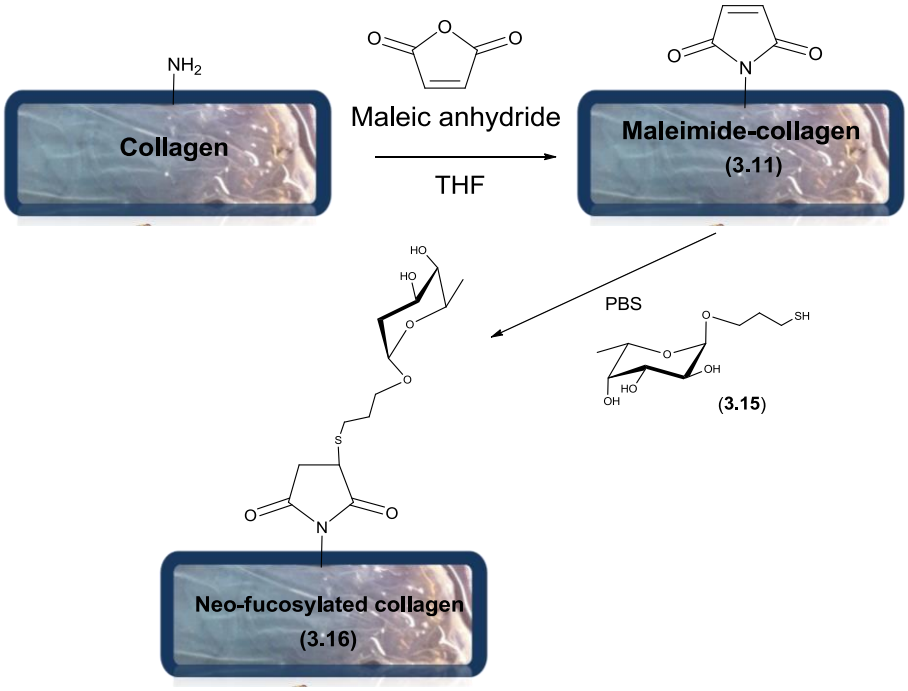

Scheme 3.2. Synthetic strategy for collagen film functionalization with fucose.

^{1}H NMR spectroscopy has been used to determine the efficacy of the neoglycosylation reaction; following the disappearance of maleimide signals, we quantified the sugar amount. In particular about 30% of total lysine side-chains amino groups have been functionalized with the sugar.

3.2.4 Collagen functionalization *via* thiol-ene reactions

Collagen functionalization and characterization

Since collagen contains few or no cysteine or cysteine residues,[136] thiol groups have been added reacting lysine side-chain amino groups with γ-thiobutyrolactone, obtaining thiolated collagen **3.17**. Selected

sugars have been allyl α-D-glucopyranoside and allyl β-D-galactopyranoside. Thiol-ene reaction was conducted at room temperature for 1 h in a MeOH:H_2O (1:2) solution by irradiation with a UV lamp at 365 nm (Raionet) using 2,2-dimethoxy-2-phenylacetophenone (DPAP) as a radical photoinitiator. The efficacy of collagen thiolation was checked by ^{1}H NMR spectroscopy: derivatization of the treated and untreated samples with 5,5'-Dithiobis(2-nitrobenzoic acid) (DTNB, **Figure 3.18**) has been conducted. DTNB is a reagent able to form disulfide bridges with free thiol groups;[137] the reaction was performed to label and quantify inserted −SH groups (untreated collagen was used as the control). The resulting collagen-S-TNB film **3.18** (**Figure 3.18**) presents additional protons resonating in the characteristic aromatic region (6.4−7.5 ppm) deriving from the TNB moiety, if compared to pristine collagen characterized by a low number of aromatic amino acids (Phe, Tyr, and His).

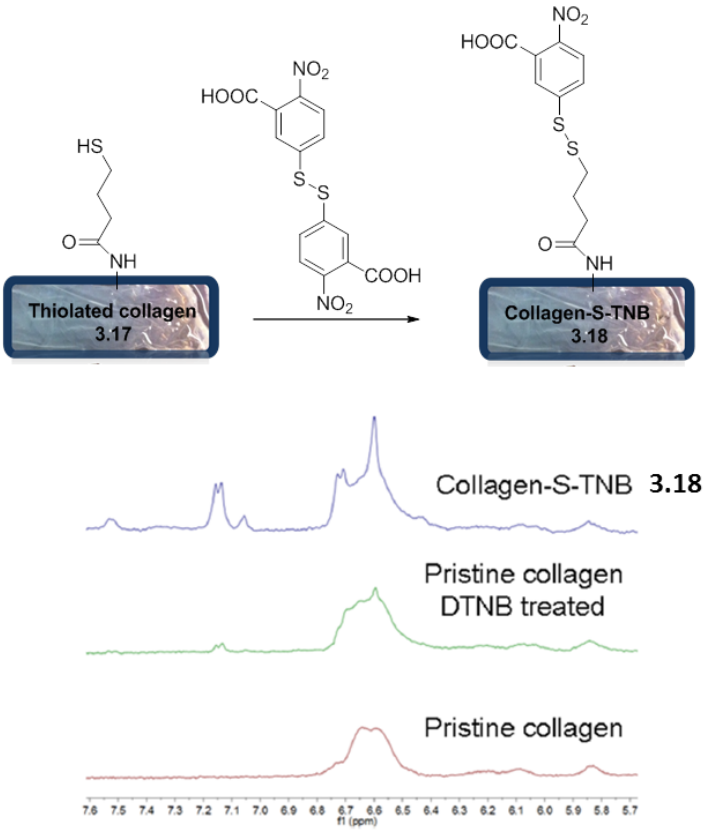

Figure 3.18. DTNB reaction with thiolated collagen 3.17 and ^{1}H-NMR of the aromatic region for quantification.

From the variation of intensities in the aromatic region (δ 6.4−7.5 ppm) of the spectra after DTNB reaction, we were able to evaluate that approximately 60% of the total lysines are functionalized with the −SH group necessary for the following coupling to carbohydrates. In order to verify the presence of adsorbed DTNB, pristine collagen (non-thiolated) was also reacted with DTNB, and ^{1}H NMR was recorded. The efficacy of the photoclick neoglycosylation, that has

led to the production of collagen **3.19** and **3.20** (**Scheme 3.3**), was again determined by DTNB treatment: integral values show the absence of additional aromatics due to TNB, evidencing that the thiol–ene reaction goes to completion on sulphydryl groups (**Figure 3.19**).

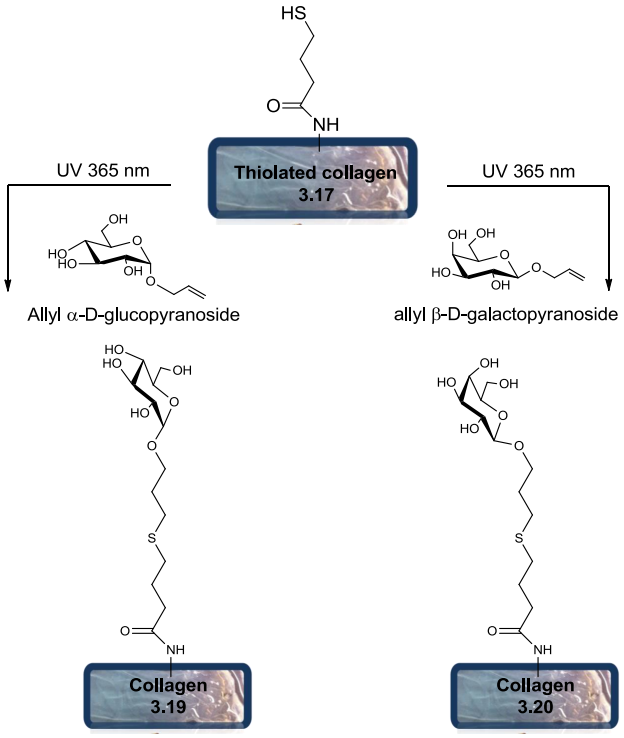

Scheme 3.3. Thiol-ene reaction between thiolated collagen and allyl α-D-glucopyranoside and allyl β-D-galactopyranoside.

Given the amino acid composition of collagen being about 300 µmol lysine content per gram of protein, we calculated the sugar content in approximately 180 µmol/g of collagen. FT-IR spectroscopy has also

been performed, and ELLA assays demonstrated the correct spatial presentation for recognition.

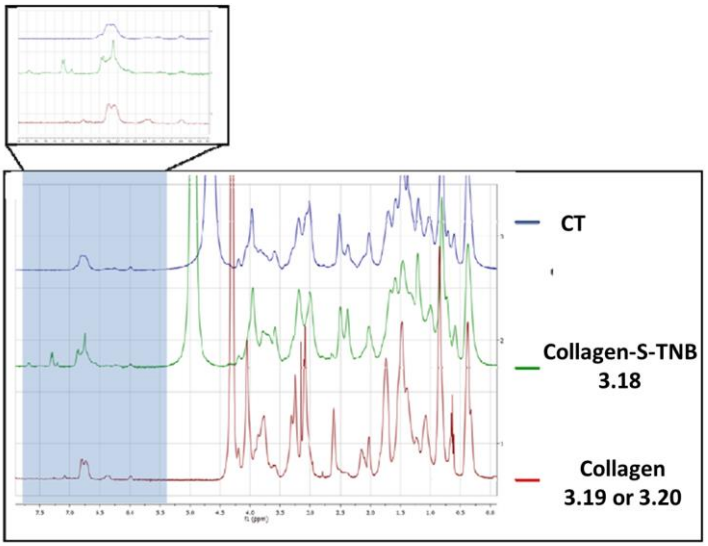

Figure 3.19. NMR spectra of collagen patches before and after the thiol-ene mediated neoglycosylation reaction.

The addition of sugar moieties to thiolated collagen **3.17** was confirmed by FT-IR spectroscopy. The infrared amide I bands (1700−1600 cm^{-1}, due to the C=O stretching vibration of the peptide bond) of pristine collagen, thiolated (**3.17**), and glycosylated **3.19** and **3.20** (full lines of **Figure 3.20**) were almost superimposable; this suggests that the native protein secondary structures were mostly maintained after the sample treatments. On the contrary, we observed some spectral variations on the carbohydrate marker bands in the 1200−900 cm^{-1} region. We also measured the FT-IR spectra of the film external layers (dashed lines of **Figure 3.20**), obtained by

scraping the collagen films. In the case of glucosylated and galactosylated patches, the spectra of the materials scraped out from the film exhibited variable intensities in the 1200–900 cm^{-1} spectral region.

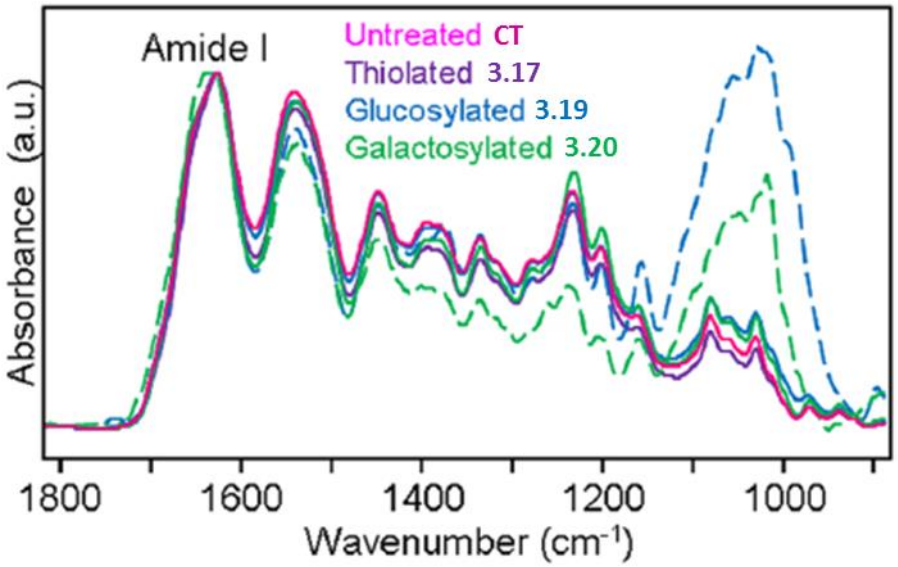

Figure 3.20. FT-IR spectra of collagen samples; the FT-IR spectra of the external layers are also reported (dashed lines).

In order to verify if the exposed monosaccharides were able to exploit their biological signaling function upon recognition of their complementary receptor, ELLAs on the neoglycosylated collagen samples (**Figure 3.21**) were performed. Commercially available peroxidase conjugated lectins were used; peanut agglutinin (PNA) has been chosen based on its ability to recognize β-galactosides, while Concanavalin-A (ConA) has been selected on its ability to recognize α-glucosides. The ELLA assays show effective recognition of

each monosaccharide by its complementary lectin: these results clearly show not only the presence but also the right exposition of the monosaccharides on film surfaces.

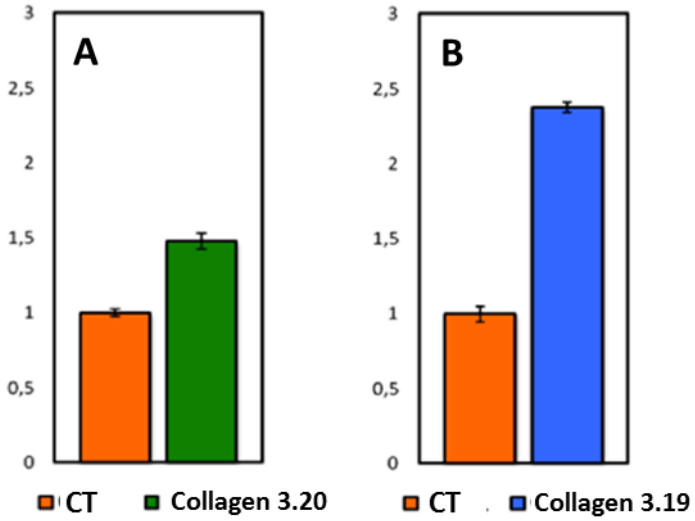

Figure 3.21. ELLA assays on glycosylated collagens 3.19 and 3.20 patches from three independent experiments.

3.3 Conclusions

This chapter describes the development of collagen films and soluble collagen functionalized with different sugar moieties; in particular glucose, galactose, sialic acid, fucose and chondroitin sulfate have been taken into account. Three different functionalization strategies have been adopted; in all cases free lysine side-chains amino groups have been useful for collagen modification. The first strategy has considered the reductive amination, directly on collagen free amino groups, in the second one lysine side-chain amino groups have been used to add maleimido groups on collagen surface to allow the

selective functionalization with sugar modified with thiols, and finally the addition of thiol groups on collagen has allowed the thiol-ene reaction in the presence of allylated sugars. All the materials were characterized in term of their functionalization by different methods: FTIR, NMR, and AFM. Moreover, in order to assess if the exposed sugar moieties can also exploit their biological signaling functions upon recognition of its complementary receptor, ELLA assays have been conducted on collagen functionalized with glucose and galactose moieties.

Biological evaluations of neoglycosylated collagens have been conducted, in term of cell proliferation and differentiation; very interesting results have been obtained, proving the relevant role of carbohydrates as signaling cues when covalently linked to biomaterial surfaces. Neogalactosylated collagen matrices can be used as good substrate for the growth of MG63 cells; potentially, this chemical modification could be used to implement cell colonization of collagen-based scaffolds for tissue engineering approaches. F11 cells seeded on collagen matrices functionalized with glucose moieties were driven to differentiate into functional neurons without the use of added conventional differentiating agents in the culture medium. Finally, we evaluated *in vitro* collagen films exposing on their surface two different sialosides with mMSCs for their ability to influence gene expression toward osteogenesis or chondrogenesis. These preliminary results demonstrated that sialylated collagen films

provide a “functional network” for suitable MSCs/material interactions and cell stimulations for osteochondral tissue engineering.

Deeper biological studies are needed in order to clarify the role of different carbohydrates in the differentiation processes of different cell lines. However, these data lay the basis for the development of a new generation of smart biomaterials, able to modulate cell fate.

Chapter 4

Elastin-based biomaterials

4.1 Introduction

Elastin is an extracellular matrix protein with the ability to provide elasticity to tissues and organs. Elastin is most abundant in organs where elasticity is of major importance, like in blood vessels; it stretches and relaxes more than a billion times during life, in elastic ligaments, in lung and in skin. Another important property of the precursor of elastin, tropoelastin and elastin-like peptides is their potential to self-assemble under physiological conditions. The coacervation is at the base of these processes, which probably induces the alignment of tropoelastin molecules previous to intermolecular crosslinking.[138] The resulting elastin, that is insoluble, has a half-life of 70 years; it is one of the most stable proteins known. It is not only a structural protein.[139] Elastin is formed in the process of elastogenesis through the assembly and cross-linking of the protein tropoelastin (**Figure 4.1**).

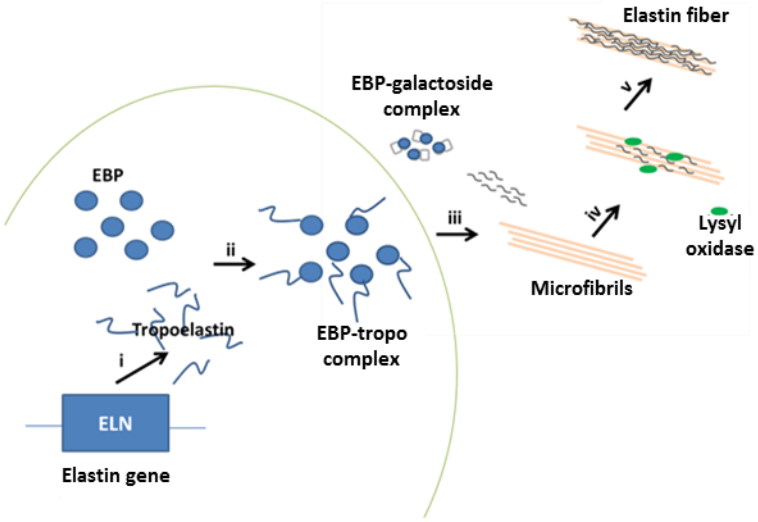

Figure 4.1. Elastogenesis stages: i) tropoelastin is transcribed and translated from the elastin (ELN) gene and (ii) transported to the plasma membrane in association with EBP. (iii) Tropoelastin is released and aggregates on the cell surface, while EBP dissociates to form a complex with available galactosides. (iv) Tropoelastin aggregates are oxidized by lysyl oxidase leading to crosslinked elastin that accumulates on microfibrils which help to direct elastin deposition. (v) The process of deposition and cross-linking continues to give rise to mature elastic fibers.

The tropoelastin monomer is developed from expression of the elastin gene during perinatal development by elastogenic cells such as smooth muscle cells (SMCs), endothelial cells, fibroblasts and chondroblasts.[140] The tropoelastin transcript is subjected to extensive alternative splicing causing the removal of entire domains from the protein. In humans, this splicing results in different tropoelastin isoforms, the most common lacks exon 26A.[141] Mature, intracellular tropoelastin connects with the elastin binding protein (EBP) and then this complex is secreted to the cell surface.[142] EBP has galacto-lectin properties (it is an enzymatically spliced variant of the lysosomal β-galactosidase); it binds the hydrophobic VGVAPG sequence in elastin,

the cell membrane, and galactosugars via three separate sites. Binding of galactosugars to the lectin site of the 67-kD EBP lowers its affinity for both tropoelastin and for the cell binding site, resulting in the release of bound elastin and the dissociation of the 67-kD subunit from the cell membrane. Galactosugar-containing microfibrillar glycoproteins may therefore be involved in the coordinated release of tropoelastin from the 67-kD binding protein on the cell membrane to the growing elastin fiber. An excess of galactose-containing components of the extracellular matrix, e.g., glycoproteins, glycosaminoglycans, or galactolipids may, however, impair elastin assembly by causing premature release of tropoelastin and the elastin-binding protein from the cell surface.[143] Previous studies show impaired formation of mature elastin fibers in cultured or transplanted elastin-producing cells treated with agarose[144] or following the addition of excess free non-sulfated galactosugars such as lactose, galactose, or galactosamine.[145]

Released tropoelastin on the cell surface aggregates by coacervation. During this process, the hydrophobic domains of tropoelastin associate and tropoelastin molecules become concentrated and more and more aligned permitting the subsequent formation of crosslinks. Coacervated tropoelastin is deposited onto microfibrils which probably act as a scaffold to conduct tropoelastin cross-linking and consequential elastic fiber formation. Cross-linking is promoted by the enzyme lysyl oxidase; this enzyme deaminates lysine side

chains in tropoelastin to build allysine sidechains that can consequently react with adjacent allysine or lysine side chains to form cross-links.[146] Additionally, these cross-links can react to form desmosine and isodesmosine cross-links between tropoelastin molecules (**Figure 4.2)**.[147] Multiple cross-links generate the mature insoluble elastic fiber.

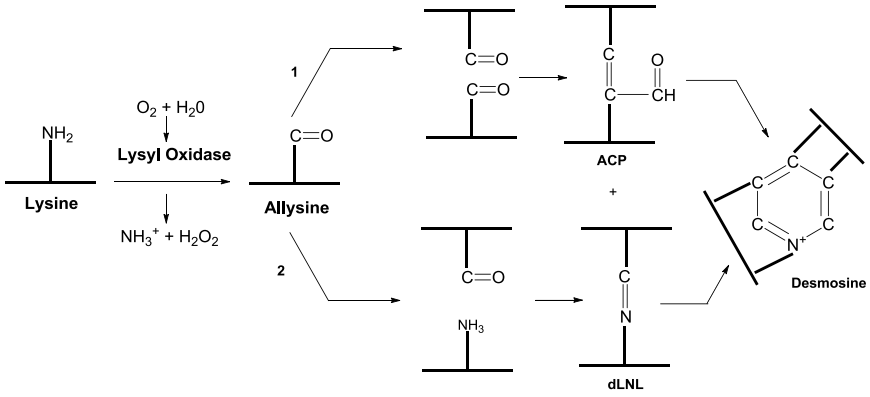

Figure 4.2. Cross-linking of elastin monomers is initiated by the oxidative deamination of lysine side chains by the enzyme lysyl oxidase in a reaction that consumes molecular oxygen and releases ammonia. The aldehyde (allysine) that is formed can condense with another modified side chain aldehyde (1) to form the bivalent aldol condensation product (ACP) cross-link. Reaction with the amine of an unmodified side chain through a Schiff base reaction (2) produces dehydrolysinonorleucine (dLNL). ACP and dLNL can then condense to form the tetrafunctional cross-link desmosine or its isomer isodesmosine.

Elastin comprises up to 70% of the dry weight in elastic ligaments, about 50% in large arteries, 30% in lung, and 2–4% in skin. In general, elastic fibers are present as rope-like structures like in ligaments, in the media of elastic arteries and skin. Elastin confers flexibility and elasticity indispensable to the function of these tissues. The disposition of elastin in the extracellular matrix differs between various tissues to yield a lot of structures with specific elastic

properties. For example, elastin in the form of thin lamina in the arterial wall is responsible for the strength and elasticity essential for vessel expansion and regulation of blood flow.[148] Moreover, in the lung, elastin is organized as a latticework that promotes the opening and closing of the alveoli;[149] in skin, elastin fibers are enriched in the dermis where they give skin flexibility and extensibility.[150]

Elastin has key biological roles in the regulation of cells native to elastic tissues. Researches about elastin knockout mice show a central role for elastin in arterial morphogenesis through regulation of smooth muscle cells proliferation and phenotype.[151] This model is sustained by *in vitro* studies demonstrating that elastin is able to inhibit SMCs (smooth muscle cells) proliferation in a dose dependent manner.[152] Moreover, elastin can influence the adhesion and proliferation of endothelial cells from several vascular origins.[153] Analogous effects have been observed for dermal fibroblasts.[154] Elastin is also a chemoattractant for SMCs, endothelial cells and monocytes. Several cell receptors have been found for elastin, in particular EBP, which binds to multiple sites including the VGVAPG sequence on exon 24 of tropoelastin.[155] This elastin binding activates intracellular signaling pathways implicated in cell proliferation, chemotaxis, migration and cell morphology for different cell types (SMCs, endothelial cells, fibroblasts, monocytes, leukocytes and mesenchymal cells). Glycosaminoglycans on the SMCs and

chondrocyte cell surface dominate binding to the C-terminus of bovine tropoelastin.[156]

Elastin can be used as biomaterial in various forms, including insoluble elastin in autografts, allografts, xenografts, decellularised ECM, and in purified elastin preparations. Moreover, insoluble elastin can be hydrolysed to get soluble elastin preparations. Repeated elastin-like sequences can be generated by synthetic or recombinant means. Additionally, recombinant tropoelastin or tropoelastin fragments can be used in biomaterials.[157]

- Elastin in autografts, allografts and xenografts. Obviously, autografts, allografts and xenografts contain elastic fibers. Common examples are split-skin autografts for burn wounds, autologous saphenous veins and umbilical vein allografts for coronary artery by-pass graft surgery, and aortic heart valve xenografts.
- Decellularised tissues containing elastin. These tissues are tissue pieces that are purified to remove cells but maintaining their 3D architecture. Cells have to be removed, because cellular remains inevitably lead to an immunological response. The advantage of decellularised tissues is that the structural design is maintained in contrast to the preparation of constructs from purified components. On the other hand, this restricts its application primarily to the tissue it is obtained from, for example, decellularised esophagus for esophagus tissue engineering[158] and decellularised heart valves and vasculature for heart valve replacement and vascular grafts.[159] Other disadvantages of decellularised tissues are that it is complicated to produce highly purified preparations from intact tissue (if compared to pulverised material), and that decellularised tissue could result in undefined preparations with large batch-to-batch variations. Decellularisation is executed with different extraction

methodologies, for example detergents (Triton, SDS) and enzyme digestions (e.g. trypsin). Decellularisation by Triton or trypsin also changes the extracellular matrix composition. It is difficult to compare results obtained from different laboratories; in fact, each protocol will result in its own set of remaining ECM components.

- Purified elastin preparations. Purification is important when studying the effect of mature extracellular elastin in fibrous form (containing its natural crosslinks like (iso)desmosine) without introducing artefacts by impurities. In applied research, for example the use of elastin as biomaterials in tissue engineering, the purified intact fibres could be advantageous when manufacturing molecularly-defined scaffolds from scratch thus avoiding undesired immunological reactions to contaminations, and allowing studies to the body's response to one single component: elastin.[160] Due to the intermolecular crosslinks, elastin is highly insoluble. Indeed, elastin can only be dissolved after hydrolysing some peptide bonds. This insolubility is often used for isolation of elastin from tissues. Throughout history, bovine and equine ligamentum nuchae have been used as a source for insoluble elastin, because a large percentage of its dry weight is elastin. For example, Lansing et al.[161] isolated elastin from ligamentum nuchae based on treatment with 0.1 M NaOH at 95°C for 45 min.

  An advantage of purified elastin is that it can be modeled into different shapes. Purified elastin allows the production of highly defined scaffolds.
- Hydrolysed elastin: soluble forms of elastin. Hydrolysed elastin (or elastin peptides) is also used as biomaterial. Usually, methods to prepare soluble elastin are treatment with 0.25 M oxalic acid at 100°C[162] and 1 M KOH in 80% ethanol at 37°C.[163] Proteolytic enzymes that are able to degrade elastic fibres, including serine-type elastases from polymorphonuclear leukocytes and several metallo-elastases of monocyte/macrophage origin, also result in solubilised

elastin.[164] These methods are all based on the hydrolysis of some peptide bonds of insoluble elastin. Elastin peptides obtained after the treatment with oxalic acid can be coacervated after suspension in 10 mM sodium acetate with 10 mM NaCl set to pH 5.5 with acetic acid, followed by heating and centrifugation at 37°C. In this way two fractions will be formed: in particular α-elastin (a viscous coacervate) and β-elastin (in the supernatant). Using KOH, *k*-elastin is produced; it is a heterogeneous mixture of elastin peptides with a mean molecular mass of about 70 kDa, soluble in aqueous solutions. A significant advantage of these preparations is their solubility which makes handling and analysis of the material simpler. In addition, elastin peptides influence signalling, proliferation and protease release *via* the elastin receptor.[165] Biomaterials having hydrolysed elastin can exert biological effects (like enhancing elastin synthesis) on a lot of cell types. Consequently, the presence of these molecules in biomaterials is suggested. The cell biological effect may be modulated by the amount of solubilised elastin in the material and the extent of crosslinking. Materials based on *k*-elastin or elastin fibers with types I and III collagen can be prepared, for example in combination with glycosaminoglycans[166] or calcium phosphate. Elastin preparations combined with fibrin have also been prepared.[167] The potential of collagen-elastin and collagen-fibrin biomaterials were considered in *in vivo* models, e.g. as a tympanic membrane.[168] Finally, solubilised elastin has been used to enhance the biocompatibility of synthetic materials such as polyethylene glycol terephthalate (PET).[169]

Biomaterials derived from (bio)synthetic elastin. Using protein engineering, numerous different parameters of elastin-like molecules can be controlled, including amino acid sequence, peptide length, and, in the case of block copolymers, the length and number of the blocks. Another advantage is the opportunity to incorporate specific sequences that possess cell biological effects. Recombinant expression systems result

in highly homogeneous protein preparations (composition, sequence and molecular mass) as opposed to molecules prepared by peptide synthesis. On the contrary, with peptide synthesis it is simpler to incorporate non-natural amino acids which can be useful in modification or crosslinking reactions. The thermally responsive behavior of elastin-like polypeptides may also be exploited in biomaterials, for example as injectable biomaterials.

4.2 Elastin functionalization and characterization

Elastin-based biomaterials that have been taken into account are in form of 2D matrices and hydrolysed elastin. In particular elastin 2D scaffolds were obtained from a commercial insoluble elastin from bovine neck ligament (Sigma-Aldrich, cotalog no. E1625). The procedure has considered a solvent casting method, by using acetic acid 0.5 M as solvent; in this way we were able to obtained elastin matrices (**Figure 4.3A**). One of the major problems that we have observed in the scaffolds production is the elastin batch variation: being this protein extracted from natural sources, various elastin lots have shown differences in scaffolds production (**Figure 4.3B**); so, in some cases, we had to tune 2D-scaffolds preparation conditions.

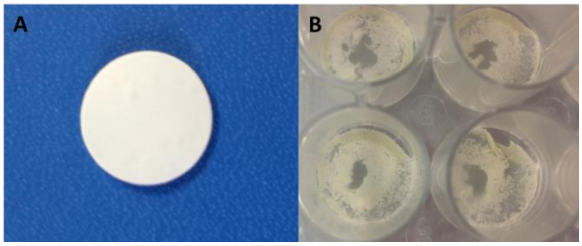

Figure 4.3. Pictures of elastin scaffolds. (A) Normal elastin scaffold. (B) Elastin scaffolds obtained maintaining the same elastin concentration, but changing elastin lot.

Then, we decided, as in the case of collagen, to functionalize elastin matrices with carbohydrates, for the reasons previously discussed. The functionalization strategy that has been adopted is the reductive amination of lysine residues in citrate buffer (pH 6.0); maltose and lactose have been chosen as model sugars in order to expose α-glucosides and β-galactosides on elastin surface (**Scheme 4.1**). Elastin matrices **4.1** and **4.2** have been obtained.

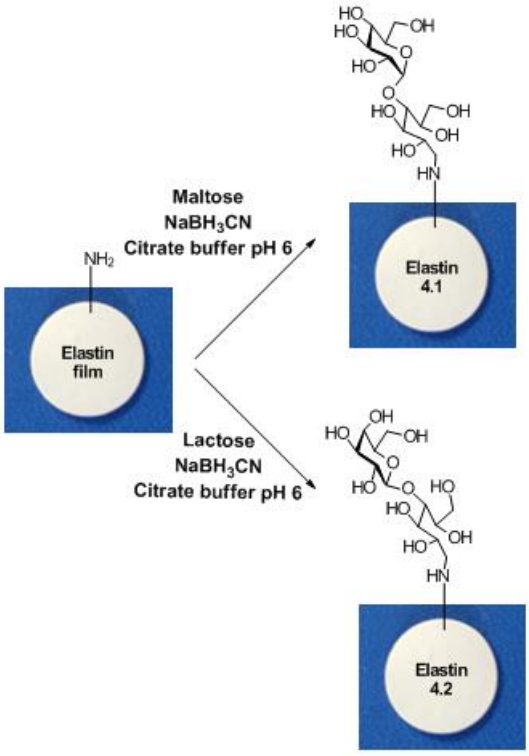

Scheme 4.1. Reductive amination between elastin lysine residues and maltose or lactose.

These resulting matrices were characterized by Fourier transform infrared (FTIR) spectroscopy and scanning electron microscopy (SEM). Moreover, a swelling test, to determine the amount of liquid

material that can be absorbed, has been performed. By FTIR, the analysis of the external layers of elastin scaffolds confirmed the success of the neoglycosylation reactions as indicated by the raising of the carbohydrate marker bands, in the 1200-900 cm^{-1} region, only in the case of the treated samples, glucosylated and galactosylated (**Figure 4.4**).

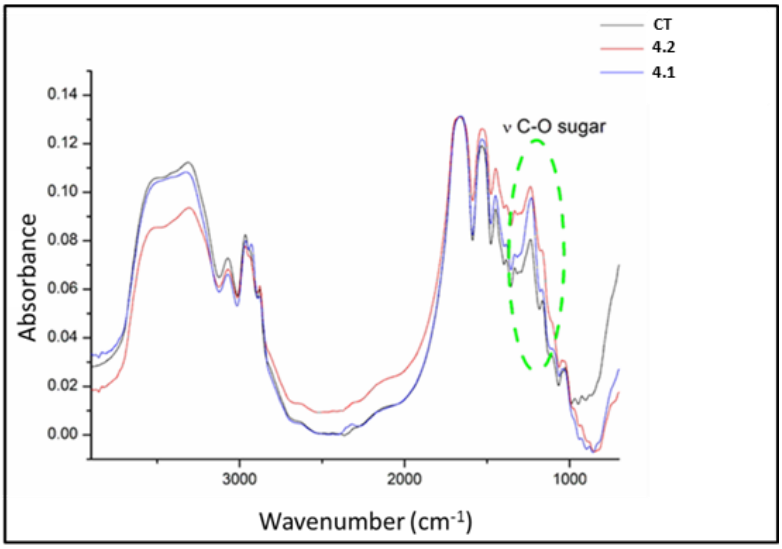

Figure 4.4. FTIR absorption spectra of untreated (grey line), neogalactosylated 4.2 (red line) and neoglucosylated 4.1 (blue line) elastin samples.

In **figure 4.5** and **4.6**, we can see SEM images of untreated and neoglycosylated elastin, pre- and post-swelling.

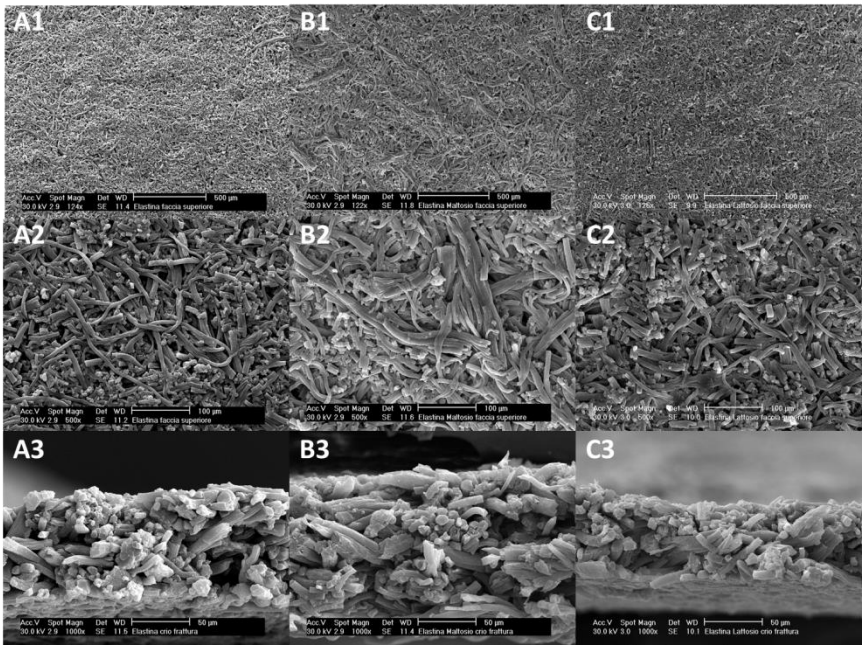

Figure 4.5. SEM images of elastin before the swelling test. A1 and A2 upper side of untreated elastin (low and high magnification), A3 internal side of untreated elastin after cryo-fracture. B1 and B2 upper side of glucosylated elastin 4.1 (low and high magnification), B3 internal side of glucosylated elastin 4.1 after cryo-fracture. C1 and C2 upper side of galactosylated elastin 4.2 (low and high magnification), C3 internal side of galactosylated elastin 4.2 after cryo-fracture.

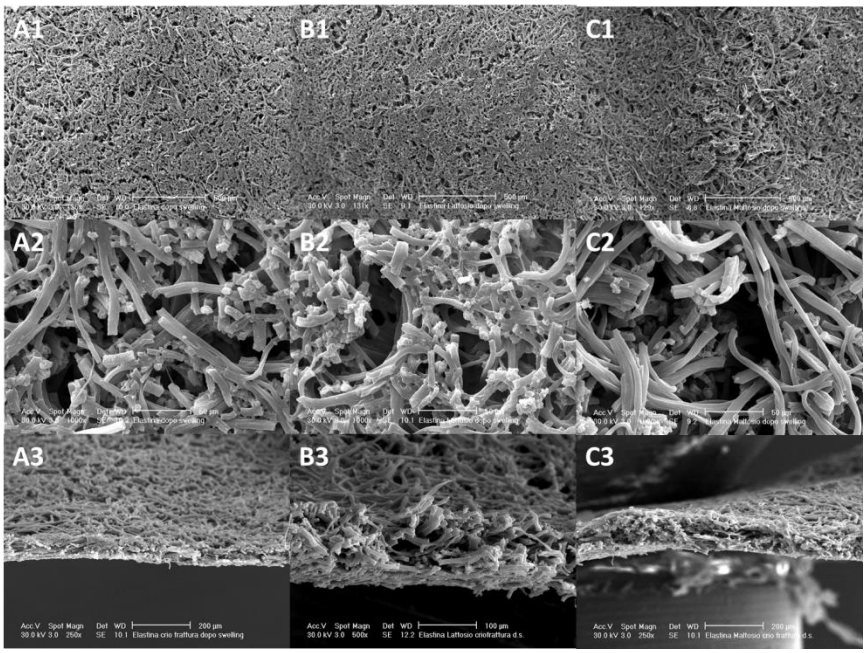

Figure 4.6. SEM images of elastin after the swelling test. A1 and A2 upper side of untreated elastin (low and high magnification), A3 internal side of untreated elastin after cryo-fracture. B1 and B2 upper side of galactosylated elastin 4.2 (low and high magnification), B3 internal side of galactosylated elastin 4.2 after cryo-fracture. C1 and C2 upper side of glucosylated elastin 4.1 (low and high magnification), C3 internal side of glucosylated 4.1 elastin after cryo-fracture.

The swelling test has been performed; in particular elastin matrices were immersed in water and after 1 hour were immediately weighed. The swelling capacity was calculated according to the following equation:

$$\% S = \frac{(m_w - m_i)}{m_i} x\ 100$$

where *% S* is swelling ratio, m_w is the weight of samples after swelling test performing (water immersion), and m_i is the initial weight. The graph in **Figure 4.7** shows the results.

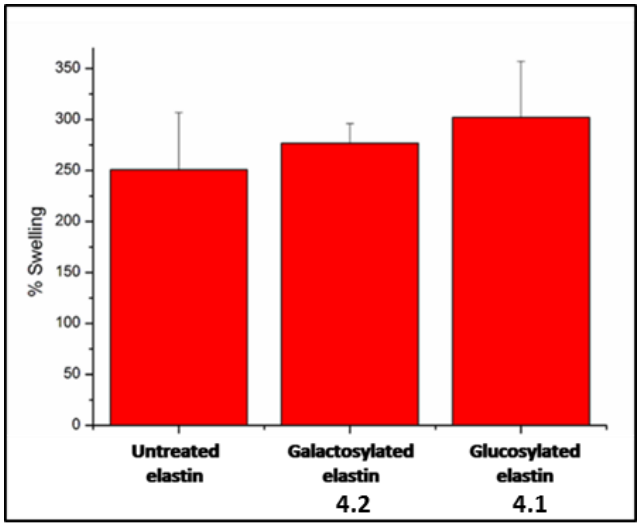

Figure 4.7. Bar chart indicating percentage of swelling of untreated and neoglycosylated elastin scaffolds.

The same functionalization strategy has been adopted for the neoglycosylation of hydrolysed elastin; in particular soluble elastin has been functionalized with lactose (elastin **4.3**), maltose (elastin **4.4**), cellobiose (elastin **4.5**), 3'-sialyllactose (elastin **4.6**) and 6'-sialyllactose (elastin **4.7**). The resulting neoglycosylated elastins were characterized by Fourier transform infrared (FTIR) spectroscopy; the success of the neoglycosylation reaction is demonstrating by the raising of the carbohydrate marker bands, in the 1200-900 cm^{-1} region, only in the case of the functionalized samples (**Figure 4.8**).

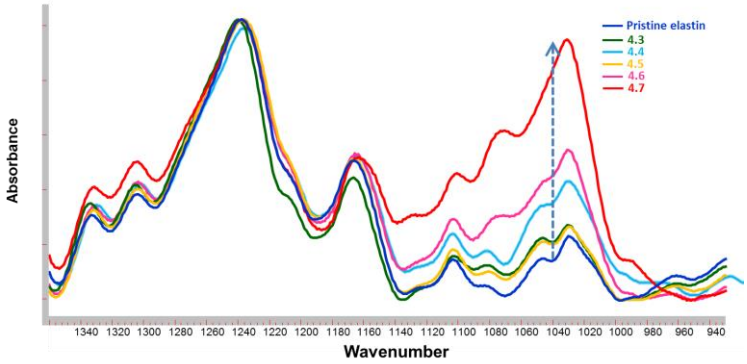

Figure 4.8. FTIR absorption spectra of soluble untreated elastin (blue line), elastin functionalized with maltose (light blue line), cellobiose (yellow line), lactose (green line), 3'-sialyllactose (pink line), or 6'-sialyllactose (red line).

The amount of sugar on elastin matrix surfaces and on soluble elastin was quantified by using the ninhydrin assay. Ninhydrin, in fact, is a chemical able to react with ammonia or primary and secondary amines, and when reacting with these free amines, a deep blue or purple color, known as Ruhemann's purple, is produced. By reading the absorbance (570 nm), we calculated the percentage of elastin free amino groups, therefore the sugar amount on elastin (insoluble and soluble). In table **4.1** we can observe that by increasing the sugar quantity at the beginning of the reaction, we have been able to increase the functionalization rate, both on insoluble and soluble elastin. Moreover, in the case of soluble elastin, the functionalization degree was higher if compared to insoluble elastin as expected, being the reductive amination reaction executed in a heterogeneous phase in the presence of a water soluble protein.

Table 4.1. Ninhydrin assays of insoluble (A) and soluble elastin (B).

A *Insoluble elastin*

Sugar eq	%functionalized amines	nmol (sugar)/mg (protein)
10	26	~90
50	36	~120
100	45	~150

B *Soluble elastin*

Sugar eq	%functionalized amines	nmol (sugar)/mg (protein)
10	49	~170
50	65	~240
100	79	~270

4.3 Conclusions

This chapter describes elastin matrices production and elastin (soluble and insoluble) functionalization with carbohydrates. In particular, elastin matrices were successfully neoglycosylated with galactose and glucose moieties, as demonstrated by FTIR analysis. Moreover, these materials have been characterized by scanning electron microscopy (SEM). On the other hand, soluble elastin was functionalized with galactose, glucose, and sialic acid epitopes. The functionalized samples have been characterized by FTIR analysis. Moreover, the amount of sugar on elastin matrix surfaces and on hydrolysed elastin was quantified by using the ninhydrin assay.

Biological assays with elastin scaffolds decorated with glucose moieties are in due course. In order to give a comparison with biological assays conducted with neoglucosylated collagen scaffolds, F11 cells have been chosen for these experiments. In particular, we want to understand if, by changing matrices, but maintaining the same functionalization, cell response will vary.

Chapter 5

Gelatin-based hydrogels for tissue engineering applications

5.1 Introduction

Hydrogels have become one of the most used platforms for three-dimensional (3D) cells cultures. The big versatility of hydrogel biomaterials makes it possible to design and produce scaffolds with established mechanical properties, as well as with desired biofunctionality. 3D hydrogel scaffolds have been used for a multiplicity of applications, including tissue engineering of microorgan systems, drug delivery and screening, and cytotoxicity testing. Furthermore, 3D culture is applied for studying cellular physiology, stem cell differentiation, and tumor models and for investigating interaction mechanisms between the extracellular matrix and cells.[170]

Hydrogels in tissue engineering must have smart properties to function appropriately and promote new tissue formation. These

properties include both classical physical parameters in order to allow degradation and have good mechanical features, as well as biological performance parameters (e.g., cell adhesion). One of the main critical parameters is the biocompatibility of hydrogels. Biocompatibility is based on the material's ability to stay within the body without causing detrimental effects on adjacent cells or lead significant scarring, or else evoke a response that detracts from its desired function. The inflammatory response to a hydrogel can affect the immune response toward the transplanted cells and vice versa. Hydrogels are composed of hydrophilic polymer chains that can be either synthetic or natural in origin. The structural integrity of hydrogels depends on crosslinks generated between polymer chains with different chemical bonds and physical interactions. Hydrogels structural properties should be similar to tissues and the ECM, and they can be delivered in a minimally invasive manner.

5.1.1 Hydrogels forming materials

A variety of naturally and synthetic derived materials may be used to produce hydrogels for tissue engineering scaffolds. Typical naturally derived polymers include gelatin, collagen, alginate, chitosan, fibrin, and hyaluronic acid (HA); on the other hand, synthetic materials include poly(ethylene oxide) (PEO), poly(vinyl alcohol) (PVA), poly(acrylic acid) (PAA), poly(propylene fumarate-co-ethylene glycol) (P(PF-co-EG)), and polypeptides.[171]

- Naturally derived materials: naturally derived hydrogels have usually been used in tissue engineering applications being either components of ECM or having macromolecular properties similar to the natural ECM. Likewise, hyaluronic acid is found in different amounts in all tissues of adult animals. Also alginate and chitosan, like hyaluronic acid, are hydrophilic and linear polysaccharides. Collagen fibers and scaffolds can be created and their mechanical properties improved by inserting various chemical crosslinkers (e.g., glutaraldehyde, carbodiimide), by crosslinking with physical treatments (e.g. UV irradiation, and heating), and by the combination with other polymers (e.g. hyaluronic acid, polylactic acid, poly(glycolic acid), poly(lactic-coglycolic acid), chitosan, PEO). Collagen is naturally degraded by metalloproteases, in particular collagenases, and serine proteases, allowing engineered tissue cells to degrade it. Gelatin is hydrolysed collagen, formed by breaking the natural triple-helix structure of collagen into single-strand molecules. There are two types of gelatin, gelatin A and gelatin B; gelatin A is prepared by using acidic conditions before thermal denaturation, while gelatin B is obtained with alkaline treatments that cause a high carboxylic content. Gelatin simply forms gels by changing the temperature of its solution. Gelatin-based hydrogels have been used in many tissue engineering applications due to their biocompatibility and facility of gelation. Gelatin hydrogels have also been used for delivery of growth factors to promote vascularization of engineered new tissues. Nevertheless, the weakness of the gels has been a problem, and a number of chemical modification methods have been considered to ameliorate the mechanical properties of gelatin hydrogels. HA is the simplest glycosaminolglycan (GAG) and is found in almost every mammalian tissue and fluid. It was found prevalently during wound healing and in synovial fluids of joints. It is a linear polysaccharide composed of a repeating disaccharide of (1–3) and (1–4)-linked β-D-glucuronic acid and N-acetyl-β-D-

glucosamine units. Hydrogels of HA have been produced by covalent crosslinking for example with hydrazide derivatives,[172] by esterification, and by annealing.[173] Additionally, HA has been combined with both collagen and alginate to form composite hydrogels.[174] HA is naturally degraded by hyaluronidase. Alginate has been used in different medical applications such as cell encapsulation and drug delivery, because it is able to gel under mild conditions, and has low toxicity. Alginate is a linear polysaccharide copolymer of (1–4)-linked β-D-mannuronic acid (M) and α-L-guluronic acid (G) monomers, and is derived primarily from brown seaweed and bacteria; the M and G monomers are sequentially distributed in either repeating or alternating blocks. Hydrogels are produced when divalent cations such as Ca^{2+}, Ba^{2+}, or Sr^{2+} cooperatively interact with blocks of G monomers to form ionic-bridges between different polymer chains; the crosslinking density and so mechanical features and pore size of the ionically crosslinked hydrogels can be readily manipulated by using different M and G ratio and molecular weight of the polymer chain. Hydrogels can also be created by covalently crosslinking alginate with adipic hydrazide or PEG using common carbodiimide chemistry.[175] Chitosan has been studied for many tissue engineering applications; in fact it is structurally similar to naturally occurring GAGs and is degradable by human enzymes. It is a linear polysaccharide of (1–4)-linked D-glucosamine and N-acetyl-D-glucosamine residues derived from chitin, which is found in arthropod exoskeletons. Chitosan is soluble in dilute acids which protonate the free amino groups, so, chitosan can be gelled, for example, by increasing the pH. Its derivatives and mixtures have also been gelled *via* glutaraldehyde crosslinking,[176] UV irradiation,[177] and thermal variations.[178] Chitosan is degraded by lysozyme.

- Synthetic materials: synthetic hydrogels are interesting biomaterials for tissue engineering because their chemistry and properties can be controlled and reproducible. For

example, synthetic polymers can be reproducibly created with specific molecular weights, degradable linkers, and crosslinking modes. Consequently, these properties regulate gel formation dynamics, crosslinking density, material mechanical properties and degradation. Examples of synthetic materials are PEO ((poly(ethylene oxide)), PVA (poly(vinyl alcohol)), and P(PF-co-EG) (poly(propylene furmarate-co-ethylene glycol). PEO is currently FDA approved for a lot of medical applications and is one of the most usally applied synthetic hydrogel polymers for tissue engineering. PEO and poly(ethylene glycol) (PEG) are hydrophilic polymers that can be photocrosslinked by modifying each end of the polymer with either acrylates or methacrylates.[179] Hydrogels are produced modifying PEO or PEG, mixing them with the appropriate photoinitiator and crosslinked *via* UV light exposure. Thermally reversible hydrogels have also been produced from block copolymers of PEO and poly(l-lactic acid) (PLLA) and PEG and PLLA.[180] Another synthetic hydrophilic polymer largely used in space filling and drug delivery applications is PVA; it can be physically crosslinked by repeated freeze-thawing cycles of aqueous polymer solutions or chemically crosslinked with glutaraldehyde or succinyl chloride to form hydrogels.[181]

5.1.2 Applications of hydrogels in tissue engineering

There are a lot of applications in regenerative medicine where hydrogels have found efficacy. Langer and Vacanti[182] first elucidated the basic methods utilized in tissue engineering to repair damaged tissues, and the ways by which polymer gels are used in these techniques. Hydrogels, in regenerative medicine, have been used as scaffolds to supply structural integrity and bulk for cellular organization and morphogenic guidance, to be useful as tissue

barriers and bioadhesives, to function as drug depots, to deliver bioactive molecules that drive the natural reparative processes, and to embed and deliver cells.[183]

- Hydrogels as scaffold materials: hydrogels are interesting scaffolding materials having mechanical properties that can be adapted to mimic those of natural tissues. Hydrogels are used as scaffold to give bulk and mechanical organization to a tissue construct, whether cells are adhered to or suspended within the 3D gel framework. A powerful strategy to allow and enhance cellular adhesion is the inclusion of the well known RGD adhesion peptide sequence, recognized by fibroblasts, endothelial cells, osteoblasts, and chondrocytes. One essential trait of tissue scaffold is to preserve cellular proliferation and desired cellular distribution. The importance of scaffold degradation in tissue cultures has been demonstrated by studying cellular viability in non-degradable scaffolds. For example, poly(ethylene glycol)-dimethacrylate (PEGDMA) and PEG have been photopolymerized to form hydrogel networks with embedded chondrocytes for cartilage regeneration,[184] but after photopolymerization, cells encapsulated into scaffold were viable and evenly dispersed, but, being these scaffolds non-degradable, the number of cells has the tendency to decrease significantly in the time. Mann et al.[185] utilized PEG-diacrylate derivatives functionalized with RGD-peptides to create photopolymerized hydrogels as scaffolds for vascular smooth muscle cells. These cells remained viable within scaffolds, continued to proliferate, and produced ECM proteins. Cells were shown to have the ability to spread and migrate in proteolytically degradable scaffolds, but they were spherical and banded together in non-degradable hydrogels. It was shown that in proteolytically degradable hydrogels, cells proliferation and ECM production over cells in non-degradable PEG-diacrylate scaffolds are increased. Even if many objectives have been achieved with the use of hydrogel scaffolds for tissue

regeneration applications, these materials should usually be biodegradable to maximize the ability of scaffolds to encourage proliferating replacement tissues.

- Hydrogels as barriers: to enhance the healing response succeeding tissue damage, hydrogels have been utilized as barriers in order to defend against restenosis or thrombosis caused by post-operative adhesion formation.[186] It has been demonstrating that building a thin hydrogel layer intravascularly with interfacial photopolymerization will inhibit restenosis by reducing intimal thickening and thrombosis. The thin hydrogel layer is able to decrease intimal thickening because it furnishes a barrier to impede platelets, coagulation factors, and plasma proteins from the contact with the vascular wall; contacting these factors to vessel walls stimulates smooth muscle cell proliferation, migration, and ECM synthesis events that bring to restenosis. Hydrogel barriers have also been used to prevent post-operative adhesion formation. For example, poly(ethylene glycol-co-lactic acid) diacrylate hydrogels were produced by bulk photopolymerization on intraperitoneal surfaces. These hydrogel barriers were able to avoid fibrin deposition and fibroblast attachment at the tissue surface.[187]
- Hydrogels with drug delivery capabilities: due to their hydrophilicity and biocompatibility, hydrogels are often used as localized drug depots, having also drug release rates that can be controlled[188] and triggered smartly by interactions with biomolecular stimuli.[189] Macromolecular drugs, such as proteins or oligonucleotides that are hydrophilic, can be used as hydrogels. By monitoring the degree of swelling, crosslinking thickness, and degradation rate, delivery kinetics can be designed in accordance with the desired drug release plan. In addition, photopolymerized hydrogels are very useful for localized drug delivery having the ability to adhere and conform to targeted tissue when developed *in situ*. Drug delivery features in hydrogels can be used to work together with the barrier role of hydrogels to deliver therapeutic

agents locally while inhibiting post-operative adhesion formation. Take as an example, hydrogels assembled on the inner surface of blood vessels *via* interfacial photopolymerization that have been used for intravascular drug delivery.[190] These gels can be formed in bilayers, where the inner layer is less permeable than the outer layer near the vessel wall. A lower molecular weight polymer precursor is used to produce the luminal layer, making it less permeable. The function of this bilayer hydrogel structure is to improve the delivery of released proteins into the arterial media. Moreover, different drug concentrations can be encapsulated into each layer during synthesis of a multilayer matrix device to obtain excellent release behavior.

- Hydrogels for cell encapsulation: cell transplantation can be realized with hydrogels because they can supply immunoisolation while still enabling oxygen, nutrients, and metabolic products to distribute with facility into the hydrogel. For the design and production of a bio-artificial endocrine pancreas, photopolymerized PEG diacrylate (PEGDA) hydrogels have been formed to transplant islets of Langerhans.[191] In these researches, islet cells were suspended in a photopolymerizable PEG diacrylate prepolymer solution, and the solution was used to create PEG-based microspheres that captured the islets. The first formulation of these microspheres contributed to sufficient immunoisolation; nevertheless, the nutrients diffusion to the entrapped cells was constrained. Another formulation takes into account a reduction in thickness of the interfacially photopolymerized hydrogels to enhance the diffusion of nutrients to the encapsulated islets. By reducing thickness, encapsulated islets are viable for long periods and the hydrogel preserves its immunoisolation function.

5.1.3 Methods of preparation of hydrogels

Hydrogels can be prepared by various methods depending on the designed structure and the desired application. Some of these methods are discussed below and summarized in **Figure 5.1**.

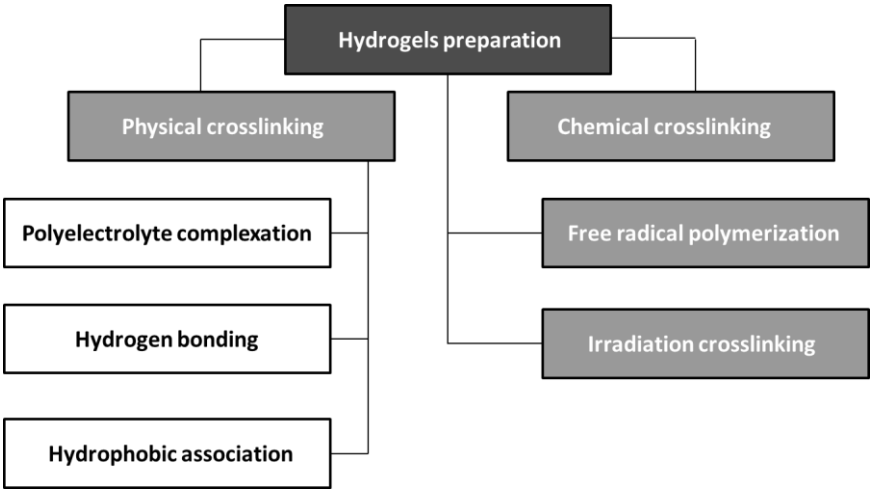

Figure 5.1. Schematic diagram showing the most common methods of preparation of hydrogels.

- Free radical polymerization: traditional free radical polymerization is the favourite technique for development of hydrogels based on monomers such as acrylates, amides and vinyl lactams.[192,193] It can also be used for the production of natural polymers-based hydrogels on condition that these polymers have appropriate functional groups or have been decorated with radically polymerizable groups. For example, this approach has been used to create different chitosan-based hydrogels.[194] This method requires the typical free radical polymerizations steps, which are: initiation, propagation, chain transfer and termination. In the initiation step a lot of visible, thermal, ultraviolet and red-ox initiators can be utilized for radical generation; these radicals then can react with monomers transforming them into active forms that react with more monomers and so on in the propagation step. The developed long chain radicals are subjected to

termination either by chain transfer or by radical combination producing polymeric matrices. This approach can be executed either in solution or neat (bulk). Solution polymerization is attractive during synthesis of large amount of hydrogels and, in this condition, water is the most generally used solvent. Bulk polymerization is faster than solution polymerization and does not require a solvent removal, which is usually time consuming.

- Irradiation crosslinking of hydrogel polymeric precursors: ionizing-radiation techniques, especially if in combination with a concurrent sterilization procedure, are very efficient approaches for synthesis of hydrogels. Ionizing radiations, such as electron beam and γ–rays, have high energy enough to ionize simple molecules either in air or water. During irradiation of a polymer solution, a lot of reactive sites are created along the polymer strands. Furthermore, the combination of these radicals brings to generation of a wide number of crosslinks. Production of hydrogels using this technique can be achieved *via* irradiation of the polymers in bulk or in solution. Nevertheless, irradiation of a polymer solution is the preferred because of the less energy needed for production of macroradicals. Moreover, in solution the efficiency of radicals is high because of the reduced density of reaction mixture. Administering irradiation to hydrogel development gives many advantages over other preparation techniques in which, during the irradiation process, no catalysts or additives are required to initiate the reaction. Moreover, irradiation approaches are easy and the crosslinking extent can be checked simply by changing the irradiation dose.[195] This method has been utilized for creating a variety of hydrogels for many biomedical applications, where even the smallest contamination is not desirable. For example, it has been used efficiently to form acrylic acid hydrogels and PEG/carboxymethyl chitosan-based pH-responsive hydrogels.[196] However, this method is not suggested for generation of hydrogels from some polymers

that can undergo degradation under the ionizing irradiation.[197]

- Chemical crosslinking of hydrogel polymeric precursors: chemical crosslinking of hydrophilic polymers is one of the main used techniques for hydrogel preparation. In this method, a bi-functional crosslinking agent is added to a solution of a hydrophilic polymer and the polymer may have an appropriate functionality in order to react with the crosslinking agent; this technique is adequate for generation of hydrogels from both natural and synthetic hydrophilic polymers. For example, albumin and gelatin–based hydrogels were produced using dialdehyde or formaldehyde as crosslinking agents. Also hydrogels with high water content based on crosslinking of functionalized PEG and a lysine-containing polypeptide have been fabricated by this method.[198]
- Physical crosslinking of hydrogel polymeric precursors: crosslinking with physical interactions of polymers is one of the general techniques for hydrogel development. This physical crosslinking comprehends interactions such as polyelectrolyte complexation, hydrogen bonding and hydrophobic association, and the hydrogels produced by this approach are commonly fabricated under mild conditions.

  a) Polyelectrolyte complexation (ionic interactions): by using this method, hydrogels are produced through development of polyelectrolyte complexes, where links are generated between pairs of charged sites on the polymer backbones. The produced electrolytic links differ in their stabilities based on the pH of the system. Hydrogels produced by this technique are those obtained from the polyelectrolyte complexation of the carboxylate groups of sodium alginate with the amino groups of chitosan chains.

  b) Hydrogen bonding: hydrogen bonding between polymer chains can contribute to hydrogel development, for example, in producing gelatin-based hydrogels. A hydrogen bond is formed through the association of an electron deficient

hydrogen atom and a functional group of high electronegativity. Hydrogels generated by this method are altered by many factors: polymer concentration, molar ratio of each polymer, type of solvent, solution temperature, and the degree of association between the polymer functionalities.

c) Hydrophobic association: polymers and copolymers, such as graft and block copolymers, generally form structures disconnected by hydrophobic micro-domains. These hydrophobic domains act as associated crosslinking points in the entire polymeric structure, and are surrounded by hydrophilic water absorbing regions; this method has been used to create a hydrogel based on a graft-type copolymer made up of hydrophilic poly(hydroxyethyl methacrylate) (PHEMA) as a backbone and a small amount of hydrophobic poly(methylmethacrylate) (PMMA) as a long branch.

Generally, the mechanical features of these hydrophobically combined polymers are poor because of the poor interfacial adhesion. Nevertheless, this technique for hydrogel formation has some advantages such as the low cost of the system.

5.2 Gelatin-based hydrogels

During my PhD, I focused my attention, principally on gelatin based-hydrogels obtained with different synthetic strategies, and their biological evaluation.

5.2.1 Hydrogels *via* thiol-ene chemistry and biological assays

Click-chemistry is almost the most popular biocompatible approach[199] for *in situ* hydrogel formation. Metal-free click reactions, such as Diels-Alder, strain-induced coupling and radical reactions based on (metha)acrylate systems or thiol-based photo-

polymerizations (i.e. thiol-ene[200] and thiol-yne chemistry[201]) are the most relevant. Radical reactions are the most widely used, since they usually occur on a time scale that does not significantly impact on cell viability, they can be performed in cell-friendly solvents (i.e. water) in mild conditions. The thiol-ene photopolymerization is largely used for hydrogel fabrication.[202,203]

In light of these premises we synthesized new hydrogels obtained by thiol-ene photopolymerization of differently functionalized gelatin precursors. The major problem of gelatin is that it dissolves at physiological temperature (37°C), so we decided to synthesize a thiolated gelatin (gelatin lacks of thiol groups, since cysteine is not present in its primary structure) and a pentenoyl-gelatin that, with its double bonds, can react with a thiol-ene reaction in the presence of a photoinitiatior.

Alkene functionalities have been introduced into gelatin by reaction with pentenoic anhydride in the presence of pyridine in dimethylformamide (DMF, **Scheme 5.1A**), while gelatin was thiolated by reaction with γ-thiobutyrolactone in phosphate buffer saline and ethanol (**Scheme 5.1B**).

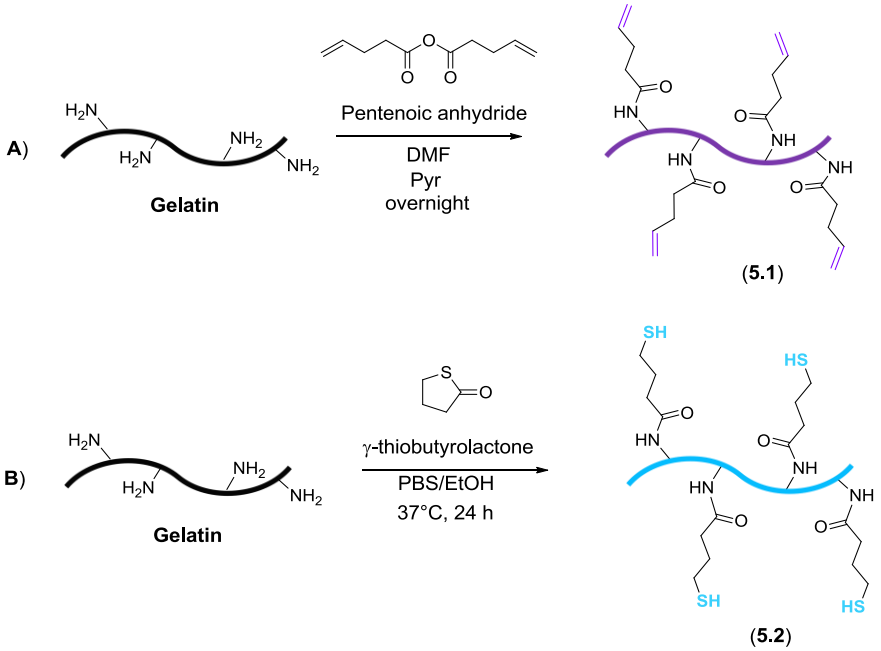

Scheme 5.1. Synthesis of pentenoyl gelatin 5.1 (A) and thiolated gelatin 5.2 (B).

Hence thiolated gelatin (**5.2**) can be photopolymerized with pentenoyl gelatin (**5.1**) *via* the thiol–ene reaction under physiological conditions (**Scheme 5.2**).

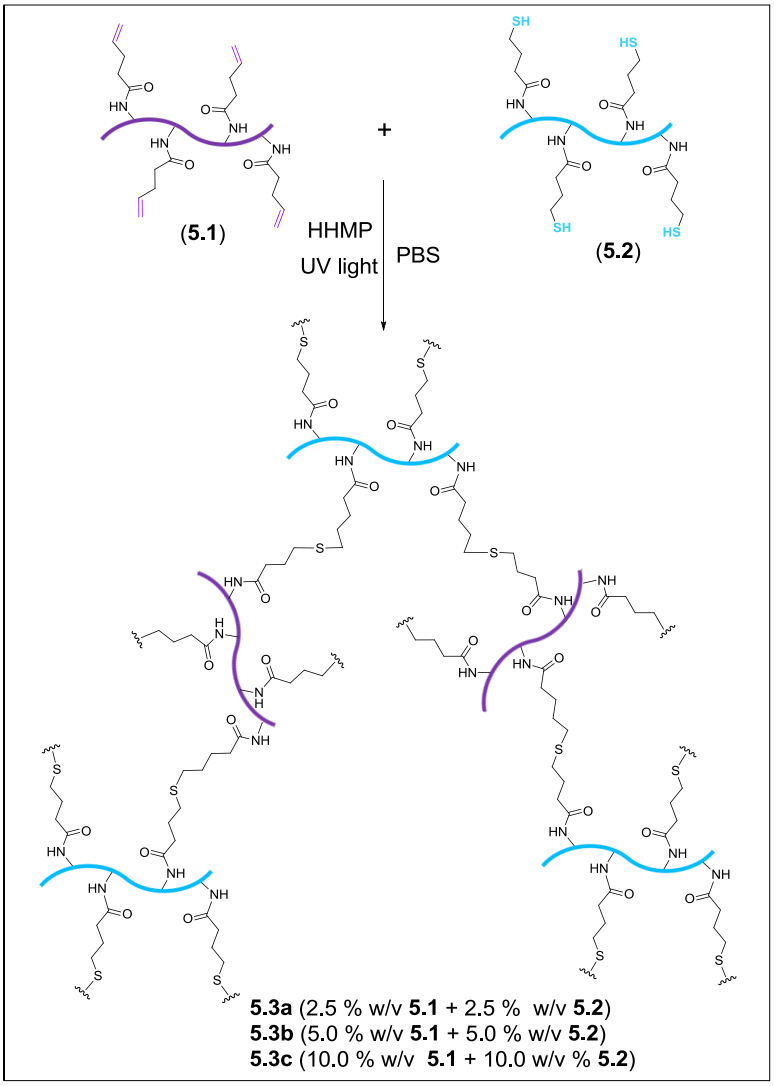

Scheme 5.2. Photopolymerization of gelatin 5.1 with gelatin 5.2 to obtain hydrogels 5.3a, 5.3b, and 5.3c.

Aiming at synthesizing a novel hydrogel formulation, three different gelatin concentrations have been evaluated: 2.5 % w/v, 5% w/v and 10 % w/v of both components (**5.1** and **5.2**) were used.

Biological assays

Although any hydrogel should have unique physicochemical features, tailored around the specific applications, all hydrogels for biological employments, necessitate to satisfy the typical requirement of cytocompatibility. Therefore, preliminary biological experiments were performed embedding hBMSCs (human bone marrow stromal cells) into hydrogels in order to evaluate their effect on cellular behavior and metabolic activity after 3 days of culture. Two concentrations (hydrogels **5.3a** and **5.3b**) resulted appropriate for cellular encapsulation in a 3D environment; the highest concentration mixture polymerized too quickly, thus not allowing efficient cell encapsulation. Both hydrogels (**5.3a** and **5.3b**) preserved their original shape throughout the culture time, even though few non-homogeneities were noticeable immediately after polymerization (**Figure 5.2**).

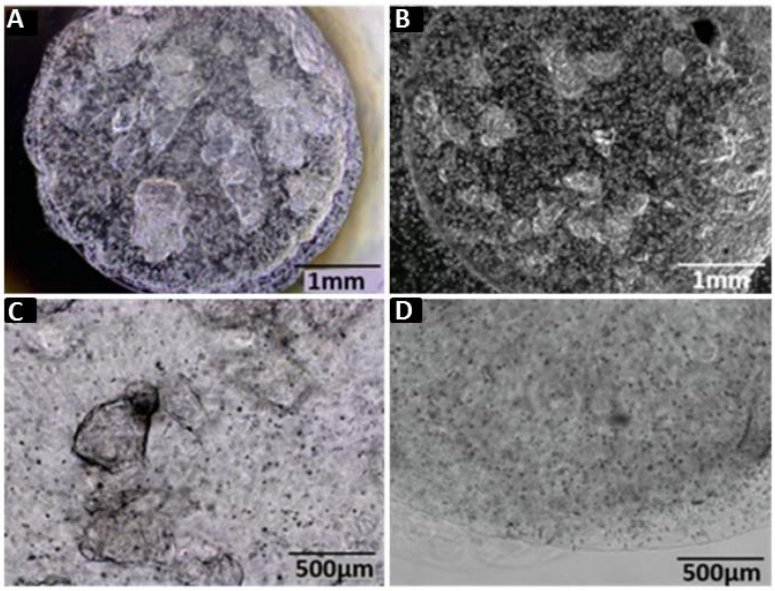

Figure 5.2. hBMSCs embedded in hydrogels cross-linked with UVA light for 5 min. After 1 day of culture both hydrogels 5.3a (A) and 5.3b (B) maintained the original 3D shape, both starting to promote cell spreading (C, D).

After 3 days in culture, hBMSCs exhibited an elongated morphology in hydrogel **5.3a**, indicating its tendency to promote cell spreading (**Figure 5.3A**). Moreover, cells remained viable, as underlined by MTT assay performed on hydrogel **5.3a**, confirming hydrogel cytocompatibility (**Figure 5.3B**). Additionally, cells embedded and cultured in hydrogel **5.3a** showed a statistically significantly higher metabolic activity if compared to hydrogel **5.3b** ($10.7 \times 10^4 \pm 5.9 \times 10^3$ *vs* $5.6 \times 10^4 \pm 5.2 \times 10^3$, respectively), suggesting that the lower hydrogel concentration has mechanical and chemical properties that better sustain cell culture (**Figure 5.3C**). Further studies are needed

to fully characterize the new hydrogels behavior in biological systems.

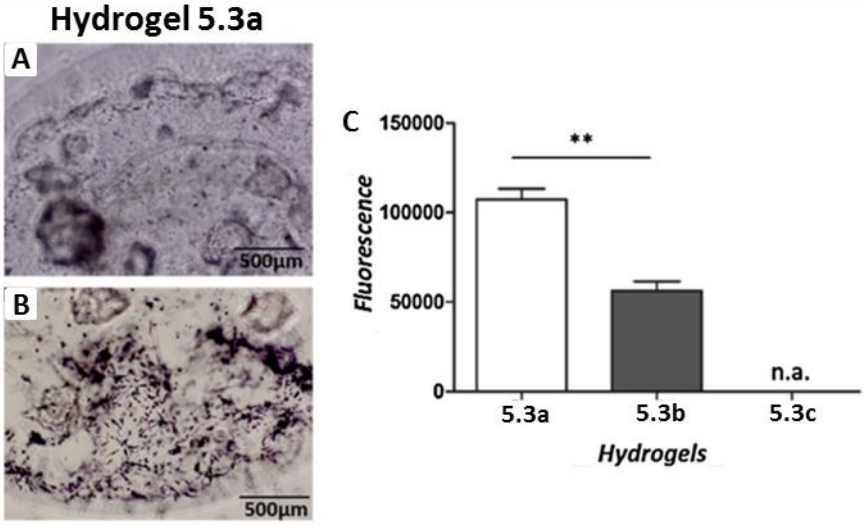

Figure 5.3. After 3 days in culture, hydrogel 5.3a promote hBMSC spreading as highlighted both in the phase contrast image (A) and by the MTT colorimetric assay (B). The higher compatibility of hydrogel 5.3a was also confirmed by the quantification of specific metabolic activity of hBMSCs cultured up to 3 days within the hydrogels, which resulted statistically higher in the hydrogel 5.3a (C). Statistical analyses were performed using the Student's t-test. *p<0.05, **p<0.01, and ***p<0.001.

5.2.2 Hydrogels with thiolated gelatin and gelatin modified with maleimido groups

Thiolated gelatin (**5.2**) was also used for hydrogels production with a different synthetic strategies; in particular we obtained stable hydrogels by reacting it with gelatin modified with maleic anhydride. The functionalization of gelatin with maleic anhydride has been conducted in tetrahydrofuran (THF) overnight, obtaining gelatin **5.4** (**Scheme 5.3**).

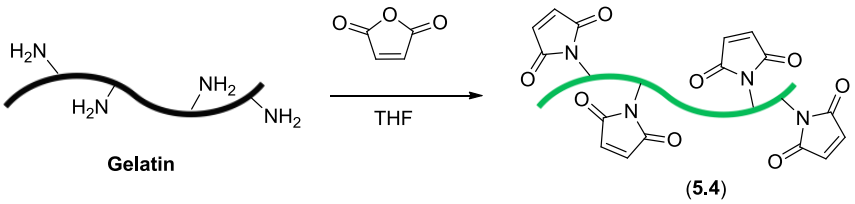

Scheme 5.3. Synthesis of gelatin 5.4.

Hydrogel **5.5** has been obtained by reacting the two modified gelatins in PBS (**Scheme 5.4**).

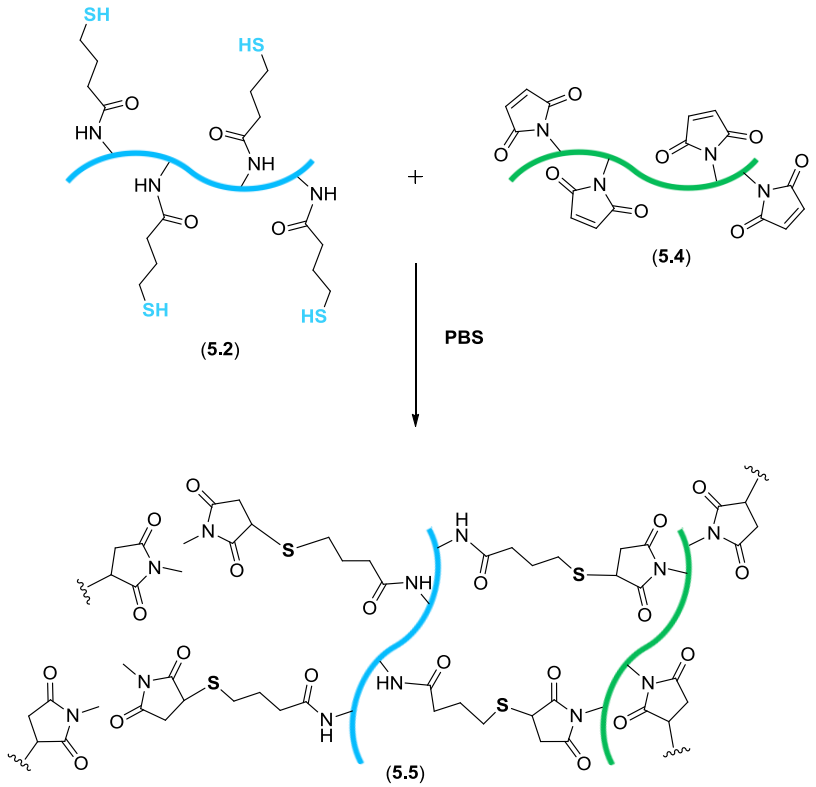

Scheme 5.4. Synthesis of hydrogel 5.5.

5.2.3 Hydrogels with gelatin and PEG derivatives

By reacting pentenoyl-gelatin (**5.1**) with a PEG derivatives, a new stable hydrogel has been obtained; in particular the commercial available poly(ethylene oxide), 4-arm, thiol terminated, in the presence of a photinitiator, under UV light (**scheme 5.5**) lead to the production of hydrogel **5.6**.

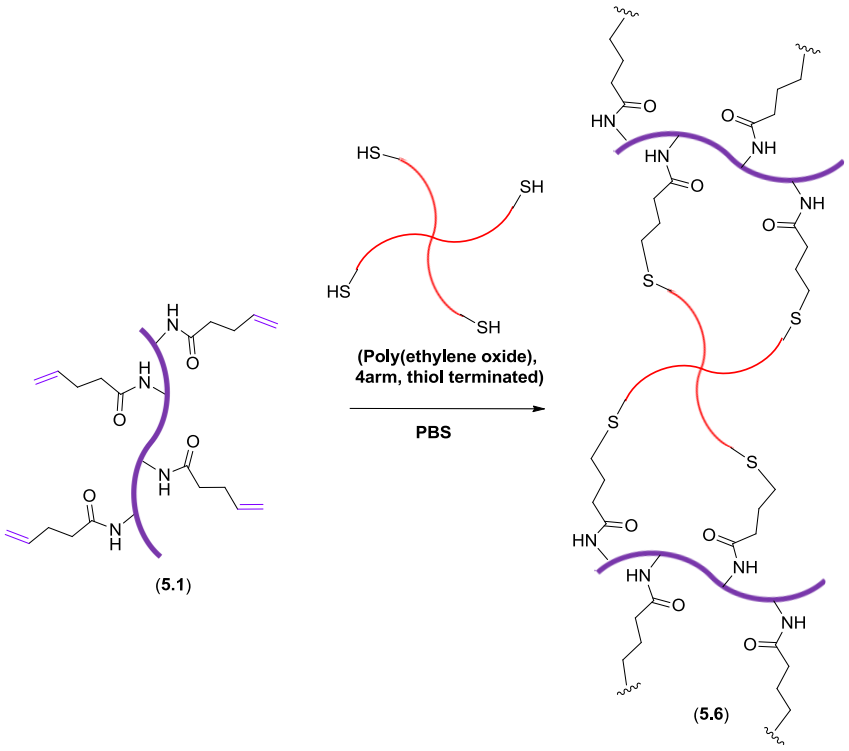

Scheme 5.5. Synthesis of hydrogel 5.6.

5.2.4 Hydrogels with gelatin and dimethyl squarate

Another method used for the production of hydrogels has been based on the reaction of gelatin with 3,4-dimethoxy-3-cyclobutene-

1,2-dione (dimethyl squarate). Hydrogel **5.7** has been obtained in carbonate buffer (pH 9.2) (**Scheme 5.6**, **Figure 5.4**).

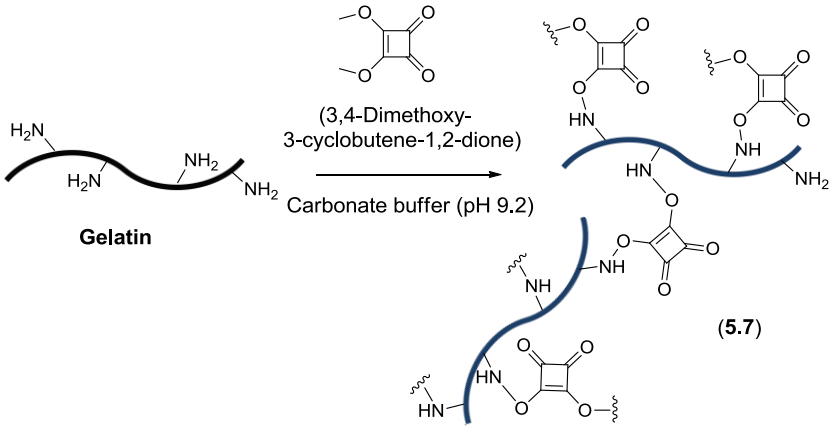

Scheme 5.6. Synthesis of hydrogel 5.7.

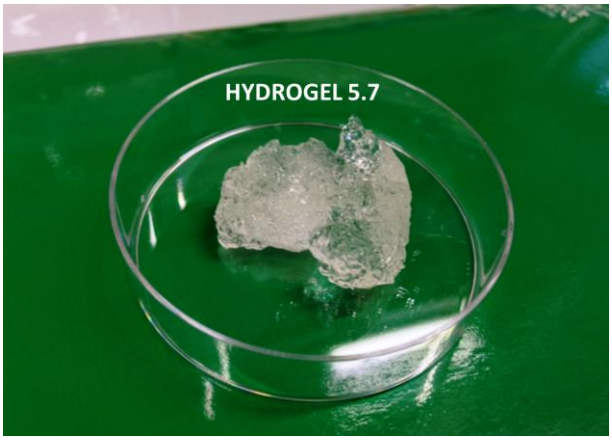

Figure 5.4. Photograph acquired by a standard camera of hydrogel 5.7.

5.3 Conclusions

In this chapter, the synthesis of differently modified gelatins and the production of hydrogels are discussed. Mild reaction conditions were

used for the synthesis of all gelatin-based hydrogels. Regarding hydrogels **5.3a** and **5.3b**, biological assays with hBMSCs embedded on them have been conducted, highlighting the hydrogels ability to sustain cell growth, providing a good 3D cell environment. With regard to all other synthesized hydrogels, we are now planning future biological assays, in order to verify their ability to support cell culture conditions. In particular, we should produce hydrogels functionalized with specific biomolecules, such as carbohydrates, that could be good candidates as smart biomaterials for regenerative medicine.

Chapter 6

General conclusions and remarks

My PhD project has led to the development of different biomaterials based on collagen, elastin, or gelatin. Regarding the first two proteins, their insoluble and soluble forms have been used for biomaterials production. Carbohydrates, due to their biological relevance, have been considered as excellent candidates for the decoration of these biomaterials, with the aim to study their potential effect on different biological systems. The functionalization with carbohydrates has been achieved using different chemical strategies; neoglycosylated collagen and elastin have been successfully obtained, as demonstrated by their physico-chemical characterizations.

Collagen films decorated with carbohydrates have been employed in different biological assays with several cell-lines. In all cases, collagen matrices have not caused any detrimental effect on cell growth and proliferation. Moreover, based on the sugar exposed, collagen matrices have been able to modulate cell fate. Morphological and

functional analysis have shown that collagen matrices decorated with glucose moieties were able to drive F11 cells to differentiate without the addition of any chemical differentiating agents in the culture medium. Collagen films exposing on their surface two different sialosides epitopes have influenced mMSCs gene expression toward osteogenesis or chondrogenesis. These results reinforce the idea that glycobiology represents an important tool of enlightenment for cellular and molecular medicine for tissue repair processes.

Sugar-decorated elastin will be used in future experiments, in order to evaluate the effective role of sugars on cell differentiation.

Deeper studies on cell-scaffold interactions are needed to understand the mechanisms underlying these findings.

Moreover, the production of soluble injectable biomaterials could be used to study the potential role of carbohydrates in *in vivo* models.

Finally, gelatin-based hydrogels have been synthesized using different synthetic strategies. Preliminary cell biocompatibility data with hydrogels obtained *via* thiol-ene chemistry have been reported; these new hydrogels have provided a good 3D cell microenvironment. Additional experiments will be useful to fully characterize the new biomaterials behavior in biological systems.

Chapter 7

Materials and methods

7.1 Collagen

7.1.1 Collagen films preparation

Type I collagen films were produced by a solvent-casting method. Briefly, collagen type I (from bovine Achilles tendon - Sigma-Aldrich, catalog no. C9879) was dissolved in acetic acid 0.5 M for 4 h at 40 °C. The suspension was homogenized with a mixer for 2 min at maximum speed. After removal of the aggregates, 40 mL of collagen solution was poured into an 8.5 × 12.5 cm^2 culture multiwell lid and the solvent evaporated in the fume hood for 2 days. The collagen matrices were produced as thin transparent films (1 mg/cm^2).

7.1.2 General procedure for collagen films neoglycosylation with maltose, cellobiose, and lactose (collagens 3.1, 3.2, and 3.3)

A piece of collagen patch (80 mg, 12 cm × 7 cm) was immersed in 20 mL of 0.06 M sugar solution followed by the sequential addition of 0.03 M $NaBH_3CN$ in citrate buffer (pH 6.00) and reacted overnight.

After this time, the collagen film was thoroughly washed first with 20 mL of milliQ (mQ) H_2O three times for 20 min, and finally with 20 mL of ethanol for 10 min.

7.1.3 General procedure for collagen films neoglycosylation with 3'-sialyllactose and 6'-sialyllactose (collagens 3.4 and 3.5)

A collagen patch (80 mg, 12 cm × 7 cm) was immersed in 20 mL of 0.006 M 6'-sialyllactose or 3'-sialyllactose solution followed by the sequential addition of 0.003 M $NaBH_3CN$ in citrate buffer (pH 6.00) and reacted overnight. After this time, the collagen film was thoroughly washed first with 20 mL of mQ H_2O three times for 20 min, and finally with 20 mL of ethanol for 10 min.

7.1.4 Synthesis of insoluble collaggrecan (collagen 3.6)

A piece of collagen patch (2 mg) was immersed in 2 mL of 1.5 mM chondroitin-6-sulfate (from shark cartilage, CAS number 12678-07-8) solution followed by the addition of 0.75 mM $NaBH_3CN$ in citrate buffer (pH 6.00) and reacted overnight at room temperature. The collagen film was then washed with 2 mL of HCl 0.1 M for 10 min, 2 mL of NaOH 0.1 M for 10 min, 2 mL of mQ water three times for 20 min, and finally with 2 mL of ethanol for 10 min.

7.1.5 General procedure for hydrolyzed collagen neoglycosylation with maltose, 3'-sialyllactose and 6'-sialyllactose (collagens 3.7, 3.8, and 3.9)

100 mg of soluble collagen (Semed S collagen powder - DSM Biomedical - PN 20003-01) was dissolved in 8 mL of citrate buffer (pH 6.00). The selected carbohydrate (0.2 M) and $NaBH_3CN$ (0.1 M) was sequentially added to the collagen solution and reacted overnight. The reaction mixture was purified with dialysis tubing (MWCO 14000 Da - Sigma-Aldrich, catalog no. D9527) against water and then lyophilized.

7.1.6 Synthesis of soluble collaggrecan (collagen 3.10)

100 mg of soluble type I bovine collagen (Kensey Nash, from bovine) was dissolved in 10 mL of 0.16 mM chondroitin-6-sulfate aqueous solution followed by the sequential addition of 0.08 mM $NaBH_3CN$ in citrate buffer (pH 6.00) and reacted for 24 h at room temperature. The reaction mixture was purified with Vivaspin 20 centrifugal concentrators (MWCO 100,000 Da), 4 washings for 15 min at 3000 rpm (i.e., until no unreacted chondroitin-6-sulfate was detectable by FT-IR), and lyophilized.

7.1.7 Neoglycosylated collagens characterizations

- **NMR Quantification**

Derivatization of the native and neoglycosylated collagen samples with maleic anhydride was performed to label and quantify $-NH_2$ groups of lysine residues. Collagen films (32 mg) were immersed in a THF solution (0.04 M) of maleic anhydride in the presence of $NaHCO_3$. The reaction was carried out at room temperature overnight. After thoroughly washing with mQ H_2O, followed by ethanol, collagen films were dried under vacuum and then dissolved in 0.6 mL of 2 M NaOD in D_2O. ^1H NMR spectra were recorded using a Varian 400 MHz Mercury instrument, operating at a proton frequency equal to 400 MHz, at room temperature. The 90° pulse-width (pw90) was calibrated, the number of scans varied depending on the signal-to-noise ratio, and the recycling delay was 5 s.

- **Atomic Force Microscopy (AFM) (*In collaboration with Prof. Mario Raspanti - Insubria University*)**

Specimens were dehydrated with increasing concentrations of ethanol and then with hexamethyldisilazane (HMDS, Sigma), immobilized onto biadhesive tape and observed with a Digital Instruments Multi-Mode Nanoscope IIIa equipped with a Digital Instruments phase Extender and fitted with Nanosensors Tesp-SS or with Olympus OTESPA silicon probes ($k \approx 42$ N m^{-1} and $f \approx 300$ kHz, for both). Images were obtained *via* tapping-mode atomic force

microscopy in air, at a scan speed of 1.5−2 Hz, and at a resolution of 512 × 512 pixel.

- **Fourier Transform Infrared (FTIR) Spectroscopy (*In collaboration with Dr. Antonino Natalello - Department of Biotechnology and Biosciences, University of Milano-Bicocca*)**

FTIR spectra in attenuated total reflection (ATR) were collected by using the Golden Gate device (Specac) equipped with a single reflection diamond element. The Varian 670-IR spectrometer (Varian Australia Pty Ltd., AU) was used under the following conditions: 2 cm^{-1} spectral resolution, 25 kHz scan speed, 512 scan coadditions, triangular apodization and nitrogen-cooled mercury cadmium telluride detector. A qualitative ATR/FTIR characterization of the surface of the collagen patches was obtained by scraping out their external layers on the ATR element and collecting the spectra of the materials moved out from the film. The absorption spectra were reported after baseline correction between 1800 and 900 cm^{-1} and normalization at the amide I band intensity to compensate for the different protein content. In the case of the soluble samples, 2 µL of the sample solution in milliQ water were deposited onto the diamond element of the ATR device. After solvent evaporation, the sample was then washed with milliQ water, air dried, and measured as reported above for the solid samples

7.1.8 ELLA Assays (Enzyme Linked Lectin Assay) on collagen matrices exposing glucose and galactose

Pristine collagen and glycosylated collagen samples were blocked with a solution of 2% BSA in PBS (100 µL) and shaken (14 h, 5 °C), according to manufacturer's protocol. The films were then removed and respectively incubated at room temperature with a solution of the lectin from peanut (*Arachis hypogaea*) and from *Canavalia ensiformis* (Jack bean) peroxidase labeled (Sigma-Aldrich, catalog no. L7759 and L6397) (0.01 mg/mL, 200 µL) in PBS for 2 h with shaking. The films were then thoroughly washed with PBS to remove unbound lectin and then treated with a solution of OPD (SIGMAFAST^{TM} OPD, Sigma-Aldrich, catalog no. P9187) (500 µL, 1 h). The absorbance of an aliquot of this solution (200 µL) was measured at 450 nm.

7.1.9 MG63 cell culturing and proliferation assay on neogalactosylated collagen matrices (*In collaboration with Prof. Rodolfo Quarto - University of Genova)*

Human osteosarcoma MG63 cells were cultured in Coon's modified F12 Medium (F12; Biochrom AG, Berlin, Germany) containing 10% foetal calf serum (FCS; GIBCO Invitrogen Corp., Milano, Italy) at 37°C and 5% CO_2. The pristine and chemically modified collagen matrices, layered onto support polystyrene plates, were placed into the wells of 24-well plates, previously coated with a sterile 1% agarose solution to avoid cell attachment and growth outside the matrices; cells were

then seeded onto the matrices at a density of 25 x 10^4 cells per well and let adhere for 4 h. As an alternative, control cultures were executed also on the untreated standard plastic ware; for each culture condition six independent replica wells were prepared. Unattached cells were removed and each well was washed twice with sterile phosphate buffered solution (PBS), pH 7.4. A fresh medium, supplemented with 10% Alamar Blue™ (Life Science Invitrogen, Milano, Italy) was added and the plates were incubated at 37°C in the dark for the following 4 h. Supernatants were collected and briefly centrifuged (14000 rpm, 30 s) while each well was replenished with fresh F12 + 10% FCS. This procedure was repeated after 2, 4 and 7 days of culture. To evaluate cell growth in each culture condition at each time point, equal volumes of supernatants (200 µL) were assessed in duplicates, according to the manufacturer's instructions, at 570 and 600 nm using a Spectra MR spectrophotometer (Dynex Technologies, Chantilly, VA, USA). After 7 days of culture, matrix samples were washed twice in PBS, accurately removed from the polystyrene plates and placed onto a glass slide. Collagen matrices were then fixed in 4% formaldehyde in PBS for 30 min at RT and consequently exposed to a 3 µM solution of DAPI (Invitrogen Molecular Probes; Milano, Italy) in PBS for 15 min. Stained matrices were then re-washed in PBS, layered with a drop of Dako Fluorescent mounting medium (Dako North America Inc., Carpinteria, CA, USA) and covered with a cover slip glass. Images

were acquired using a Nikon Digital Sight DS-5Mc camera mounted on an Olympus BX51 fluorescence microscope.

7.1.10 F11 cell cultures and immunofluorescence analysis on neoglycosylated collagen matrices (*In collaboration with Dr. Marzia Lecchi - Department of Biotechnology and Biosciences, University of Milano-Bicocca*)

F11 cells (mouse neuroblastoma N18TG-2 x rat DRG[17]) were seeded on native and functionalized collagen patches at 60000 cells/35 mm dish and were maintained without splitting until the day of the experiment. They were cultured in Dulbecco's modified Eagle's medium (Sigma-Aldrich), 10% of fetal calf serum (Sigma- Aldrich), 2 mM glutamine (Sigma-Aldrich) and incubated at 37°C in a humidified atmosphere with 5% CO_2. They received fresh medium twice per week. Following a 7-day incubation period, the cells underwent morphological and functional analysis.

Transmission images of F11 cells on the collagen matrices were obtained by the laser scanning confocal microscope Leica Mod, TCS-SP2 (Leica Microsystems Heidelberg GmbH, Mannheim, Germany) coupled to a DMIRE2 inverted microscope, using the 20X objective HC PL FLUOTAR with N.A. of 0.5. Image processing was performed with Leica Confocal Software (LCS) and Adobe Photoshop Software. For each experiment 10 images were analyzed.

For immunofluorescence assays F11 cells were seeded onto coverslips coated with neoglycosylated collagen patches (30000 cells/coverslip) and grown for 7 days, receiving fresh medium twice per week. Cells were fixed for 20 min in 4% (w/v) paraformaldehyde in PBS and permeabilized by incubation in the presence of 0.3% (v/v) Triton-X100 for 90 min at room temperature. After blocking with 10% normal goat serum, cells were incubated overnight at 4 °C with anti-β-tubulinIII antibody (1:400, Covance, Princeton). After removal of the primary antibody and extensive washes with PBS, cells were incubated at room temperature for 45 min with a secondary antibody labeled with Alexa Fluor 546 (1:800, Molecular Probes). Samples were finally incubated for 10 min with DAPI (0.3 mg/mL, Roche Applied Science, Penzberg, Germany) for nuclear staining and rinsed with PBS for mounting and analysis. Microphotographs were taken using a Zeiss Axiovert 200 direct epifluorescence microscope (Zeiss Axioplan 2, Germany).

7.1.11 F11 Patch-Clamp Recordings

Electrophysiological recordings were performed by the patch-clamp technique in the whole-cell configuration. The standard extracellular solution was applied and contained the following (mM): NaCl 135, KCl 2, $CaCl_2$ 2, $MgCl_2$ 2, hepes 10, glucose 5, pH 7.4. The standard pipet solution contained the following (mM): potassium aspartate 130, NaCl 10, $MgCl_2$ 2, $CaCl_2$ 1.3, EGTA 10, hepes 10, pH 7.3. Recordings

were acquired by the pClamp8.2 software and the MultiClamp 700A amplifier (Axon Instruments), in the voltage-clamp or current-clamp mode. The information we extracted from the experiments were represented by sodium and potassium current densities, the resting membrane potential (V_{rest}), and the presence of action potentials evoked by depolarizing currents. Sodium and potassium currents were recorded by applying a standard protocol: starting from a holding potential of −60 mV, cells were conditioned at −90 mV for 500 ms and successively tested by depolarizing potentials in 10 mV increments, from −80 to +40 mV. Series resistance errors were compensated for to a level of up to 85−90%. The electrical activity was evoked by hyperpolarizing the V_{rest} at approximately −75 mV and by subsequently depolarizing with 600 ms long current pulses. The depolarization peaks were considered action potentials when they were higher than 0 mV. For the analysis, Origin 8 (Microcal Inc., Northampton, MA) and Excel were routinely used. Data are presented as mean ± SEM. Statistical evaluations were obtained using the oneway analysis of variance (ANOVA), followed by the Tukey post hoc test, and the χ^2 test.

7.1.12 mMSCs cell cultures on neoglycosylated collagen with 3'-sialyllactose and 6'-sialyllactose (*In collaboration with Dr. Silvia Panseri- National Research Council - Faenza)*

Mouse mesenchymal stem cells (C57BL/6 mMSCs, GIBCO) were cultured in DMEM Glutamax medium (Gibco) containing 10% Fetal Bovine Serum and 1% penicillin-streptomycin (100 U/mL to 100 µg/mL) and kept at 37°C in an atmosphere of 5% CO_2. Cells were detached from culture flasks by tripsinization, centrifuged and resuspended. Cell number and viability were assessed with the trypan-blue dye exclusion test. The neoglycosylated collagen films, and pristine collagen (used as control group, CT) were previously washed in EtOH 70% for 10 min, followed by a wash in PBS 1× for 10 min, air-dried and sterilized by UV irradiation for 15 min per side under laminar flow hood. In detail 10.0 mm × 10.0 mm films for cell morphology, cell viability and proliferation assay and 50.0 mm × 30.0 mm films for gene expression profiling were used. Samples were placed one per well in a 24-multiwell plate or in 90.0 mm-Petri dish (depending on dimension) and presoaked in PBS 1× for 4 h. Then cells were plated at a density of 2.5×10^3 cells/cm^2 on collagen films. In detail, a drop of 1 mL and 200 µL of culture medium, depending of the membrane dimension, containing cells were seeded on the upper collagen films allowing cell attachment for 1 h in the incubator before adding 9.0 or 1.0 mL of standard culture medium (αMEM Glutamax, 10% Fetal Bovine Serum and 1% penicillin-streptomycin 100 U/mL −

100 µg/mL) without any osteogenic and chondrogenic supplements. All cell-handling procedures were performed in a sterile laminar flow hood. All cell culture incubation steps were performed at 37 °C with 5% CO_2. The media were changed every 2 days.

7.1.13 mMSCs morphology on neoglycosylated collagen matrices

Samples were washed with 1x PBS for 5 min, fixed with 4% (w/v) paraformaldehyde for 15 min and washed with 1x PBS for 5 min. Cellular permeabilization was performed with 1x PBS with 0.1% (v/v) Triton X-100 for 5 min. FITC-conjugated Phalloidin (Invitrogen) 38 nM in 1× PBS was added for 20 min at room temperature in the dark. Cells were washed with 1× PBS for 5 min and incubated with DAPI (Invitrogen) 300 nM in 1× PBS for 5 min. Images were acquired by inverted microscope (Ti-E fluorescence Nikon). One sample per group was analyzed at day 1.

7.1.14 mMSCs viability and proliferation assay on neoglycosylated collagen matrices with 3'-sialyllactose and 6'-sialyllactose

The MTT reagent (3-(4,5-dimethylthiazol-2-yl)-2,5-diphenyl tetrazolium bromide) was prepared at 5 mg/mL in 1x PBS. Cells were incubated with the MTT reagent 1:10 for 2 h at 37°C. Medium was collected and cells incubated with 1 mL of dimethyl sulfoxide for 15 min. In this assay, the metabolically active cells react with the tetrazolium salt in the MTT reagent to produce a formazan dye that

can be observed at λ_{max} of 570 nm, using a Multiskan FC Microplate Photometer (Thermo Scientific). Using a calibration curve, we represented the mean of the total cells detected on each film (N. 5 films per group) at day 1, 2, 3, 7, and 14.

7.1.15 mMSCs - Quantitative Real-Time Polymerase Chain Reaction (qPCR)

At day 7 and 14, mMSCs grown on neoglycosylated and pristine collagen films, used as calibrator, were homogenized and total RNA extraction was performed by use of the Tri Reagent, followed by the Direct-zol RNA MiniPrep kit (Euroclone) according to manufacturer's instructions. RNA integrity was analyzed by native agarose gel electrophoresis and quantification performed by the Qubit 2.0 Fluorometer together with the Qubit RNA BR assay kit, following manufacturer's instructions. Total RNA (500 ng) was reverse transcribed to cDNA using the high-capacity cDNA reverse transcription kit, according to manufacturer's instructions. Quantification of gene expression, using Taqman assays (Applied Biosystems), for Runt-related transcription factor 2 (RUNX2, Mm01340178), alkaline phosphatase (ALP, Mm00475834), transcription factor SOX-9 (SOX9, Mm00448840), Aggrecan (ACAN, Mm00545794) and glyceraldehyde 3-phosphate dehydrogenase, used as housekeeping gene, (GAPDH, Mm99999915) was performed by use of the StepOne Real-Time PCR System (Applied Biosystems).

Experiment was done in triplicate, using three technical replicates for each experiment. Data were collected using the OneStep Software (v.2.2.2) and relative quantification was performed using the comparative threshold (Ct) method (ΔΔCt), where relative gene expression level equals $2^{-\Delta\Delta C}$.

7.1.16 Synthesis of maleimide-collagen (3.11)

A collagen patch (80 mg, 12 cm × 7 cm) was immersed in a THF solution (0.06 M) of maleic anhydride in the presence of $NaHCO_3$. The reaction was carried out at room temperature overnight. The collagen patch was washed with 20 mL mQ H_2O three times for 20 min, and finally with 20 mL of ethanol for 10 min.

7.1.17 Synthesis of thiolated fucose

General methods

Solvents were dried over molecular sieves, for at least 24 h prior to use, when required. When dry conditions were required, the reaction was performed under Ar atmosphere. Thin-layer chromatography (TLC) was performed on silica gel 60F254 coated glass plates (Merck) with UV detection when possible, charring with a conc. H_2SO_4/EtOH/H_2O solution (10:45:45 v/v/v), or with a solution of $(NH_4)_6Mo_7O_{24}$ (21 g), $Ce(SO_4)_2$ (1 g), conc. H_2SO_4 (31 mL) in water (500 mL) and then heating to 110°C for 5 min. Flash column chromatography was performed on silica gel 230-400 mesh (Merck).

Routine ^{1}H and ^{13}C NMR spectra were recorded at 400 MHz (^{1}H) and at 100.57 MHz (^{13}C). Chemical shifts are reported in parts per million downfield from TMS as an internal standard; *J* values are given in Hz. Mass spectra were recorded on a System Applied Biosystems MDS SCIEX instrument (Q TRAP, LC/MS/MS, turbon ion spray) or on a System Applied Biosystem MDS SCIEX instrument (Q STAR elite nanospray).

Synthesis of fucose derivative 3.12

To a stirred solution of L-fucose (2 g, 12.18 mmol) in allyl acohol (8.285 mL, 121.83 mmol), acetyl chloride (1.73 mL, 24.36 mmol) was added dropwise at 0°C under argon atmosphere. The solution was stirred at 65°C for 3.5 hours and then it was neutralized adding $NaHCO_3$ saturated solution. The mixture was concentrated under reduced pressure. The product was purified by flash column chromatography (8:2, EtOAc:EtOH) affording **3.12** (1.6363 g, 66% yield) (mixture of α- and β-anomers).

NMR and mass data are in agreement with those reported in literature.[204]

Synthesis of fucose derivative 3.13

To a stirred solution of **3.12** (1.6363 g, 8.013 mmol) in DCM dry (80 mL), pyridine (2.935 mL), acetic anhydride (3.4 mL, 36 mmol) and DMAP (catalytic amount) were added. The reaction was stirred for 24

hours, and then EtOH is added. The mixture is extracted with DCM and HCl 5%, the organic layers were collected, dried over Na_2SO_4 anhydrous and the solvent was evaporated at reduced pressure. The product was purified by flash column chromatography (8:2, PE:acetone) affording **3.13** (2.2512 g, 85% yield).

^{1}H NMR (400 MHz, $CDCl_3$) δ: 5.91 – 5.80 (m, 1H, OCH_2CHCH_2), 5.37 (dd, $^3J_{3,2}$ = 10.8, $^3J_{3,4}$ = 3.3 Hz, 1H), 5.32 – 5.26 (m, 2H, 4-H, 1 x OCH_2CHCH_2), 5.19 (dd, $^3J_{3'a,2'}$ = 13.5, $^2J_{3'a,3'b}$ = 3.0 Hz, 1H, 1 xOCH_2CHCH_2), 5.13 (dd, $^3J_{2,3}$ = 10.8, $^3J_{2,1}$ = 3.7 Hz, 1H, 2-H), 5.08 (d, $^3J_{1,2}$ = 3.7 Hz, 1H, 1-H), 4.20 – 4.14 (m, 2H, 5-H, 1 x OCH_2CHCH_2), 4.00 (dd, $^2J_{1'b,1'a}$ = 13.1, $^3J_{1'b,2}$ = 6.1 Hz, 1H, 1 x OCH_2CHCH_2), 2.16 (s, 3H, CH_3CO), 2.07 (s, 3H, CH_3CO), 1.98 (s, 3H, CH_3CO), 1.13 (d, $^3J_{6,5}$ = 6.6 Hz, 3H, 6-H).

^{13}C NMR ($CDCl_3$) δ: 170.63 (s, CH_3CO), 170.45 (s, CH_3CO), 170.06 (s, CH_3CO), 133.43 (d, OCH_2CHCH_2) , 117.69 (t, OCH_2CHCH_2), 95.27 (d, 1-C), 71.16 (d, 4-C), 68.55 (t, OCH_2CHCH_2), 68.10, 68.02 (d, 2-C, 3-C), 64.42 (d, 5-C), 20.85 (q, CH_3CO), 20.72 (q, CH_3CO), 20.68 (q, CH_3CO), 15.83 (q, 6-C).

MS: m/z = 353.1 [M+Na], 369.1 [M+K]

Synthesis of fucose derivative 3.14

To a stirred solution of **3.13** (892 mg, 2.70 mmol) and thioacetic acid (3.859 mL, 54 mmol) in 1,4-dioxane dry (0.575 mL),

azobisisobutyronitrile (AIBN) (2.216 g, 13.50 mmol) was added at 50°C under argon atmosphere for 3 hours. Then the reaction was allowed to cool to room temperature and cyclohexene was added and the mixture was stirred for 30 minutes at room temperature. The solvent was evaporated at reduced pressure. The product was purified by flash chromatography (8:2 until 7:3 PE:AcOEt) affording **3.14** (1 g, 91% yield).

^{1}H NMR (400 MHz, $CDCl_3$) δ: 5.16 (dd, $^{3}J_{3,2}$ = 10.7, $^{3}J_{3,4}$ = 3.3 Hz, 1H, 3-H), 5.12 (d, $^{3}J_{4,3}$ = 3.3 Hz, 1H, 4-H), 4.93 (dd, $^{3}J_{2,3}$ = 10.7, $^{3}J_{2,1}$ = 3.7 Hz, 1H, 2-H), 4.86 (d, $^{3}J_{1,2}$ = 3.7 Hz, 1H, 1-H), 4.01 – 3.95 (m, 1H, 5-H), 3.59 (dt, $^{2}J_{1'a,1'b}$ = 11.4, $^{3}J_{1'a,2'}$ = 5.8 Hz, 1H, 1'a-H), 3.28 (dt, $^{2}J_{1'b,1'a}$ = 11.4, $^{3}J_{1'b,2'}$ = 6.2 Hz, 1H, 1'b-H), 2.80 (t, $^{3}J_{3',2'}$ = 7.0 Hz, 2H, 2'H), 2.17 (s, 3H, CH_3COS), 2.00 (s, 3H, CH_3CO), 1.91 (s, 3H, CH_3CO), 1.81 (s, 3H, CH_3CO), 1.75 – 1.67 (m, 2H, 2'-H), 0.97 (d, $^{3}J_{6,5}$ = 6.5 Hz, 3H, 6-H).

^{13}C NMR ($CDCl_3$) δ: 195.21 (s, CH_3*C*OS), 170.34 (s, CH_3*C*O), 170.20 (s, CH_3*C*O), 169.80 (s, CH_3*C*O), 96.09 (d, 1-C), 96.09 (d, 1-C), 70.99 (d, 4-C), 67.95, 67.83 (d, 2-C, 3-C) 66.36 (t, O*C*$H_2CH_2CH_2SH$), 64.25 (d, 5-C), 30.43 (q, *C*H_3COS), 29.03 (t, OCH_2CH_2*C*H_2SH), 25.59 (t, OCH_2*C*H_2CH_2SH), 20.61-20.42 (q, *C*H_3CO), 15.71 (d, 6-C).

MS: m/z = 429.1 [M+Na], 445.0 [M+K]

Synthesis of fucose derivative 3.15

To a solution of **3.14** (935 mg, 2.30 mmol) in dry methanol (19 mL) sodium methoxide (186 mg, 3.45 mmol) was added. The reaction mixture was allowed to stir till completion (12 hours), then Amberlite IR 120 H^+ was added till solution neutrality. The resin was filtered off and the solvent was evaporated to dryness. The product was purified by flash chromatography (72:28, AcOEt:EtOH) affording thiolated fucose **3.15** (408 mg, 87% yield).

^{1}H NMR (400 MHz, D_2O) *δ:* 4.73 (d, $^3J_{1,2}$ = 3.8 Hz, 1H, H-1), 3.93 (q, $^3J_{5,6}$ = 6.5 Hz, 1H, H-5), 3.76 – 3.54 (m, 4H, 2-H, 3-H, 4-H, 1'a-H), 3.50 – 3.38 (m, 1H, 1'b-H), 2.81 – 2.63 (m, 2H, 3'-H), 1.94 – 1.83 (m, 2H, 2'-H), 1.08 (d, $^3J_{6,5}$ = 6.5 Hz, 3H, 6-H).

^{13}C NMR (D_2O) *δ*: 98.30 (d, 1-C), 71.73, 69.53, 67.90 (d, 2-C, 3-C, 4-C), 66.57 (d, 5-C), 66.06 (t, 1'-C), 34.66 (t, 3'-C), 28.05 (t, 2'-C), 15.27 (q, 6-C).

MS: m/z = 239.1 [M+H].

7.1.18 Neoglycosylation of maleimide-collagen with thiolated fucose (collagen 3.16)

A collagen patch (50 mg) was immersed in a PBS solution (0.015 M) of thiolated fucose (**3.15**). The reaction was carried out at room temperature for 24 h. The collagen patch was washed with 20 mL mQ

H_2O three times for 20 min, and finally with 20 mL of ethanol for 10 min.

7.1.19 Synthesis of thiolated collagen (collagen-SH 3.17)

A collagen patch (80 mg, 12 × 7 cm) was immersed in 20 mL of EtOH:PBS 1:1 v/v solution containing 0.025 M γ-thiobutyrolactone at room temperature for 24 h. Thiolated collagen was washed first with 20 mL of 0.1 M aq HCl for 10 min, next with 20 mL mQ H_2O for 10 min three times, and finally with 20 mL ethanol for 10 min.

7.1.20 Photoclick reaction of collagen-SH with α-D-glucopyranoside or β-D-galactopyranoside (collagens 3.19 and 3.20)

Coupling of collagen-SH (12 mg, 5 cm × 2 cm) with allyl α-D-glucopyranoside (27 mg) or allyl β-D-galactopyranoside (27 mg) was carried out at room temperature for 1 h in 30 mL of MeOH:H_2O (1:2) by irradiation with a UV lamp (λ_{max} = 365 nm) using 2,2-dimethoxy-2-phenylacetophenone (DPAP, 17 mg) as a radical initiator. Neoglycosylated collagen was than washed with 20 mL of 0.1 M aq HCl for 10 min, next with 20 mL mQ H_2O for 15 min three times, and finally with 20 mL ethanol for 10 min.

7.1.21 Labeling and quantification of collagen-SH thiol groups by NMR

Collagen-SH (12 mg) was immersed in an aqueous solution (0.035 M) of DTNB and (0.05 M) DIPEA. The reaction was carried out at room temperature for 24 h. Collagen-S-TNB was thoroughly washed with 20 mL of 0.1 M aq HCl for 10 min, with 20 mL of mQ H_2O for 15 min three times, and finally with 20 mL ethanol for 10 min. Collagen was dried under vacuum and then dissolved in 0.6 mL of a NaOD 2 M solution in D_2O. ^1H NMR spectra were recorded using a Varian 400 MHz Mercury instrument, operating at a proton frequency equal to 400 MHz, at room temperature. The 5 mm diameter NMR tubes were sealed and kept closed during the full duration of the experiment. The 90° pulse width (pw90) was calibrated; the number of scans varied depending on the signal-to-noise ratio, and the recycling delay was 5 s.

7.2 Elastin

7.2.1 Elastin films preparation

Elastin films were produced by a solvent-casting method. Elastin from bovine neck ligament (Sigma-Aldrich, catalog no. E1625) was dissolved in acetic acid 0.5 M for 4 h at 40°C. The suspension was homogenized with a mixer for 2 min at maximum speed. 2 mL of elastin solution was poured in multiwell plates (24) and the solvent

evaporated in the fume hood for 2 days. The elastin films were produced as white matrices (~10 mg/cm^2).

7.2.2 General procedure for elastin films neoglycosylation (elastin 4.1 and 4.2)

An elastin film (10 mg, 1 cm × 1 cm) was immersed in 2 mL of 0.08 M sugar solution (maltose or lactose) followed by the sequential addition of 0.04 M $NaBH_3CN$ in citrate buffer (pH 6.00) and reacted overnight. After this time, the elastin film was thoroughly washed first with 2 mL of mQ H_2O three times for 15 min, and finally with 2 mL of ethanol for 10 min.

7.2.3 General procedure for hydrolyzed elastin neoglycosylation (elastins 4.3, 4.4, 4.5, 4.6, and 4.7)

To a stirred solution of soluble elastin from bovine neck ligament (Sigma-Aldrich, catalog no. E6527) (100 mg) in 5 mL of citrate buffer (pH 6.0), sugar (lactose, maltose, cellobiose, 3'-sialyllactose, or 6'-sialyllactose) (1.71 mmol) and $NaBH_3CN$ (0.855 mmol) were added. The reaction was stirred overnight and then was purified with dialysis tubing (MWCO 14000 Da - Sigma-Aldrich, catalog no. D9527) against water and then lyophilized.

7.2.4 Ninhydrin assay

To a solution of ninhydrin (2 mL, 10 mg/mL) in ethanol, 10 mg of elastin (untreated or neoglycosylated) were added. The mixture was heated at 70°C for 30 min, then, after cooling to room temperature, the absorbance was recorded (570 nm).

7.2.5 Scanning Electron Microscopy (SEM - *In collaboration with Prof. Brigida Bochicchio - University of Basilicata)*

SEM was performed using the environmental scanning electron microscope ESEM XL30 FEI with a beam acceleration voltage of 30kV. The samples were mounted on aluminum stubs with double-sided carbon tape and coated with a thin layer of gold in a Sputter Coater prior to analysis. For internal analysis the sheets were cryo-fractured by immersion for 1 minute into a liquid N_2 bath and subsequently fractured using a scalpel blade prior to gold sputtering.

7.3 Hydrogels

7.3.1 Synthesis of pentenoyl gelatin (5.1)

Gelatin from porcine skin (2 g) (Sigma-Aldrich, catalog no. G2500) was suspended in 4 mL of DMF. Pyridine (1.49 mL, 18.47 mmol) and pentenoic anhydride (3.376 mL, 18.47 mmol) were added. The reaction was conducted at room temperature overnight. The pentenoyl gelatin was purified by dialysis against water (MWCO 14000 Da) and then freeze-dried.

7.3.2 Synthesis of thiolated gelatin (5.2)

Gelatin (2 g) was dissolved in 10 mL of PBS (pH 7.4) and a solution of 2.13 mL γ-thiobutyrolactone (24.63 mmol) in 10 mL of ethanol was added. The reaction was conducted at 37°C for 24 h. The thiolated gelatin was purified by dialysis against water (50°C) and then freezedried.

7.3.3 Hydrogels 5.3a-c preparation

Hydrogels were prepared reacting thiolated gelatin and pentenoyl gelatin in different concentrations (2.5% w/v (**5.3a**), 5.0% w/v (**5.3b**), 10.0% w/v (**5.3c**) of each component) in phosphate buffered saline (PBS, pH = 7.4, 30 µL), in the presence of 0.05% w/v 2-hydroxy-4'-(2-hydroxyethoxy)-2-methylpropiophenone (HHMP, as the photoinitiator). The mixture was polymerized for 5 min under ultraviolet light (λ_{max} = 365 nm).

7.3.4 hBMSCs isolation and expansion (*In collaboration with Dr. Marco Rasponi - Politecnico di Milano)*

Primary human bone marrow stromal cells (hBMSCs) were isolated by adherence from bone marrow aspirates of donors undergoing orthopedic surgery, after written informed consent. Briefly, bone marrow was centrifuged and freshly isolated cells were plated at 1 x 10^5 cells/cm^2 and cultured overnight to allow cell adhesion. Suspended cells were then removed, and nucleated cells were

expanded. hBMSCs were cultured in complete medium including α-modified Eagle's medium, 10% fetal bovine serum, 10 mM HEPES, 1 mM sodium pyruvate, 100 U/mL penicillin, 100 µg/mL streptomycin and 292 µg/mL L-glutamine (all GIBCO) and supplemented with 5 ng/mL fibroblast growth factor 2 (Peprotech). hBMSCs were harvested after reaching 70–80% confluence and re-seeded at a lower density (3 x 10^3 cells/cm^2) in new tissue culture treated flasks (CytoOne, USA Scientific, Florida, USA). Medium was changed twice weekly and cells were finally harvested at the third passage.

7.3.5 Cytocompatibility assays of hydrogels 5.3a and 5.3b

In vitro cytocompatibility evaluation was performed embedding hBMSCs within the synthesized hydrogels **5.3a** and **5.3b** and assessing cellular behavior and metabolic activity after 3 days in culture. More in detail, pre-polymer solutions with final concentrations of 5% w/v (**5.3a**) and 10% w/v (**5.3b**) were prepared by reacting thiolated gelatin (**5.2**) with pentenoyl gelatin (**5.1**) at ratio 1:1 (w/w) and adding HHMP at 0.05% w/v. Cells were trypsinized, counted and resuspended in the pre-polymer solutions at a final concentration of 1 x 10^6 cells/mL. The photo-polymerization reaction was carried out maintaining sterile conditions by irradiating samples for 5 min with the UVA light source (λ_{max} = 365 nm) directly within multiwell plates. Obtained cell laden hydrogels were incubated and cultured under standard culture conditions (RH 95%, CO_2 5%, T =

37°C). Samples were monitored daily under optical microscope (Olympus IX-71; Olympus, Hamburg, Germany) and phase contrast images were acquired to evaluate hydrogel morphological modifications over time and cellular behavior within hydrogels at different concentrations. After 3 days in culture, AlamarBlue assay was performed rinsing samples with PBS and incubating them for 4 h at 37°C in 10% v/v of AlamarBlue solution (Invitrogen Corporation, Isbad, CA). Samples solutions were then measured at 540 nm using a spectrophotometer (Victor X3; PerkinElmer, Waltham, MA). MTT colorimetric assay was also performed to qualitatively assess cell viability and morphology. The MTT working solution was obtained dissolving thiazolyl blue tetrazolium bromide powder in DMEM without phenol red at a final concentration of 0.5 mg/mL. Samples were first rinsed in PBS and incubated in the MTT working solution for 4 h at 37°C in the dark. Phase contrast images of colored hBMSCs embedded in hydrogel **5.3a** were finally acquired under optical microscope.

7.3.6 Synthesis of maleimide gelatin (5.4)

To a solution of maleic anhydride (1.53 M) in THF, 1 g of gelatin was added. The reaction was conducted at 37°C overnight. The maleimide gelatin was purified by dialysis against water (50°C) and then freezedried.

7.3.7 Hydrogel 5.5 preparation

Hydrogel **5.5** were prepared reacting thiolated gelatin (**5.2**) and maleimide gelatin (**5.4**) (5% w/v of each component) in phosphate buffered saline (PBS, pH = 7.4, 30 µL). The mixture was reacted for 10 min at room temperature.

7.3.8 Hydrogel 5.6 preparation

Hydrogel 6 was prepared reacting pentenoyl gelatin (**5.1**) (5% w/v) and poly(ethylene oxide), 4-arm, thiol terminated (Sigma-Alrich, catalog no. 565725) (0.01 mmol) in phosphate buffered saline (PBS, pH = 7.4, 30 µL), in the presence of 0.05% w/v 2-hydroxy-4'-(2-hydroxyethoxy)-2-methylpropiophenone (HHMP, as the photoinitiator). The mixture was polymerized for 5 min under ultraviolet light (λ_{max} = 365 nm).

7.3.9 Hydrogel 5.7 preparation

To a solution of gelatin (250 mg) in carbonate buffer (2.5 mL, pH = 9.2), 3,4-dimethoxy-3-cyclobutene-1,2-dione (Sigma-Aldrich, catalog no. 377406) was added and the mixture was reacted at 50°C for 20 h.

References

[1] Lee, E. J.; Kasper, F. K.; Mikos, A. G. *Ann. Biomed. Eng*. **2014**, *42*(2), 323–337.
[2] Ratner, B. D.; Hoffman, A. S.; Schoen, J. F.; Lemons, J. E. Biomaterials Science, an Introduction to Materials in Medicine 1–8 (Academic, San Diego, **1996**).
[3] Peppas, N. A.; Langer, R. *Science* **1994**, *263*, 1715–1720.
[4] Bell, E.; Ivarsson, B.; Merrill, C. *Proc. Natl. Acad. Sci. USA* **1979**, *76*, 1274–1278.
[5] Langer, R. *Nature* **1998**, *392*(Suppl.), 5–10.
[6] Langer, R. *Science* **2001**, *293*, 58–59.
[7] Vacanti, J. P.; Langer, R. *Lancet* **1999**, *354*, 32–34.
[8] Langer, R.; Tirrell, D. A. *Nature* **2004**, *428*, 487-492.
[9] Yurchenco, P. D.; Birk, D. E.; Mecham, R. P. (eds) Extracellular Matrix Assembly and Structure (Academic, San Diego, **1994**).
[10] van Hest, J. C. M.; Tirrell, D. A. *Chem. Commun.* **2001**, *19*, 1897–1904.
[11] Alsberg, E.; Anderson, K.W.; Albeiruti, A.; Rowley, J. A.; Mooney, D. J. *Proc Natl Acad Sci*. *USA* **2002**, *99*, 12025–12030.
[12] Ratner, B. D.; Bryant, S. J. *Annu. Rev. Biomed. Eng.* **2004**, *6*, 41–75.
[13] Anderson, J. M.; Rodriguez, A.; Chang, D. T. *Semin. Immunol.* **2008**, *20*, 86–100.
[14] Mager, M. D.; LaPointe, V.; Stevens, M. M. *Nature Chem.* **2011**, *3*, 582–589.
[15] Hozumi, K.; Otagiri, D.; Yamada, Y.; Sasaki, A.; Fujimori, C.; Wakai, Y.; Uchida, T.; Katagiri, F.; Kikkawa, Y.; Nomizu, M. *Biomaterials* **2010**, *31*, 3237–3243.
[16] Johnson, K.; Zhu, S.; Tremblay, M. S.; Payette, J. N.; Wang, J.; Bouchez L. C.; Meeusen, S.; Althage, A.; Cho, C. Y.; Wu, X.; Schultz, P. G. *Science* **2012**, *336*, 717–721.
[17] Zhou, Z.; Yu, P.; Geller, H. M.; Ober, C. K. *Biomaterials* **2012**, *33*, 2473–2481.
[18] a) Service, R. F.; *Science* **2012**, *338*, 321−323; b) Stallforth, P.; Lepenies, B.; Adibekian, A.; Seeberger, P. H. *J. Med. Chem.* **2009**, *52*, 5561–5577; c) Hart, G. W.; Copeland, R. J. *Cell* **2010**, *143*, 672−676; d) Seeberger, P. H. *Nat. Chem. Biol.* **2009**, *5*, 368−372.
[19] a) Cipolla, L.; Russo, L.; Taraballi, F.; Lupo, C.; Bini, D.; Gabrielli, L.; Capitoli, A.; Nicotra, F. In Specialist Periodical Reports-Carbohydrate Chemistry. (Eds. Royal Society of Chemistry (London) Ch. 17, **2012**); b) Chawla, K.; Yu, T.; Stutts, L.; Yen, M.; Guan, Z. *Biomaterials* **2012**, *33*, 6052−6060; c) Sapsford, K. E.; Algar, W. R.; Berti, L.; Gemmill, K. B.; Casey, B. J.; Oh, E.; Stewart, M. H.; Medintz, I. L. *Chem. Rev*. **2013**, *113*, 1904–2074; d) Koepsel, J. T.; Murphy, W. L. *Chem. Bio. Chem.* **2012**, *13*, 1717−1724; e) Slaney, A. M.; Wright, V. A.; Meloncelli, P. J.; Harris, K. D.; West, L. J.; Lowary, T. L.; Buriak, J. M. *ACS Appl. Mater. Interfaces* **2011**, *3*, 1601−1612; f) Santoyo-Gonzalez, F.; Hernandez-Mateo, F. *Chem. Soc. Rev.* **2009**, *38*, 3449−3462.
[20] Werz, D. B.; Ranzinger, R.; Herget, S.; Adibekian, A.; von der Lieth, C. W.; Seeberger, P. H. *ACS Chem. Biol.* **2007**, *2*, 685–691.
[21] Kelley, W.; Moremen, M. T.; Nairn, A. V. *Nature Rev.* **2012**, *13*, 448–462.

[22] Cipolla, L.; La Ferla, B.; Airoldi, C.; Zona, C.; Orsato, A.; Shaikh, N.; Russo, L.; Nicotra, F. *Future Med. Chem.* **2010**, *2*, 587–599.
[23] Ohtsubo, K.; Marth, J. D. *Cell* **2006**, *126*, 855–867.
[24] Jurgensen, H. J.; Madsen, D. H.; Ingvarsen, S.; Melander, M. C.; Gårdsvoll, H.; Patthy, L.; Engelholm, L. H.; Behrendt, N. A. J. *Biol. Chem.* **2011**, *286*, 32736–32748.
[25] Barish, R. D.; Schulman, R.; Rothemund, P. W.; Winfree, E. *PNAS* **2009**, *106*, 6054–6059.
[26] Bryksin, A. V.; Brown, A. C.; Baksh, M. M.; Finn, M. G.; Barker, T. H. *Acta Biomater.* **2014**, *10*, 1761–1769.
[27] Holzapfel, B. M.; Reichert J. C.; Schantz J. T.; Gbureck U.; Rackwitz L.; Nöth U.; Jakob F.; Rudert M.; Groll J.; Hutmacher D. W. *Adv. Drug Deliver. Rev*. **2013**, *65*(4), 581-603.
[28] Abramson S.; Alexander H.; Best S.; Bokros J. C.; Brunski J. B.; Colas A. S.L.; Cooper S. L.; Curtis J.; Haubold A.; Hensch L. L.; Hergenrother, R. W.; Hoffman, A. S.; Hubbel, J. E.; Jansen, J. A.; King, M. W.; Kohn, J.; Lamba, N. M. K.; Langer, R.; Migliaresci, C.; More, R. B.; Peppas, N. A.; Ratner, B. D.; Visser, S. A.; Recum, A.; Weinberg, S.; Yannas, I. V. Classes of materials used in medicine (Eds. Ratner, B. D.; Hoffmann, A. S.; Schoen, F. J.; Lemons, J. E., Biomaterials Science: An Introduction to Materials in Medicine, Elsevier Academic Press, London, **2004**, pp. 67–137).
[29] McGregor, D. B.; Baan, R. A.; Partensky, C.; Rice, J. M.; Wilbourn, J. D. *Eur. J. Cancer* **2000**, *36*, 307–313.
[30] Wapner, K. L. *Clin. Orthop. Relat. Res.* **1991**, *271*, 12–20.
[31] Geetha, M.; Singh, A. K.; Asokamani, A.; Gogia, A. K. *Prog. Mater. Sci.* **2009**, 54, 397–425.
[32] Witte, F. *Acta Biomater.* **2010**, *6*, 1680–1692.
[33] Kamitakahara, M.; Ohtsuki, C.; Miyazaki, T. *J. Biomater. Appl.* **2008**, *23*, 197–212.
[34] Paul, W.; Sharma, C. P. *J. Biomater. Appl.* **2003**, *17*, 253–264.
[35] Lieberman, I. H.; Togawa, D.; Kayanja, M. M. *Spine J.* **2005**, *5*(6 Suppl), 305S–316S.
[36] Suzuki, O. *Acta Biomater*. **2010**, *6*, 3379–3387.
[37] Hench, L. L.; Splinter, R. J.; Allen, W. C.; Greenlee, T. K. *J. Biomed. Mater. Res.* **1972**, *2*, 117–41.
[38] Moimas, L.; Biasotto, M.; Di Lenarda, R.; Olivo, A.; Schmid, C. *Acta Biomater.* **2006**, *2*, 191–199.
[39] Fukui, K.; Kaneuji, A.; Sugimori, T.; Ichiseki, T.; Kitamura, K.; Matsumoto, T. *J. Arthroplasty* **2011**, *26*, 45–49.
[40] Dawson, E.; Mapili, G.; Erickson, K.; Taqvi, S.; Roy, K. *Adv. Drug Deliv. Rev.* **2008**, *60*, 215–228.
[41] Lee, C. H.; Singla, A.; Lee, Y. *Int. J. Pharm.* **2001**, *221*, 1–22.
[42] Park, S. N.; Park, J. C.; Kim, H. O.; Song, M. J.; Suh, H. *Biomaterials* **2002**, *23*, 1205–1212.

[43] Young, S.; Wong, M.; Tabata, Y.; Mikos, A. G. *J Control Release* **2005**, *109*, 256–274.
[44] Reece, T. B.; Maxey, T. S.; Kron, I. L. *Am. J. Surg.* **2001**, *182*, 40S–44S.
[45] Lippiello, L. *Osteoarthr. Cartil.* **2003**, *11*, 335–342.
[46] Pieper, J. S.; van Wachem, P. B.; van Luyn, M. J. A.; Brouwer, L. A.; Hafmans, T.; Veerkamp, J. H.; van Kuppevelt, T. H. *Biomaterials* **2000**, *21*, 1689–1699.
[47] Afify, A. M.; Stern, M.; Guntenhoner, M.; Stern, R. *Arch. Biochem. Biophys.* **1993**, *305*, 434–441.
[48] Kogan, G.; Soltes, L.; Stern, R.; Gemeiner, P. *Biotechnol. Lett.* **2007**, *29*, 17–25.
[49] Wang, D. A.; Varghese, S.; Sharma, B.; Strehin, I.; Fermanian, S.; Gorham, J.; Fairbrother, D. H.; Cascio, B.; Elisseeff, J. H. *Nat. Mater.* **2007**, *6*, 385–392.
[50] Khor, E.; Lim, L. Y. *Biomaterials* **2003**, *24*, 2339–2349.
[51] Chenite, A.; Chaput, C.; Wang, D.; Combes, C.; Buschmann, M. D.; Hoemann, C. D.; Leroux, J. C.; Atkinson, B. L.; Binette, F.; Selmani, A. *Biomaterials* **2000**, *21*, 2155–2161.
[52] George, M.; Abraham, T. E. *J. Control Release* **2006**, *114*, 1–14.
[53] Uludag, H.; De Vos, P.; Tresco, P. A. *Adv. Drug. Deliv. Rev.* **2000**, *42*, 29–64.
[54] Groenewold, M. D.; Gribnau, A. J., Ubbink, D. T. *BMC Surg.* **2011**, *11*, 15.
[55] Grayson, W. L.; Martens, T. P.; Eng, G. M.; Radisic, M.; Vunjak-Novakovic, G. *Semin. Cell. Dev. Biol.* **2009**, *20*, 665–673.
[56] Yurchenco PD. In Yurchenco, P. D., Birk, D. E.; Mecham, R. P. (Eds Extracellular Matrix Assembly and Structure, Academic, San Diego, **1994**).
[57] Wade, R. J.; Burdick, J. A. *Mater. Today* **2012**, *15*(10), 454-459.
[58] Russo, L.; Sgambato, A.; Bini, D.; Calloni, I.; Origgi, D.; Cetin Telli, F.; Cipolla, L. Imperial College Press. (Ed. L Cipolla, Ch. 16, Carbohydrate, Biomaterials, and Tissue Engineering Applications, **2015**).
[59] Behonick, D. J.; Werb, Z. *Mech. Dev.* **2003**, *120*, 1327-1336.
[60] Stevens, M. M.; George, J. H. *Science* **2005**, *310*, 1135-1138.
[61] Xu, T.; Zhang, N.; Nichols, H. L.; Shi, D.; Wen, X. *Mater. Sci. Eng. C* **2007**, *27*, 578.
[62] Langer, K.; Coester, C.; Weber, C.; Von Briesen, H.; Kreuter, J. *Eur. J. Pharm. Biopharm.* **2000**, *49*, 303–307.
[63] Goddard, J. M.; Hotchkiss, J. H. *Prog. Pol. Sci.* **2007**, *32*, 698-725.
[64] a) Whittlesey, K. J.; Shea, L. D. *Exp. Neurol.* **2004**, *190*, 1-16; b) Simmons, C. A.; Alsberg, E.; Hsiong, S.; Kim, W. J.; Mooney, D. J. *Bone* **2004**, *35*, 562-569; c) Kroese-Deutman, H. C.; Ruhe, P. Q.; Spauwen P. H.; Jansen, J. A. *Biomaterials* **2005**, *26*, 1131–1138.
[65] Lutolf, M. P. *Adv. Mater.* **2003**, *15*, 888-892.
[66] Zhang, Y.; Moheban, D. B.; Conway, B. R.; Bhattacharyya, A.; Segal, R. A. *J. Neurosci.* **2000**, *20*, 5671–78.
[67] Kuhl, P. R.; Griffith-Cima, L. G. *Nat. Med.* **1996**, *2*, 1022–1027.

[68] Kirkwood, K.; Rheude, B.; Kim, Y. J.; White, K.; Dee, K. C. *J. Oral. Implantol.* **2003**, *29*, 57–65.
[69] Karageorgiou, V.; Meinel, L.; Hofmann, S.; Malhotra, A.; Volloch, V.; Kaplan, D. *J. Biomed. Mater. Res. A* **2004**, *71*, 528–37.
[70] Zisch, A. H.; Lutolf, M. P.; Ehrbar, M.; Raebar, G. P.; Rizzi, S. C.; Davies, N.; Shmökel, H.; Bezuidenhout, D.; Djonov, V.; Zilla, V.; Hubbel, J. A. *FASEB J.* **2003**, *17*, 2260–2262.
[71] Lee, A. C.; Yu, V.; M.; Lowe, J. B.; Brenner, M. J.; Hunter, D. A.; Mackinnon, S. E.; Sakiyama-Elbert, S. E. *Exp. Neurol.* **2003**, *184*, 295–300.
[72] Taylor, S. J., McDonald, J. W. J.; Sakiyama-Elbert, S. E. *J. Control. Release* **2004**, *98*, 281-94.
[73] Seliktar, D.; Zisch, A. H.; Lutolf, M. P.; Wrana, J. L.; Hubbel, J. A. *J. Biomed. Mater. Res. A* **2004**, *68*, 704–716.
[74] Dinbergs, I. D.; Brown, L.; Edelman, E. R. *J. Biol. Chem.* **1996**, *271*, 29822–29829.
[75] Hersel, U.; Dahmen, C.; Kessler, H. *Biomaterials* **2003**, *24*, 4385-415.
[76] La Ferla B.; Zona, C.; Nicotra, F. *Synlett* **2009**, *14*, 2325−2327.
[77] Dubruel, P.; Vanderleyden, E.; Bergadà, M.; De Paepe, I.; Chen, H.; Kuypers, S.; Luyten, J.; Schrooten, J.; Van Hoorebeke, L.; Schacht, E. *Surface Science* **2006**, *600*, 2562-2571.
[78] Stern, R.; Jedrzejas, M. J.*Chem. Rev.* **2008**, *108*, 5061–5085.
[79] Del Valle, E. M. M. *Process. Biochem.* **2004**, *39*, 1033–1046.
[80] Moremen, K. W.; Tiemeyer, M.; Nairn, A. V. *Nat. Rev. Mol. Cell. Biol.* **2012**, *13*, 448-462.
[81] Varki, A. *Cold Spring Harb. Perspect. Biol.* **2011**, *3*(6), a005462.
[82] Hynes, R. O.; Naba, A. *Cold Spring Harb. Perspect. Biol.* **2012**, *4*, a004903.
[83] Lauc, G.; Krištić, J.; Zoldoš, V. *Front. Genet.* **2014**, *5*, 145.
[84] Ruoslahti, E.; Hayman, E. G.; Pierschbacher, M. D. *Arteriosclerosis* **1985**, *5*, 581–594.
[85] Smethurst, P. A.; Onley, D. J.; Jarvis, G. E.; O'Connor, M. N.; Knight, C. G.; Herr, A. B.; Ouwehand, W. H.; Farndale, R. W. *J. Biol. Chem.* **2007**, *282*, 1296–1304.
[86] Konitsiotis, A. D.; Raynal, N.; Bihan, D.; Hohenester, E.; Farndale, R. W.; Leitinger, B. *J. Biol. Chem.* **2008**, *283*, 6861–6868.
[87] Gullberg, D.; Gehlsen, K. R.; Turner, D. C.; Ahlen, K.; Zijenah, L. S.; Barnes, M. J.; Rubin, K. *EMBO J.* **1992**, *11*, 3865–3873.
[88] Pierschbacher, M. D.; Ruoslahti, E. *Nature* **1984**, *309*, 30–33.
[89] Fiedler, L. R.; Schonherr, E.; Waddington, R.; Niland, S.; Seidler, D. G.; Aeschlimann, D.; Eble, J. A. *J. Biol. Chem.* **2008**, *283*, 17406–17415.
[90] Gattazzo, F.; Urciuolo, A.; Bonaldo, P. Biochim. Biophys. Acta **2014**, *1840*(8), 2506–2519.
[91] Xu, T.; Molnar, P.; Gregory, C.; Das, M.; Boland, T.; Hickman, J. J. *Biomaterials* **2009**, *30*, 4377–4383.

[92] Gingras, M.; Beaulieu, M. M.; Gagnon, V.; Durham, H. D.; Berthod, F. *Glia* **2008**, *56*, 354–364.
[93] Che, Z. M.; Jung, T. H.; Choi, J. H.; Yoon do, J.; Jeong, H.J .; Lee, E. J.; Kim, J. *Biochem. Biophys. Res. Commun.* **2006**, *346*, 268–275.
[94] Sabeh, F.; Shimizu-Hirota, R.; Weiss, S. J. *J. Cell Biol.* **2009**, *185*, 11–19.
[95] Inoue, T.; Toda, S.; Narisawa, Y.; Sugihara, H. *J. Invest. Dermatol.* **2001**, *117*, 244–250.
[96] Shanmugasundaram, N.; Ravichandran, P.; Reddy, P. N.; Ramamurty, N.; Pal, S.; Rao, K.P. *Biomaterials* **2001**, *22*, 1943–1951.
[97] Spencer, N. J.; Cotanche, D. A.; Klapperich, C. M. *Biomaterials* **2008**, *29*, 1028–1042.
[98] Cortial, D.; Gouttenoire, J.; Rousseau, C. F.; Ronziere, M. C.; Piccardi, N.; Msika, P.; Herbage, D.; Mallein-Gerin, F.; Freyria, A. M. *Osteoarthritis Cartilage* **2006**, *14*, 631–640.
[99] Williams, P. A.; Peacocke, A. R. *Biochim. Biophys. Acta* **1965**, *101*(3), 327–35.
[100] Steinert, A. F.; Ghivizzani, S. C.; Rethwilm, A.; Tuan, R. S.; Evans, C.H.; Noth, U. *Arthritis Res. Ther.* **2007**, *9*(3), 213.
[101] Natalello, A.; Ami, D.; Brocca, S.; Lotti, M.; Doglia, S. M. *Biochem. J.* **2005**, *385*, 511–517.
[102] Guilbert, M.; Said, G.; Happillon, T.; Untereiner, V.; Garnotel, R.; Jeannesson, P.; Sockalingum, G. D. *Biochim. Biophys. Acta* **2013**, *1830*, 3525– 3531.
[103] Slaney, A. M.; Wright, V. A.; Meloncelli, P. J.; Harris, K. D.; West, L. J.; Lowary, T. L.; Buriak, J. M. (2011) *ACS Appl. Mater. Interfaces* **2011**, *3*, 1601– 1612.
[104] Wang, Q. Q.; Li, W.; Yang, B. C. *J. Biomed. Mater. Res.* **2011**, *99*, 125–134.
[105] Zinger, O.; Anselme, K.; Denzer, A.; Habersetzer, P.; Wieland, M.; Jeanfils, J.; Hardouin, P.; Landolt, D. *Biomaterials* **2004**, *25*, 2695–2711.
[106] Tsai, S. W.; Liou, H. M.; Lin, C. J.; Kuo, K. L.; Hung, Y. S; Weng, R. C.; Hsu, F. Y. *PLoS One* **2012**, *7*(2), e31200.
[107] Palmieri, D.; Valli, M.; Viglio, S.; Ferrari, N.; Ledda, B.; Volta, C.; Manduca, P. *Exp. Cell Res.* **2010**, *316*, 789–799.
[108] Schachner, M.; Martini, R. *Trends Neurosci.* **1995**, *18*, 183–191.
[109] Yamamoto, S.; Oka, S.; Inoue, M.; Shimuta, M.; Manabe, T.; Takahashi, H.; Miyamoto, M.; Asano, M.; Sakagami, J.; Sudo, K.; Iwakura, Y.; Ono, K.; Kawasaki, T. *J. Biol. Chem.* **2002**, *277*, 27227– 27231.
[110] Kalovidouris, S. A.; Gama, C. I.; Lee, L. W.; Hsieh-Wilson, L. C. *J. Am. Chem. Soc.* **2005**, *127*, 1340–1341.
[111] Kleene, R.; Schachner, M. *Nat. Rev. Neurosci.* **2004**, *5*, 195–208.
[112] Dani, N.; Broadie, K. *Dev. Neurobiol.* **2012**, *72*, 2–21.
[113] Ohtsubo, K.; Marth, J. D. *Cell* **2006**, *126*, 855–867.
[114] Masand, S. N.; Perron, I. J.; Schachner, M.; Shreiber, D. I. *Biomaterials* **2012**, *33*, 790–797.

[115] Platika, D.; Boulos, M. H.; Baizer, L.; Fishman, M. C. *Proc. Natl. Acad. Sci. U.S.A.* **1985**, *82*, 3499−3503.
[116] Edsjö, A.; Holmquist, L.; Påhlman, S. *Semin. Cancer. Biol.* **2007**, *17*, 248−256.
[117] Abemayor, E.; Sidellt, N. *Environ. Health Perspect.* **1989**, *80*, 3−15.
[118] Chiesa, N.; Rosati, B.; Arcangeli, A.; Olivotto, M.; Wanke, E. *J. Physiol.* **1997**, *501*, 313−318.
[119] Wieringa, P.; Tonazzini, I.; Micera, S.; Cecchini, M. T. *Nanotechnology* **2012**, *23*, 275102−275116.
[120] McDonnell, J.; Jones, G. E.; White, T. K.; Tanzer, M. L. *J. Biol. Chem.* **1996**, *271*, 7891−7894.
[121] Xiao, G.; Chung, T. F.; Pyun, H. Y.; Fine, R. E.; Johnson, R. J. *Mol. Brain Res.* **1999**, *72*, 121−128.
[122] Arcangeli, A.; Becchetti, A.; Mannini, A.; Mugnai, G.; De Filippi, P.; Tarone, G.; Del Bene, M. R.; Barletta, E.; Wanke, E.; Olivotto, M. *J. Cell Biol.* **1993**, *122*, 1131−1143.
[123] Cherubini, A.; Hofmann, G.; Pillozzi, S.; Guasti, L.; Crociani, O.; Cilia, E.; Di Stefano, P.; Degani, S.; Balzi, M.; Olivotto, M.; Wanke, E.; Becchetti, A.; De Filippi, P.; Wymore, R.; Arcangeli, A. *Mol. Biol. Cell* **2005**, *16*, 2972−2983.
[124] Bianco, P.; Riminucci, M.; Gronthos, S.; Robey, P. G. *Stem Cells* **2001**, *19*(3), 180–192.
[125] Chen, X.; Varki, A. *ACS Chem. Biol.* **2010**, *5*(2), 163–176.
[126] Xu, L.; Xu, W.; Xu, G.; Jiang, Z.; Zheng, L.; Zhou, Y.; Wie, W.; Wu, S. *Glycoconjugate J.* **2013**, *30*(7), 677-685.
[127] Kitazume, S.; Imamaki, R.; Ogawa, K.; Komi, Y.; Futakawa, S.; Kojima, S.; Hashimoto, Y.; Marth, J.D.; Paulson, J.C.; Taniguchi, N. *J. Biol. Chem.* **2010**, *285*, 6515-6521.
[128] Kitazume, S.; Imamaki, R.; Ogawa, K.; Taniguchi, N. *Glycobiology* **2014**, *24*, 1260–1264.
[129] Orlando, B.; Giacomelli, L.; Ricci, M.; Barone, A.; Covani, U. *Arch. Oral Biol.* **2013**, *58*(1), 42-49.
[130] Franceschi, R. T.; Ge, C.; Xiao, G.; Roca, H.; Jiang, D. *Ann. N. Y. Acad. Sci.* **2007**, *1116*, 196-207.
[131] Gersbach, C. A.; Byers, B. A.; Pavlath, G. K.; Garcia, A. J. *Exp. Cell Res.* **2004**, *300*(2), 406-417.
[132] Malaval, L.; Liu, F.; Roche, P.; Aubin, J. E. *J. Cell. Biochem.* **1999**, *74*(4), 616-627.
[133] Ito, A.; Nagai, M.; Tajino, J.; Yamaguchi, S.; Iijima, H.; Zhang, X.; Aoyama, T.; Kuroki, H. *PLoS One* **2015**, *10*(5), e0128082.
[134] Diekman, B. O.; Christoforou, N.; Willard, V. P.; Sun, H.; Sanchez-Adams, J.; Leong, K. W.; Guilak, F. *Proc. Natl. Acad. Sci*., *U.S.A.* **2012**, *109*(47), 19172-19177.
[135] Becker, D. J.; Lowe, J. B. *Glycobiology* **2003**, *13*(7), 41R-53R.
[136] Miller, E. J. *Cell. Biochem.* **1976**, *13*, 165−192.

[137] Riddles, P. W.; Blakeley, R. L.; Zerner, B. *Methods Enzymol.* **1983**, *91*, 49-60.
[138] Wu W. J.; Vrhovski B.; Weiss A. S. *J. Biol. Chem.* **1999**, *274*, 21719–24..
[139] Daamen, W. F.; Veerkamp, J. H.; van Hest, J. C. M.; van Kuppevelt, T. H. *Biomaterials* **2007**, *28*, 4378–4398.
[140] Uitto, J.; Christiano, A. M.; Kahari, V. M.; Bashir, M. M.; Rosenbloom, J. *Biochem. Soc. Trans.* **1991**, *19*(4), 824-829.
[141] Indik, Z.; Yeh, H.; Ornstein-Goldstein, N.; Sheppard, P.; Anderson, N.; Rosenbloom, J. C.; Peltonen, L.; Rosenbloom, J. *Proc. Natl. Acad. Sci. USA* **1987**, *84*(16), 5680-5684.
[142] Hinek, A. *Ciba F. Symp.* **1995**, *192*, 185-191; discussion 191- 196.
[143] Hinek, A; Mecham, R. P.; Keeley, F.; Rabinovitch, M. *J. Clin. Invest.* **1991**, *88*(6), 2083-2094.
[144] Hinek, A.; Kawiak, J.; Czarnowska, E.; Barcew, B. *Acta Biol. Hung.* **1984**, *35*, 245-258.
[145] Hinek, A.; Wrenn, D. S.; Mecham, R. P.; Barondes, S. H. *Science* **1988**, *239*, 1539-1541.
[146] Kagan, H. M.; Sullivan, K. A. *Methods Enzymol.* **1982**, *82*A, 637-650.
[147] Umeda, H.; Nakamura, F.; Suyama, K. *Arch. Biochem. Biophys.* **2001**, *385*(1), 209-219.
[148] Glagov, S.; Vito, R.; Giddens, D. P.; Zarins, C. K. *J. Hypertens. Suppl.* **1992**, *10*(6), S101-104.
[149] Starcher, B. *Anal. Biochem.* **2001**, *292*(1), 125-129.
[150] Pasquali-Ronchetti, I.; Baccarani-Contri, M. *Microsc. Res. Tech.* **1997**, *38*(4), 428-435.
[151] Li, D. Y.; Brooke, B.; Davis, E. C.; Mecham, R. P.; Sorensen, L.K.; Boak, B. B.; Eichwald, E.; Keating, M. T. *Nature* **1998**, *393*(6682), 276-280.
[152] Ito, S.; Ishimaru, S.; Wilson, S. E. *Angiology* **1998**, *49*(4), 289-297.
[153] Wilson, B. D.; Gibson, C. C.; Sorensen, L. K.; Guilhermier, M. Y.; Clinger, M.; Kelley, L. L.; Shiu, Y. T.; Li, D. Y. *Ann. Biomed. Eng.* **2010**, *39*(1), 337-346.
[154] Rnjak, J.; Wise, S. G.; Mithieux, S. M.; Weiss, A. S. *Tissue Eng. Part B Rev.* **2011**, *17*(2), 81-91.
[155] Rodgers, U. R.; Weiss A. S. *Pathol. Biol. (Paris)* **2005**, *53*(7), 390-398.
[156] Akhtar, K.; Broekelmann, T. J.; Song, H.; Turk, J.; Brett, T. J.; Mecham, R. P.; Adair-Kirk, T. L. *J. Biol. Chem.* **2011**, *286*(15), 13574-13582.
[157] Rodríguez-Cabello, J. C.; Piña, M. J.; Ibàñez-Fonseca, A.; Fernàndez-Colino, A.; Arias, F. J. *Bioconjugate Chem.* **2015**, *26*, 1252-1265.
[158] Bhrany, A. D.; Beckstead, B.L.; Lang, T. C.; Farwell, D.G.; Giachelli, C. M.; Ratner, B. D. *Tissue Eng.* **2006**, *12*, 319–30.
[159] Amiel, G. E.; Komura, M.; Shapira, O.; Yoo, J. J.; Yazdani, S.; Berry, J.; Kaushal, S.; Bischoff, J.; Atala, A.; Soker, S. *Tissue Eng.* **2006**, *12*, 2355–2365.

[160] Daamen, W. F.; Hafmans, T.; Veerkamp, J. H.; Van Kuppevelt, T. H. *Tissue Eng.* **2005**, *11*, 1168–1176.
[161] Lansing, A. I.; Rosenthal, T. B.; Alex, M.; Dempsey, W. *Anat. Rec.* **1952**, *114*, 555–75.
[162] Partridge, S. M.; Davis, H. F.; Adair, G. S. *Biochem. J.* **1955**, *61*, 11–21.
[163] Jacob, M. P.; Hornebeck, W. Isolation and characterisation of insoluble and kappa-elastins. In Methods of connective tissue research, vol. 4. (Eds. Robert, L.; Moczar, M.; Moczar, E. Basel, Karger, **1985**, pp. 92–129).
[164] Wei, S. M.; Katona, E.; Fachet, J.; Fülöp, Jr. T., Robert, L.; Jacob, M. P. *Int. Arch. Allergy. Immunol.* **1998**, *115*, 33–41.
[165] Duca, L.; Floquet, N.; Alix, A. J.; Haye, B.; Debelle, L. *Crit. Rev. Oncol. Hematol.* **2004**, *49*, 235–44.
[166] Lefebvre, F.; Pilet, P.; Bonzon, N.; Daculsi, G., Rabaud, M. *Biomaterials* **1996**, *17*, 1813–1818.
[167] Barbie, C.; Angibaud, C.; Darnis, T.; Lefebvre, F.; Rabaud, M.; Aprahamian, M. *Biomaterials* **1989**, *10*, 445–448.
[168] Bonzon, N.; Carrat, X.; Deminiére, C.; Daculsi, G.; Lefebvre, F.; Rabaud, M. *Biomaterials* **1995**, *16*, 881–885
[169] Dutoya, S.; Verna, A.; Lefebvre, F.; Rabaud, M. *Biomaterials* **2000**, *21*, 1521–1529.
[170] Ruedinger, F.; Lavrentieva, A.; Blume, C.; Pepelanova, I.; Scheper, T. *Appl. Microbiol. Biotechnol.* **2015**, *99*, 623–636.
[171] Drury, J. L.; Mooney, D. J. *Biomaterials* **2003**, *24*, 4337–4351.
[172] Dahlmann, J.; Krause, A.; Möller, L.; Kensah, G.; Möwes, M.; Diekmann, A.; Martin, U.; Kirschning, A.; Gruh, I.; Dräger, G.. *Biomaterials* **2013**, *34*(4), 940–951.
[173] Liu, Y.; Wang, R.; Zarembinski, T. I.; Doty, N.; Jiang, C.; Regatieri, C.; Zhang, X.; Young, M. J. *Tissue Eng. Pt A* **2013**, *19*(1-2), 135-142.
[174] Tsaryk, R.; Gloria, A.; Russo, T.; Anspach, L.; De Santis, R.; Ghanaati, S.; Unger, R. E.; Ambrosio, L.; Kirkpatrick, C. J. *Acta Biomaterialia* **2015**, *20*, 10–21.
[175] Aroguz, A. Z.; Baysal, K.; Adiguzel, Z.; Baysal, B. M. *Appl. Biochem. Biotech.* **2014**, *173*(2), 433-448.
[176] Delmar, K.; Bianco-Peled, H. *Carbohyd. Polym.* **2015**, *127*, 28–37.
[177] Li, B.; Wang, L; Xu, F.; Gang, X.; Demirci, U.; Wei, D.; Li, Y.; Feng, Y.; Jia, D.; Zhou, Y. *Acta Biomaterialia* **2015**, *22*, 59–69.
[178] Assaad, E.; Maire, M.; Lerouge, S. *Carbohyd. Polym.* **2015**, *130*, 87-96.
[179] Qiu, Y.; Park, K. *Adv. Drug Deliver. Rev.* **2012**, *64S*, 49–60.
[180] Klouda, L. *Eur. J. Pharm. Biopharm.* **2015**, *97*B, 338–349.
[181] Orienti, I.; Treré, R.; Zecchi, V. *Drug Dev. Ind. Pharm.* **2001**, *27*, 877–84.
[182] Langer, R.; Vacanti, J. *Science* **1993**, *260*(5110), 920-926.
[183] Slaughter, B. V.; Khurshid, S. S.; Fisher, O. Z.; Khademhosseini, A.; Peppas, N. A. *Adv. Mater.* **2009**, *21*, 3307–3329.

[184] Elisseeff, J.; McIntosh, W.; Anseth, K.; Riley, S.; Ragan, P.; Langer, R. *J. Biomed. Mater. Res.* **2000**, *51*, 164-171..
[185] Mann, B. K.; Gobin, A. S.; Tsai, A. T.; Schmedlen, R. H.; West, J. L. *Biomaterials* **2001**, *22*, 3045-3051.
[186] West, J. L.; Hubbell, J. A. *Proc. Natl. Acad. Sci. USA* **1996**, *93*, 13188-13193.
[187] Hill-West, L.; Dunn, R. C.; Hubbell, J. A. *J. Surg. Res.* **1995**, *59*(6), 759-763.
[188] An, Y. J.; Hubbell, J. A. *J. Control. Release* **2000**, *64*, 205-215.
[189] Bergmann, N. M.; Peppas, N. A. *Prog. Polym. Sci.* **2008**, *33*, 271-288.
[190] Vashist, A.; Vashist, A.; Gupta, Y. K.; Ahmad, *S. J. Mater. Chem. B* **2014**, *2*, 147-166.
[191] Cruise, G. M.; Hegre, O. D.; Lamberti, F. V.; Hager, S. R.; Hill, R.; Scharp, D. S.; Hubbell, J. A. *Cell Transplant.* **1999**, *8*, 293-306.
[192] Shantha, K. L.; Harding, D. R. K. *J. Appl. Polym. Sci.* **2002**, *84*, 2597–2604.
[193] Shantha, K. L.; Harding, D. R. K. *Eur. Polym. J.* **2003**, *39*, 63–68.
[194] El-Sherbiny, I. M.; Abdel-Bary, E. M.; Harding, D. R. K. *Int. J. Polym. Mater.* **2006**, *55*, 789–802.
[195] Jabbari, E.; Nozari, S. *Eur. Polym. J.* **2000**, *36*, 2685–2692.
[196] El-Sherbiny, I. M.; Smyth, H. D. C. *Carbohydr Res.* **2010**, *345*(14), 2004–2012.
[197] El-Sherbiny, I. M.; Yacoub, M. H. *Glob. Cardiol. Sci. Pract.* **2013**, *38*, 317-342.
[198] Akin, H.; Hasirci, N. *Polym. Preprint.* **1995**, *36*, 384–385.
[199] Iha, R. K.; Wooley, K. L.; Nystrom, A. M.; Burke, D. J.; Kade, M. J.; Hawker, C. J. *Chem. Rev.* **2009**, *109*, 5620-5686.
[200] Dondoni, A. *Angew. Chem. Int. Ed.* **2008**, *47*, 8995-8997.
[201] Massi, A.; Nanni, D. *Org. Biomol. Chem.* **2012**, *10*, 3791-3807.
[202] Fairbanks, B. D.; Schwartz, M. P.; Halevi, A. E.; Nuttelman, C. R.; Bowman, C. N.; Anseth, K. S. *Adv. Mater.* **2009**, *21*, 5005-5010.
[203] Anderson, S. B.; Lin, C. C.; Kuntzler, D. V.; Anseth, K. S. *Biomaterials* **2011**, *32*, 3564-3574.
[204] Vermeer, H. J.; van Dijk, C. M.; Kamerling,J. P.; Vliegenthart J. F. G. *Eur. J. Org. Chem.* **2001**, *2001*, 193–203.

List of publications

Articles:

1. The collaggrecan: synthesis and visualization of an artificial proteoglycan. Mario Raspanti, Elena Caravà, Antonella Sgambato, Antonino Natalello, Laura Russo, Laura Cipolla. *Int. J. Biol. Macromol.* **2016**, *86*, 65-70.
2. Gelatin hydrogels via thiol-ene chemistry. Laura Russo, Antonella Sgambato, Roberta Visone, Paola Occhetta, Matteo Moretti, Marco Rasponi, Francesco Nicotra, Laura Cipolla. *Monatsh. Chem.* **2015**, DOI 10.1007/s00706-015-1614-5.
3. Different sialoside epitopes on collagen film surfaces direct mesenchymal stem cell fate. Antonella Sgambato, Laura Russo, Monica Montesi, Silvia Panseri, Maurilio Marcacci, Elena Caravà, Mario Raspanti, Laura Cipolla. *ACS Appl. Mater. Interfaces* **2015**, DOI: 10.1021/acsami.5b08270.
4. New synthetic and biological evaluation of uniflorine A derivatives: towards specific insect trehalase inhibitors. Giampiero D'Adamio, Antonella Sgambato, Matilde Forcella, Silvia Caccia, Camilla Parmeggiani, Morena Casartelli, Paolo Parenti, Davide Bini, Laura Cipolla, Paola Fusi, Francesca Cardona. *Org. Biomol. Chem.* **2015**, *13*(3), 886-92.
5. N-Bridged 1-deoxynojirimycin dimers as selective insect trehalase inhibitors. Laura Cipolla, Antonella Sgambato, Matilde Forcella, Paola Fusi, Paolo Parenti, Francesca Cardona, Davide Bini. *Carb. Res.* **2014**, *389*, 46-49.
6. Response of osteoblast-like MG63 on neoglycosylated collagen matrices. Laura Russo, Antonella Sgambato, Paolo Giannoni, Rodolfo Quarto, Simone Vesentini, Alfonso Gautieri, Laura Cipolla. *Med. Chem. Comm.* **2014**, *5*, 1208-1212.
7. Neoglucosylated collagen matrices drive neuronal cells to differentiate. Laura Russo, Antonella Sgambato, Marzia Lecchi, Valentina Pastori, Mario Raspanti, Antonino Natalello,

Silvia Maria Doglia, Francesco Nicotra, Laura Cipolla. *ACS Chem. Neurosci.* **2014**, *5*, 261-265.

Book chapter:

1. Carbohydrate, biomaterials, and tissue engineering applications. Laura Russo, Antonella Sgambato, Davide Bini, Ilaria Calloni, Davide Origgi, Fatma Cetin Telli, Laura Cipolla. Imperial College Press. **2015**, DOI: 10.1142/9781783267200_0016.
2. Trehalose Mimics as Bioactive Compounds. Davide Bini, Antonella Sgambato, Luca Gabrielli, Laura Russo, Laura Cipolla. Biotechnology of Bioactive Compounds: Sources and applications (eds V. K. Gupta and M. G. Tuohy), John Wiley & Sons, Ltd, Chichester, UK. **2015**, DOI: 10.1002/9781118733103.ch14.
3. Multivalent glycidic constructs toward anticancer therapeutics. Francesco Nicotra, Luca Gabrielli, Davide Bini, Laura Russo, Antonella Sgambato, Laura Cipolla. SPR Vol 40, Chapter 23, **2014**, Print ISBN: 978-1-84973-965-8, DOI:10.1039/9781849739986-00491.

Only publications related to this thesis are attached below.